12-2009

Formation of Multiple Dimer Interfaces in the Active and Inactive States of a Model G Protein-Coupled Receptor

Hee Jung Kim
University of Tennessee - Knoxville

To the Graduate Council:

I am submitting herewith a dissertation written by Hee Jung Kim entitled "Formation of Multiple Dimer Interfaces in the Active and Inactive States of a Model G Protein-Coupled Receptor." I have examined the final electronic copy of this dissertation for form and content and recommend that it be accepted in partial fulfillment of the requirements for the degree of Doctor of Philosophy, with a major in Microbiology.

Jeffrey M. Becker, Major Professor

We have read this dissertation and recommend its acceptance:

Ana A. Kitazono, Elizabeth E. Howell, Timothy E. Sparer, Todd B. Reynolds

Accepted for the Council:
Carolyn R. Hodges

Vice Provost and Dean of the Graduate School

(Original signatures are on file with official student records.)

To the Graduate Council:

I am submitting herewith a dissertation written by Hee Jung Kim entitled "Formation of Multiple Dimer Interfaces In the Active and Inactive States of a Model G Protein-Coupled Receptor." I have examined the final electronic copy of this dissertation for form and content and recommend that it be accepted in partial fulfillment of the requirements for the degree of Doctor of Philosophy with a major in Microbiology.

Jeffrey M. Becker

Major Professor

We have read this dissertation

and recommend its acceptance:

Ana A. Kitazono

Elizabeth E. Howell

Timothy E. Sparer

Todd B. Reynolds

Accepted for the Council:

Carolyn R. Hodges

Vice Provost and Dean of the Graduate School

(Original signatures are on file with official student records.)

Formation of Multiple Dimer Interfaces

In the Active and Inactive States

of a Model G Protein-Coupled Receptor

Presented for the

Doctor of Philosophy Degree

The University of Tennessee, Knoxville

Hee Jung Kim

December 2009

Dedication

I would like to dedicate this dissertation to my parents, Jin-gun Kim and Jung-ae Park, and to my parents in-law, Woong-yeol Park and Kyung-ae Kim, who stood by me, supported me and pray for me all the times.

I would also like to dedicate this work to my husband, Giljun, Joomin and the one coming soon for all the support and encouragement they gave me. Without their love, I could never have completed this work.

"My soul finds rest in God alone; my salvation comes from him"

Acknowledgments

I am most grateful to Proffessor Jeffrey M. Becker for the privilege and opportunity to work in his laboratory and wish to thank him for the advice and encouragement based on his distinguished scientific insight and knowledge. It was really a great pleasure to work for such an enthusiastic scientist and real teacher. I am also thankful that he was so patient during the times I was struggling with problems. I am honored to work for you. I would like to thank to my committee members: Dr. Ana A. Kitazono, Dr. Elizabeth E. Howell, Dr. Timothy E. Sparer and Dr. Todd B. Reynolds for their suggestions, critical reviews and guidance during my studies. I also would like to thank to Dr. Naider for his support and valuable ideas on critical decisions throughout these studies.

In addition I wish to thank all my colleagues in Dr. Becker's laboratory. They are always kind and warm. I want to thank Dr. Melinda Hauser, Dr. Byung-Kwon Lee, and Dr. Tom Masi for their wise suggestions and help. Also, I want to thank all other Beckerians: Sarah Kauffman, George Umanah, Li-Yin Huan, and Seraj Uddin for their help and making me laugh everyday.

Finally I want to thank to my family in Korea, Giljun and Joomin for all the support that they gave me during all these years.

Abstract

G protein-coupled receptors (GPCRs) are a class of integral membrane receptor proteins that are characterized by seven-transmembrane (7TM) domains connected by intracellular and extracellular loops, an extracellular N-terminus, and an intracellular C-terminus. GPCRs recognize neurotransmitters, sensory molecules and chemotactic agents and are involved in the control of many aspects of metabolism. Since GPCRs play important roles in diverse processes such as pain perception, growth and blood pressure regulation, and viral pathogenesis, GPCRs became important target for therapeutic agents. The tridecapeptide α-factor pheromone ($W_1H_2W_3L_4Q_5L_6K_7P_8G_9Q_{10}P_{11}M_{12}Y_{13}$) of *Saccharomyces cerevisiae* and Ste2p, its cognate GPCR, have been used extensively as a model for peptide ligand-GPCR structure and function. The power of yeast genetics has been used to examine the structure and function of Ste2p. Recently, GPCR homo-dimerization has been demonstrated for many GPCRs, although the role(s) of dimerization in receptor function is disputed. In this dissertation, Ste2p has been used to investigate GPCR dimerization.

Part I of this dissertation is an overview of the GPCR structure and its ligand-induced conformational change with specific emphasis on the peptide pheromone α-factor and its receptor Ste2p. Part II of this dissertation is a study originally designed to probe inter-helical interaction between TM1 and TM7 of Ste2p. Site-directed mutagenesis and cysteine cross-linking with targeted residues of Ste2p were carried out. Although the anticipated inter-helical interactions were not identified from this study, the results provided strong evidence for Ste2p dimerization. Part III of this dissertation describes dimer interfaces including TM1 and TM7 of Ste2p. By using the disulfide

cross-linking methodology, we studied the participation of specific residues at the intracellular boundary between TM1 and intracellular loop one and the entire TM7 in Ste2p dimerization. The final part of this dissertation contains a study of the participation of the Ste2p N-terminus in homo-dimer formation and the effect of ligand binding on this interaction. This part also includes overall conclusions and suggestions for future experiments that could contribute to an understanding of the dimer interfaces in Ste2p and the role of dimerization in the function of this receptor.

Table of Contents

List of Tables

List of Figures

PART I General Introduction

CHAPTER 1 G Protein-Coupled Receptors

An overview

G protein-coupled receptors (GPCRs) are a class of membrane receptor proteins that are characterized by a signature seven-transmembrane domain (7TM) and heterotrimeric guanine nucleotide-binding proteins (G proteins) coupled to receptor [1]. GPCRs consist of large and diverse gene families found in fungi, plants, and the animal kingdom. In humans, GPCRs comprise the largest superfamily of proteins with more than 1000 different GPCRs identified [2]. GPCRs are located at the cell surface and are responsible for the transduction of an extracellular stimulus into an intracellular response [3]. The endogenous ligands of GPCRs are extraordinarily diverse, including biogenic amines (such as adrenaline, dopamine, histamine, and serotonin), peptide and protein hormones (for example,angiotensin, bradykinin, endothelin, and melanocortin), peptide pheromones (i.e. α-factor, **a**-factor of various fungal species), nucleosides and nucleotides (adenosine, adenosine triphosphate, uridine triphosphate), and lipids and eicosanoids (cannabinoids, leukotrienes, prostaglandins, and thromboxanes) [4]. Furthermore, the awareness of exogenous signals, such as light, odor, and taste, is also mediated via GPCRs [5, 6]

Heterotrimeric G proteins are regulated by GPCRs upon ligand binding to receptors. G proteins are composed of three subunits (α, βγ-dimer) and each subunit plays important roles in determining the specificity and temporal characteristics of the cellular responses to signals [7]. Conformational change of receptor accompanied by activation of GPCRs lead to release of GDP followed by binding of GTP of Gα-subunit

[1]. This change triggers the dissociation of the α-subunit from the receptor and the βγ-dimer. Both the GTP bound α-subunit and the released βγ-dimer can mediate the stimulation or inhibition of effector proteins such as enzymes and ion channels [e.g, adenylate cyclase, guanylyl cyclase, phospholipase C, mitogen-activated protein kinases (MAPKs), Ca^{+2}, and K^{+} channels]. Thus, stimulation of GPCRs with specific agonists results in changes in the concentration of second-messenger molecules [1]

Considering the wide variety of biological pathways regulated by GPCRs it is not unexpected that abnormal signaling by these receptors lead to disorders in tissues and organs in the human body [8]. Currently, GPCRs are ideal drug target for pharmaceutical companies due to the widespread physiological processes GPCRs mediated. Approximately 50% of all modern prescription drugs and 25% of the top-selling drugs directly or indirectly have an effect on GPCRs [3, 6, 9] (Table 1). However, only a very small portion of the known GPCRs represent targets of currently marketed drugs. Many GPCRs remain 'orphan', which have not been assigned functions. Even for many receptors whose ligands are known, there is a need for identifying agonist and antagonist ligands. Regarding these facts, it is suggested that GPCRs will continue to be drug targets of the future [10-12]. Thus, the studies of GPCRs will contribute significantly to the understanding and treatment of a variety of diseases.

Classification of GPCRs

Despite the fact that various agonists stimulate the special GPCR family to activate diverse secondary-messenger pathways, GPCRs share structural similarities [13].

Table 1 Examples of Top-selling GPCR drugs in 2005

Action	Trade Name	Molecular Entity	Company	Therapeutic Indication	World Sales (US$ millions)
H1[1] antagonist	Allegra/ Telfast	Fexofenadine	Sanofi-Aventis	Allergies	1792
AT1[2] antagonist	Diovan	Valsartan	Novartis	Hypertension	2214
H2[3] antagonist	Gaster	Famotidine	Yananouchi	Gastric ulcer	656
5HT10[4] agonist	Lmigran	Sumatriptan	GlaxosmithKline	Migraine	1454
LH-RH[5] agonist	Leuplin/ Lupron	Leuprorelin	Takeda/Abbott	Cancer	904
GABAb[6] agonist	Neurontin	GABApentin	Pfizer	Neurological pain	2480
B1 agonist[7]	Serevent	Salmeterol	GlaxosmithKline	Asthma	679
Mixed 5HT2[8]/D1[9]/ D2[10] antagonist	Zyprexa	Olanzapine	Eli Lilly	Schizophrenia	4905

Table modified from Jacoby *et al [6]*.

[1] H1, Histamin 1 receptor; [2] AT1, Angiotensin1 receptor; [3] H2, Histamin 2 receptor; [4]5HT10, Serotonin (5-hydroxytryptamine, 5-HT) 10 receptor; [5] LH-RH, Luteinizing hormone-releasing hormone receptor; [6] GABAb, γ-Aminobutyric acid receptor; [7] B1, Bradykinin 1 receptor; [8] 5HT2, Serotonin (5-hydroxytryptamine, 5-HT) 2 receptor; [9] D1, Dopamine 1 receptor; [10] D2, Dopamine 2 receptor

All GPCRs contain seven transmembrane-spanning α-helical segments connected by alternating intracellular and extracellular loops (IL and EL, respectively), with the amino terminus located on the extracellular side of the cytoplasmic membrane and the carboxy terminus on the intracellular side. Although GPCRs share common membrane topological features, sequence comparisons showed little or no similarities among the different GPCRs [14] and the size of the each domain vary such as extracellular N-terminal tails (7-600 amino acids), loop domains (5-230 amino acids), and C-terminal domains (12-360 amino acids) which indicate diverse functions of GPCRs [7].

The GPCR superfamily has been classified into six different families. Each class has at least 20 % identity of their amino acid sequence within the TMs (Transmembrane domains) (Table 2)[4]. The rhodopsin-like class A receptor is the most studied because it is easily obtainable in a purified form in large quantitites and it has the largest number of receptors. This class contains receptors for peptides, hormone peptide, odorants, small molecules such as the catecholamines and amines, and glycoprotein hormones (Fig.1 A) [9]. Among class A receptors, peptide receptors are the largest subgroup and mediate important physiological roles of endogenous peptides that act as neurotransmitters and hormones. Class A receptors are characterized by a series of highly conserved key residues such as the DRY motif at the bottom of transmembrane domain (TM) 3 and the NPXXY motif in TM7 (Fig. 1 A). Class B receptors are the next largest class including receptors for a variety of gastrointestinal peptide hormones (secretin, glucagons, vasoactive intestinal peptide, and growth-hormone-releasing hormone), calcitonin, corticotrophin-releasing hormone and parathyroid hormone [1]. Class B receptors do not share any of the structural features characterizing class A receptors except for the

Table 2 Sequence-based groupings within the G-protein-coupled receptors

Class: A Rhodopsin-like receptors	
Family I	Olfactory receptors, adenosine receptors, melanocortin receptors, and others
Family II	Biogenic amine receptors
Family III	Vertebrate opsins and neuropeptide receptors
Family IV	Invertebrate opsins
Family V	Chemokine, chemotactic, somatostatin, opioids and others
Family VI	Melatonin receptors and others
Class B: Calcitonin and related receptors	
Family I	Calcitonin and calcitonin-like receptors
Family II	PTH[1]/PTHrP[2] receptors
Family III	Glucagon, secretin receptors and others
Family IV	Latrotoxin receptors and others
Class C: Metabotropic glutamate and related receptors	
Family I	Metabotropic glutamate receptors
Family II	Calcium receptors
Family II	GABAb[3] receptors
Family IV	Putative pheromone receptors
Class D: STE2 pheromone receptors	
Class E: STE3 pheromone receptors	
Class F: cAMP and archaebacterial opsin receptors	

[1] PTH, Parathyroid hormone receptor; [2] PTHrP, Parathyroid hormone related peptide receptor; [3] GABAb, γ-Aminobutyric acid receptor

(Modified from Flower *et al [4])*

presence of a disulfide bridge between the first extracellular loop (EL1) and second extracellular loop (Fig.1B). The most distinguishing characteristic of class B is that the amino terminus contains several cysteines, presumably forming a network of disulfide bridges [15]. The class C is relatively a smaller group, containing the metabotropic glutamate and γ-amino-butyric acid receptors, the calcium receptors, the vomeronasal, mammalian pheromone receptors, as well as some taste receptors [16]. All receptors in class C have a very large extracellular amino terminus (500-600 amino acids) (Fig.1C) that seems to be crucial for ligand binding and activation [17, 18]. Class D is the STE2 yeast pheromone receptors, and class E is the STE3 yeast pheromone receptors. These two groups will be discussed in the next section (Chapter 2). Finally class F comprises the receptors that are related to slime mold cyclic adenosine monophosphate (cAMP) receptors and archaebacterial opsins.

The tertiary structure of GPCRs

Information about the tertiary structure of a GPCR is crucial for the understanding of its function and for the design of drugs to correct possible problems caused by failure of its function. Currently methods used to understand receptor structure and the interactions of the ligand with its receptor at the atomic level include X-ray crystallography, electron microscopy or diffraction, NMR spectroscopy and molecular modeling. One of the advantages for NMR spectroscopy compared to the other methods is that dynamic information can be obtained. However, structural information requires high concentrations of dissolved pure protein. Except for several studies where single

helices were measured in a membrane, using solid state NMR, technical problems have precluded NMR studies from yielding structural information on GPCRs [19].

Currently, five crystal structures of GPCRs have been revealed (Fig. 2). The first crystal obtained was that rhodopsin resolved as a highly organized seven transmembrane bundle with 11-cis-retinal, which is a key cofactor involved in maintaining rhodopsin in the ground state [20]. An interesting feature is that some of the transmembrane helices in rhodopsin are not regular α-helices [21]. The helices are bent around proline, one of the strongest distortion is at Pro267 in TM6 (a highly conserved residue among GPCRs). It has been shown that mutations at this residue cause conformational changes on intracellular loop 3 [22]. In addition, a pronounced kink is observed in TM2, caused by flexibility in the Gly-Gly sequence in the middle of this helix. The crystal structure also revealed a short 8^{th} helix, which runs parallel to the cytoplasmic membrane. This helix and the generated fourth cytoplasmic loop cover part of the binding site for the C-terminus of $G_{t\alpha}$ subunit and play a role in $G_{t\gamma}$ binding. A set of residues including the 8^{th} helix on the cytoplasmic surface, where G protein activation occurs, likely to undergo a conformational change upon photoactivation of the chromophore that leads to G protein activation and signal transduction [21].

Several years after the rhodopsin structure was published, Kobilka and colleagues [23-25] published two different structures of the β_2-adrenoceptor. Two initial structures of β_2AR were crystallized, one was fused with T4-lysozyme and another was bound with antagonist. Also crystal structure of β_2AR was crystallized in a complex with an anti intracellular loop (IL) 3, Fab fragment, at 3.5Å resolution. Both structures were similar indicating that the T4 lysozyme fusion had little effect on the structural properties of the

Figure 1 Classification of human GPCRs

Class A GPCRs are characterized by several highly conserved amino acids in the TMs, and there is usually a disulfide bridge linking extracellular loops 1 and 2. Most of the class A receptors have a palmitoylated cysteine residue in the intracellular C-terminal tail. The binding sites of the endogenous small-molecule hormone ligands of class A GPCRs are located within the 7 TM bundle (A-1, the ligand binding site is indicated in orange). For peptide and glycoprotein hormone receptors (A-2 and A-3, respectively), binding occurs at the N terminus, the extracellular loop segments, and the extracellular parts of the TM helices. Class B GPCRs contain a relatively long N-terminal tail (B). The class B receptors show a number of conserved proline residues within the TMs. The majority of class C receptors are characterized by very large N- and C-terminal tails, a disulfide bridge connecting the first and second extracellular loops, together with a very short and well-conserved third intracellular loop (C). A number of the strongly conserved residues of class A GPCRs are also strongly conserved in class C GPCRs. The ligand binding site is located in the N-terminal domain, which is composed of the so-called venus flytrap (VFT) module that shares sequence similarity with bacterial periplasmic amino acid binding proteins. In all class C GPCRs except the GABAB receptor, a cysteine-rich domain (CRD), which contains nine conserved cysteine residues, links the VFT to the 7 TM domain (Modified from Jacoby et al [6]).

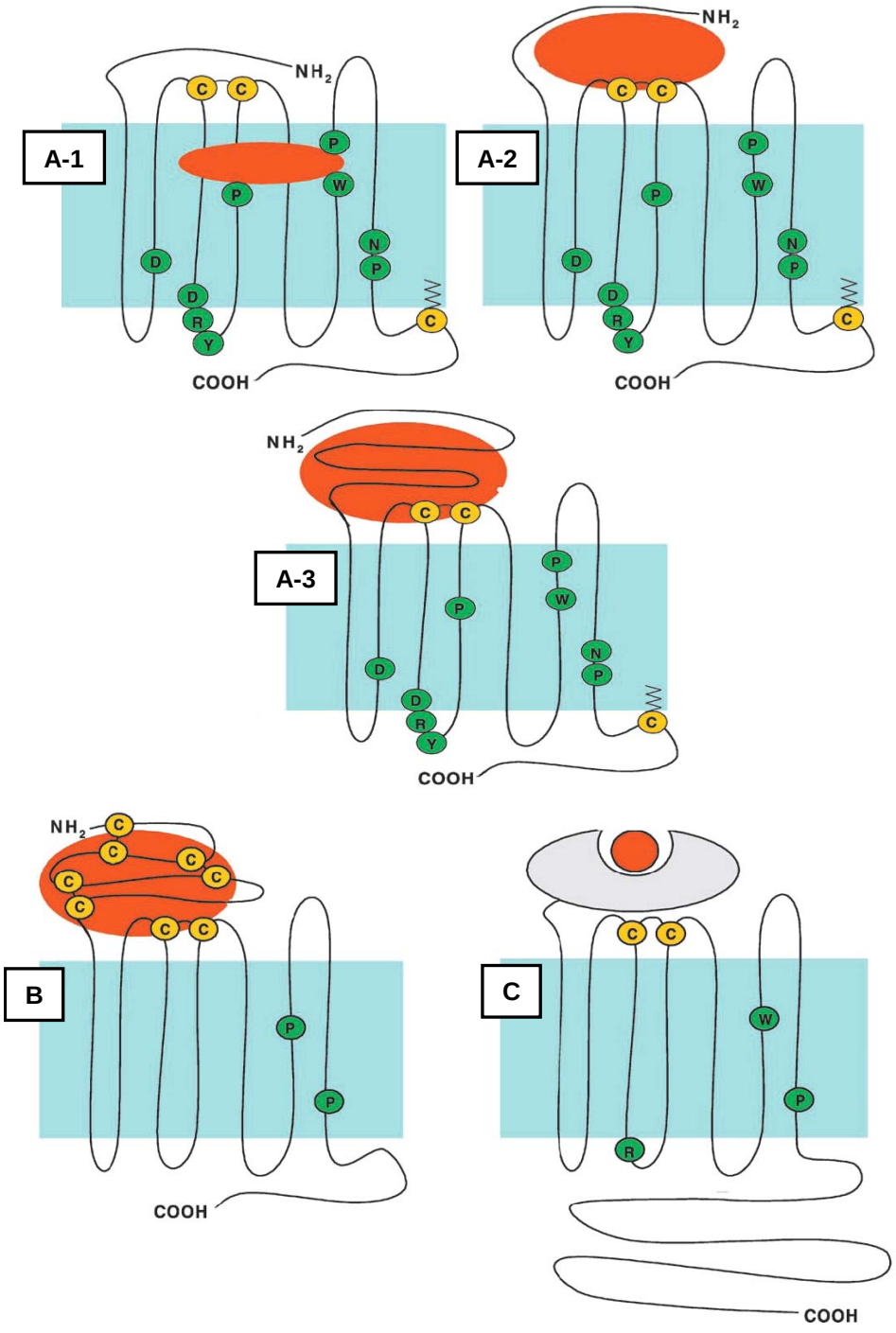
A-1
A-2
A-3
B
C
NH2
COOH
C
P
W
N
D
R
Y

antagonist bound receptor. Soon afterward, an additional structure of β_2AR-T4-lysozyme, which had a stabilizing point mutation, E122W, was solved in complex with the inverse agonist timolol revealing a cholesterol-binding site [26, 27]. Then, the turkey β_1AR structure was solved in the presence of a strong antagonist cyanopindolo [28]. The overall structure was very similar to that of human β_2AR with the exception of the second intracellular loop, a short helical segment in the turkey receptor whereas it was a random coil in human β_2AR. The adenosine A_{2a} receptor structure was also solved in complex with the antagonist ZM241385 [29]. The adenosine structure showed a shifted ligand-binding site and even greater helical shifts relative to rhodopsin and β_2AR. Then, a major breakthrough was made by Ernst and colleagues [30, 31]. They published the crystal structure of light-activated opsin in complex with the C-terminal peptide corresponding Gα subunit, transducin. Although the agonist was lacking in this structure, it may would be considered to be an active state of GPCR because of the bound C-terminal Gα peptide [32]. Importantly, the structure demonstrated significant deviation from the inactive form of rhodopsin in the arrangement of the seven helical bundles.

Compared to the rhodopsin structure, each GPCR crystal structure had similarities and differences [33, 34](Fig. 2). Sequence conservation among class A GPCRs is highest within the transmembrane regions. Thus, it is not surprising that the helical bundle orientation and packing is similar among the structures solved to date while the extracellular region of the βARs is very open compared to rhodopsin. The most prominent feature is a short helical segment within extracellular loop (EL) 2 that is supported by limited interactions with EL1 and two disulfide bridges. The extracellular

region of the adenosine receptor is highly constrained by four disulfide bridges and multiple polar and van der Waals interactions among the three loops.

The position of the antagonist-binding pocket varies significantly as a function of the receptor. The binding pocket of the β-adrenergic receptor is quite similar to that of rhodopsin, while the ligand binding pocket seems to be very different in the A2a adenosine structure. Based on sequence conservation and the initial bovine rhodopsin structure, it was considered that the DRY motif at the intracellular base of TM3 found in most class A GPCRs interact with a glutamate residue at the base of TM6. However, looking at the structure of β_2AR, β1AR, A2a, this is unlikely.

Ligand binding and receptor activation

GPCRs are activated upon binding of ligand which is varied, ranging in size from small molecules to large glycoproteins. Many studies on receptor research are focused on identification of the binding domains for ligands, using genetic, biochemical, and biophysical approaches [13]. Site-directed or random mutagenesis of receptor, domain swapping, and use of labeled probes are the most commonly used methods for understanding structure-function relationship between GPCRs and their ligands. The binding sites of endogenous "small-molecule" ligands in class A receptors, such as for the retinal chromophore in rhodopsin and catecholamines in the adrenergic receptors are the most widely studied and well characterized of these receptor-binding domains [35-37]. Recent studies on several peptide receptors such as the receptors for angiotensin [38-40], parathyroid hormone [41, 42], secretin [43], bradykinin B2 [44, 45], gonadotropin-

releasing hormone [46], opioids [47, 48], neurokinin (NK) [49, 50], vasopressin/oxytosin [51-53], cholecystokin/gastrin [54, 55], and neurotensin 1 [56] supplied valuable information on the binding domains for other classes of GPCRs. Overall similarities are observed among ligands, although there are specific and various interactions between GPCRs and their cognate ligands. For example, large ligands, such as proteins, bind to extracellular loops, while small molecules, including pharmacological agents, bind within the transmembrane region of receptor (Fig. 1). On the other hand, peptides exhibit a combined binding mode; they bind primarily to the extracellular loops while part of the ligand may penetrate into transmembrane region and interacts with residues buried in lipids [57-60].

Conformational Changes Involved in Agonist Induced GPCR Activation

For a long time, there was a simple model that receptors were depicted as bimodal switches with inactive and active forms. However, a growing body of experimental evidence provided information that GPCR is dynamic and has many different conformations [61, 62]. This newer model for GPCR activation is called multi-state model and suggests that the receptor alternate spontaneously between multiple active and inactive conformations [63]. Various GPCRs, for example 5-HT_2-serotonin receptors [64] α_{2A}-adrenoceptors [65], AT_1 receptor [66], gonadotropin-releasing hormone receptors [67], μ-opioid receptors [68] and many others, have been studied with respect to different receptor conformations supporting the multi-state model. Today, it is commonly accepted that different ligands can induce different receptor conformations [69] and this,

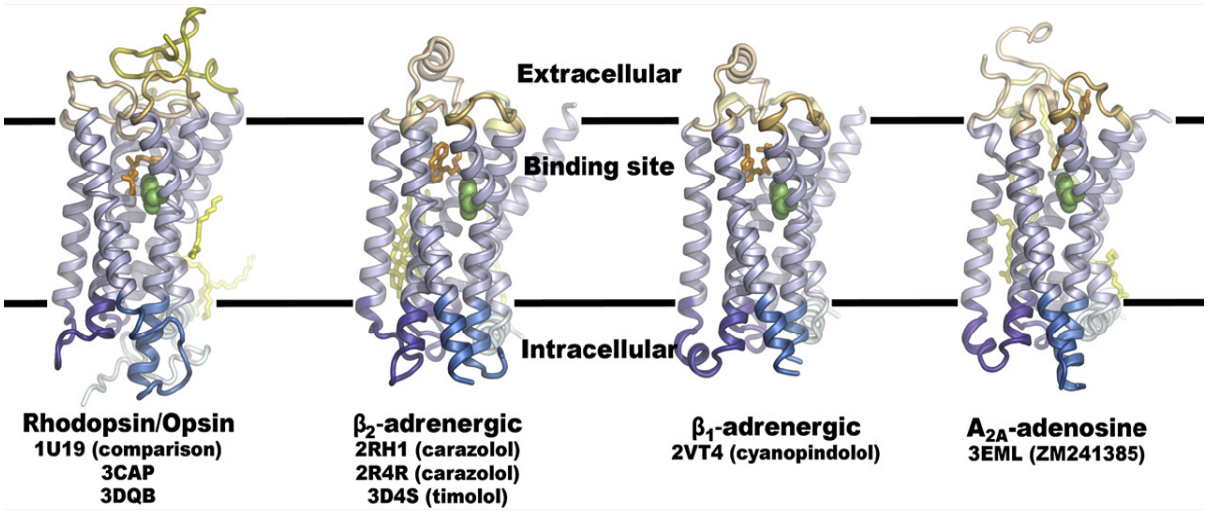

Figure 2 Panel of Representative GPCRs Solved to Date

Each group of receptors is represented by one structure (same orientation). This figure highlights the observed differences seen in the extracellular and intracellular domains as well as the small differences seen in the ligand binding orientations. Light blue indicates transmembrane domains, darker blue indicates intracellular regions, brown indicates extracellular regions, orange indicates ligand. Yellow represents bound lipids and green represents the conserved tryptophan residue. (Adapted from Hanson and Stevens [33])

phenomenon has been described by several synonyms such as ‘functional selectivity', ‘agonist-directed trafficking' or ‘biased agonism'. Recently, it has been suggested that the number of different terms be limited by using the term ‘functional selectivity’ or ‘ligand-induced differential signalling’ to describe this phenomenon [70].

The term ‘efficacy’ is used to describe the effect of ligand on the functional properties of the receptor. Agonists are defined as ligands that fully activate the receptor. ‘Partial agonists’ induce submaximal activation of the G protein even at saturating concentrations. ‘Inverse agonist’ inhibits basal activity. Antagonists have no effect on basal activity, but competitively block the access of other ligands [70].

Intramolecualr interaction of TMs and TM movements during receptor activation

The non-covalent interactions between TMs have an important role in determining the specific basal arrangement of the TM segments. For example, co-transfecting a plasmid encoding the amino terminus to TM5 of the β_2 adrenoceptor (β_2AR) and a plasmid encoding TM6 to the carboxyl terminus of β_2AR generates a functional ‘split’ receptor [71]. Also, in the M3 muscarinic receptor system, a functional receptor has been generated with discontinuity in the loop connecting TM3 and TM4, the loop connecting TM4 and TM5, and the loop connecting TM5 and TM6 [72]. In addition, analysis of the crystal structure of bovine rhodopsin suggests that the inactive state conformation of rhodopsin is stabilized by multiple interhelical salt bridges and hydrophobic interactions [73]. There is a Schiff base formation between Glu113 in TM3 and Lys296 in TM7 of bovine rhodopsin in the resting state. Single point mutations of

Glu113 and Lys296 in bovine rhodopsin have been found to lead to constitutive receptor activity [74, 75]. Site-directed mutagenesis experiments with bovine rhodopsin have demonstrated that a mutation of Gly 90 to Asp 90 in TM2 can substitute for Schiff base counterion Glu113 in TM3 [76].

Agonist binding is thought to alter the network of stabilizing intramolecular interactions to favor an active conformation. Figure 3 shows two possible ways how ligands might change intramolecular interactions and the arrangement of TM domains. First, agonists may induce a conformational change by simply disrupting intramolecular interactions (Fig. 3a), thus favoring new interactions that stabilize the molecule. Second, agonists may serve as bridges to create new interactions between TM domains (Fig. 3b). For example, catecholamines can interrupt the ionic lock of β_2AR without interacting with amino acids directly involved in the ionic lock [77].

In rhodopsin, it was reported that TM6 undergoes the largest movement upon receptor activation and smaller changes were observed for TM3 [79]. Consistent with this, movements of TM3 and TM6 during agonist-induced conformational changes have been demonstrated in β-adrenoceptor [80, 81]. The angiotensin AT_1 receptor also provides an example that Asn111 interacts with Asn295 in TM7 in the inactive state [82], while Asn111 seems to interact with Tyr4 in the active state [83]. Therefore, agonist binding might disrupt the interaction between Asn111 and Asn295. Consistent with this interpretation, mutation of Asn111 to alanine leads to constitutive activity [84]. M3 muscarinic receptor was also studied for intramolecular interactions. It was found that the cytoplasmic end of TM6 of this receptor undergoes a rotational movement [85], and the distance between the cytoplasmic ends of TM1 and TM7 was increased during activation.

In contrast the extracellular ends of TM3 and TM7 move closer to each other upon agonist stimulation [86, 87]. To gain information about the switch from an inactive conformation to active receptor conformation(s), as a method for probing spatial proximity of residues in TMs, several different techniques such as site-directed spin labeling, sulfhydryl reactivity study, and fluorescence resonance energy transfer (FRET) have been developed and used over the past decade. In addition, the disulfide cross-linking strategy has been applied to many GPCRs such as bovine rhodopsin [88-92], M3 muscarinic receptor [85, 87], and Ste2p [93]. For example, a disulfide bridge was built successfully between Val204Cys in TM5 and Phe276Cys in TM6 of bovine rhodopsin [89], which previously had been probed by metal ion site construction [94] and between Val223Cys in TM5 and Leu247Cys in TM6 of Ste2p [93]. Whereas numerous intramolecular constraints for inactive state conformations of GPCRs have been identified, much less is known about the intramolecular interactions stabilizing the active state conformations. The identification of intrahelical interactions will provide a molecular basis for understanding mechanistic information relating to GPCR activation pathways. In part II in this dissertation, the inter-helical interactions will be discussed in more detail.

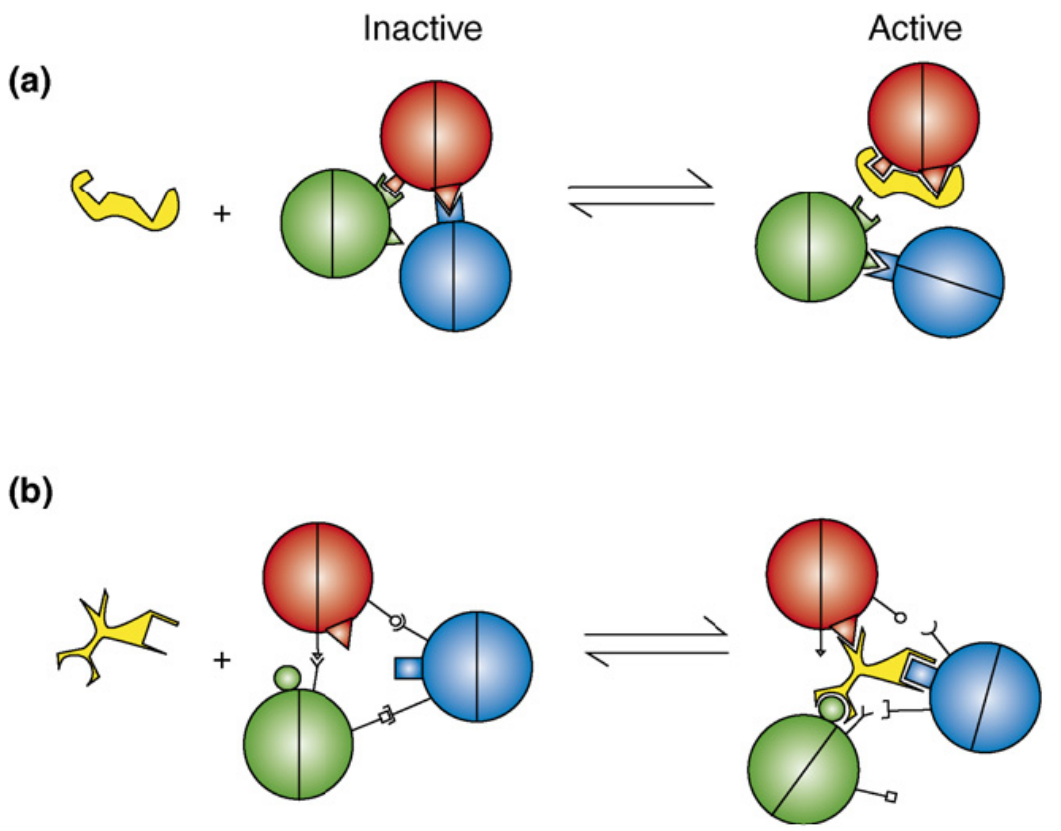

Figure 3 Possible mechanisms how agonist binding disrupts intramolecular interactions that stabilize the inactive state

(a) The agonist binds directly to amino acids involved in stabilizing the inactive state. (b) Agonist binding stabilizes new intramolecular interactions. (Adapted from Kobilka and Deupi [78])

CHAPTER 2 α-factor pheromone and its G Protein-Coupled receptor (Ste2p) in *Saccharomyces cerevisiae*

GPCRs in fungi

Since the glucose/sugar sensor in yeast, Gpr1, and homologs in other fungi are not included in the classical classification of GPCR, recently new classification system for fungal GPCRs have been proposed (Table 3). The GPCRs in fungi are categorized into six classes; Ste2p-like pheromone receptor, Ste3p-like pheromone receptor, carbon/amino acid receptor, putative nutrient receptor, cAMP receptor-like, and microbial opsin [95].

The pheromone sensing GPCRs in fungi are well studied and many pheromone receptors have been identified based on conserved sequences and structures [95]. For example, in *A. nidulans*, GprA and GprB were identified as pheromone receptors based on sequence homology to Ste2 and Ste3 of *S. cerevisiae* [96]. In addition, it is surprising that the pheromone receptors were found to be expressed constitutively even in species which have no sexual cycle documented yet, such as *Candida glabrata* and *Aspergillus fumigatus* [97-99]. The conserved MAPK cascade based on the model established in *S. cerevisiae* has also been linked to morphogenesis and virulence in many fungal pathogens such as the rice blast fungus *M. grisea*, and the human pathogens *C. albicans* and *C glabrata*. [95].

Table 3 Six classes of GPCRs in fungi

Species	Ste2-like pheromone receptor	Ste3-like pheromone receptor	Carbon /amino acid receptor	Putative nutrient receptor	cAMP receptor-like	Microbial Opsin
Ascomycetes						
Saccharomyces cerevisiae	Ste2	Ste3	Gpr1	SCRG_01312 SCRG_02823 SCRG_00179	–	–
Schizosaccharomyces pombe	Mam2	Map3	Git3	Stm1	–	–
Candida albicans	Ste2	Ste3	Gpr1	CAWG_02899 CAWG_06059 CAWG_02686	–	–
Aspergillus nidulans	GprA	GprB	GprC GprD GprE	GprF GprG AN5720	GprH GprI AN8262	AN3361
Aspergillus fumigatus	Afu3g14330	Afu5g07880	Afu7g04800	Afu5g04100 Afu1g06840 Afu1g11900	Afu3g01750 Afu5g04140 Afu3g00780	Afu7g01430
Neurospora crassa	Pre-2	Pre-1	Gpr-4	Gpr-5 Gpr-6	Gpr-1 Gpr-2 Gpr-3	Nop-1 ORP-1
Magnaporthe grisea	MGG_04711	MGG_06452	MGG_08803	MGG_04698 MGG_02855	MGG_06738	MGG_09015
Basidiomycetes						
Cryptococcus neoformans	–	Ste3α/Ste3a Cpr2	Gpr4	Gpr2 Gpr3	Gpr4 Gpr5	CNAG_03572 (Ops1)
Ustilago maydis	–	Pra1 Pra2	–	UM06006 UM01546	UM03423	UM02629 UM04125
Coprinopsis cinerea	–	Rcb1 Rcb2 Rcb3 CC1G_ 02129	–	CC1G_07132 CC1G_04180	CC1G_02288 CC1G_02310	–

-, no homolog has been identified. (Modified from Xue *et al* [95])

α-factor Pheromone and its G Protein-coupled receptor (Ste2p) in Saccharomyces cerevisiae

One of the challenges in GPCR research is the complexity of eukaryotic systems, due to the presence of receptor subtypes and cross-talk between different types of receptors regulating many different pathways. *S. cerevisiae* is a species of budding yeast which is most widely known as perhaps the most intensively studied eukaryotic model organism in molecular and cell biology. The *S. cerevisiae* α-factor receptor system has been used as an ideal system to understand GPCR structure-function as a model for peptide hormones [100]. The power of yeast genetics has been used to examine the structure –function relationship of α -factor receptor. The mitogen-activated protein kinase (MAPK) system is simple but well conserved with higher eukaryotic systems. The *S. cerevisiae* has only three GPCRs, two pheromone receptors (Ste2p and Ste3p) and the Gpr1p which is a carbohydrate sensor. Although the pheromone and carbohydrate-sensing pathways share some down-stream components, there is no cross-talk between the two systems as the pheromone receptors and the Gpr1p couple to two different G-proteins (Gpa1p and Gpa2p, respectively) [101, 102]. Thus *S. cerevisiae* provides an ideal system to study the relation between a peptide ligand and its GPCR in the absence of interfering biological complexities.

Mating in yeast, Saccharomyces cerevisiae

S. cerevisiae can exist as a haploid or diploid [103, 104]. Haploid cells have two mating cell types MATa and MATα, distinguished by the expression of a set of genes involved in mating that are not expressed in diploids. The secretion and reciprocal

detection of peptide pheromones (α -factor and **a**-factor) by GPCRs (Ste2p and Ste3p, respectively) initiate mating and eventual fusion of two haploids (Fig. 4) [100, 105]. The mating pheromones are essential to trigger the mating cycle, therefore the cells that cannot produce these molecules or lack their cognate receptors Ste2p or Ste3p become sterile. The tridecapeptide α -factor pheromone WHWLQLKPGQPMY peptide was chemically synthesized and found to exhibit all the properties of the natural pheromone [106, 107]. The **a**-factor of *S. cerevisiae* is a dodecapeptide pheromone (YIIKGVFWDPAC[Farnesyl]-OCH3) [108], and post-translational modification with a farnesyl isoprenoid and carboxymethyl group is required for full biological activity of this peptide [109].

Pheromone binding to its GPCR and activation of the βγ subunit of G protein trigger the downstream MAPK cascade which activates the transcription of genes involved in the production of pheromone itself, pheromone receptor and the proteins of the signaling pathway (Fig. 5). The cells synthesize cell surface molecules necessary for fusion with their mating partners, arrest in the G1 phase of the growth cycle by eliminating the function of G1 cyclin complex and Cdc28 protein kinase to obtain synchrony for mating, form mating projections that are involved in the fusion process, thereby exhibiting a marked change in shape, and activate a number of genes that are necessary for sexual conjugation [110, 111]. For long time, the Gα subunit Gpa1 was known as a negative regulator. However, recently new evidence was reported that pheromone signaling is also positively transmitted via Gpa1 [112]. Also it was suggested that the GTP-bound form of Gpa1 can induce mating-specific transcription and

morphogenesis in the absence of pheromone, via binding to the phosphatidylinositol-3-kinase Vps34 [113].

The activation of cells by pheromone results in morphological changes. First, conjugation projections are formed to facilitate connection of two opposite mating type cells. By the action of agglutinins, the tips of the projections fuse forming a conjugation bridge. Next, the nuclei migrate into the bridge and subsequently fuse to produce a diploid nucleus of the zygote. All these morphological processes occur with an involvement of cytoskeletal components, i.e., microtubules and actin structures, and the cell wall [114]. Many of these cellular responses have been used to measure the activity of this receptor and potency of pheromones and their analogs. Growth arrest (Halo) assay and β-galactosidase activity assay generated by a *FUS1-lacZ* construct (the *FUS1* gene is transcriptionally activated by pheromone action) are the examples of methods based on the cellular response.

Regulation of Ste2p in Saccharomyces cerevisiae and protein Signaling

Ste2p is highly regulated by several control mechanisms like many other GPCRs. Among the general regulation mechanisms, three distinct processes contribute to α-factor receptor regulation. These are (1) rapid phosphorylation and desensitization [115], (2) internalization and recycling [115] and (3) down-regulation and degradation [116, 117]. The mating process in yeast is further regulated by the control of the expression levels or the activities of the downstream elements in the signaling pathway

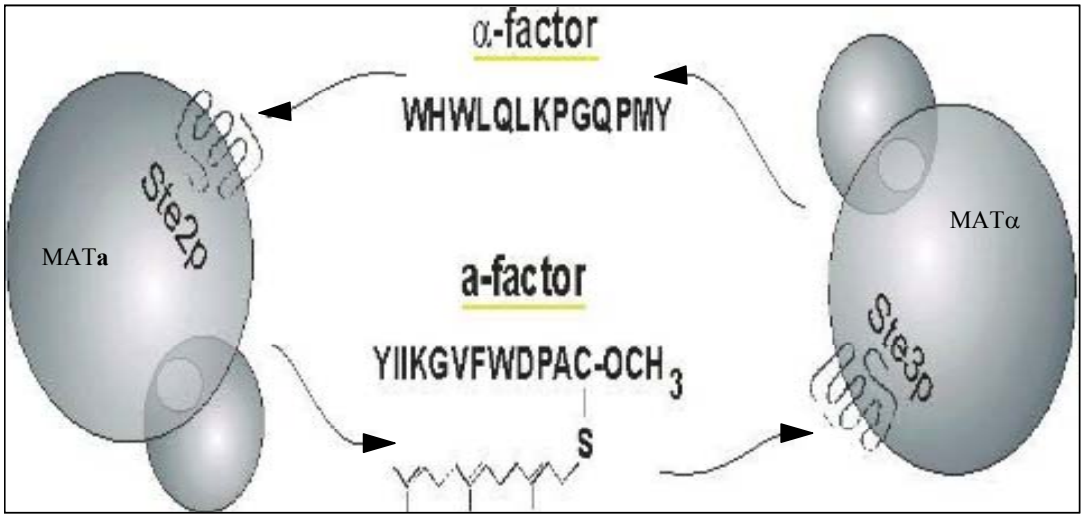

Figure 4 Pheromone mediated mating in *Saccharomyces cerevisiae*

Schematic representation of pheromone/receptor mediated communication between MAT**a** and MATα haploid cells prior to mating.

Figure 5 *Saccharomyces cerevisiae* mating pathway

Binding of pheromone to the receptor stimulates downstream responses such as transcriptional activation of pheromone-induced genes, cell-cycle arrest, and polarization of the cytoskeleton and growth components to the site of highest pheromone concentration. Receptor activation not only triggers the mitogen-activated protein kinase pathway (*light modules*) via G proteins (*spotted modules*), it also involves the receptor carboxy-terminal domain. One model is that the carboxy-terminal domain, through direct or indirect interaction (*white circle*) with the polarity-establishment complex (*dark modules*), stimulates the repolarization of the actin cytoskeleton (*speckled rectangle*) to the site of pheromone activation.

Ste5p, the scaffold protein; Ste20p, mitogen-activated protein kinase kinase kinase kinase (MKKKK); Ste11p, MKKK; Ste7p, MKK; Fus3p and Kss1p, MAPK; Far1p, Cyclin-dependent kinase inhibitor; Ste12p, Transcription factor that is activated by a MAP kinase signaling cascade; Bem1p, Protein containing SH3-domains involved in establishing cell polarity and morphogenesis functions as a scaffold protein; Cdc42p, Small rho-like GTPase; Cdc24p, Guanine nucleotide exchange factor (GEF or GDP-release factor) for Cdc42p; Bni1p, Formin, nucleates the formation of linear actin filaments; *Fus1*, gene encoding membrane protein localized to the shmoo tip and required for cell fusion. (Modified from Madden and Snyder [114]).

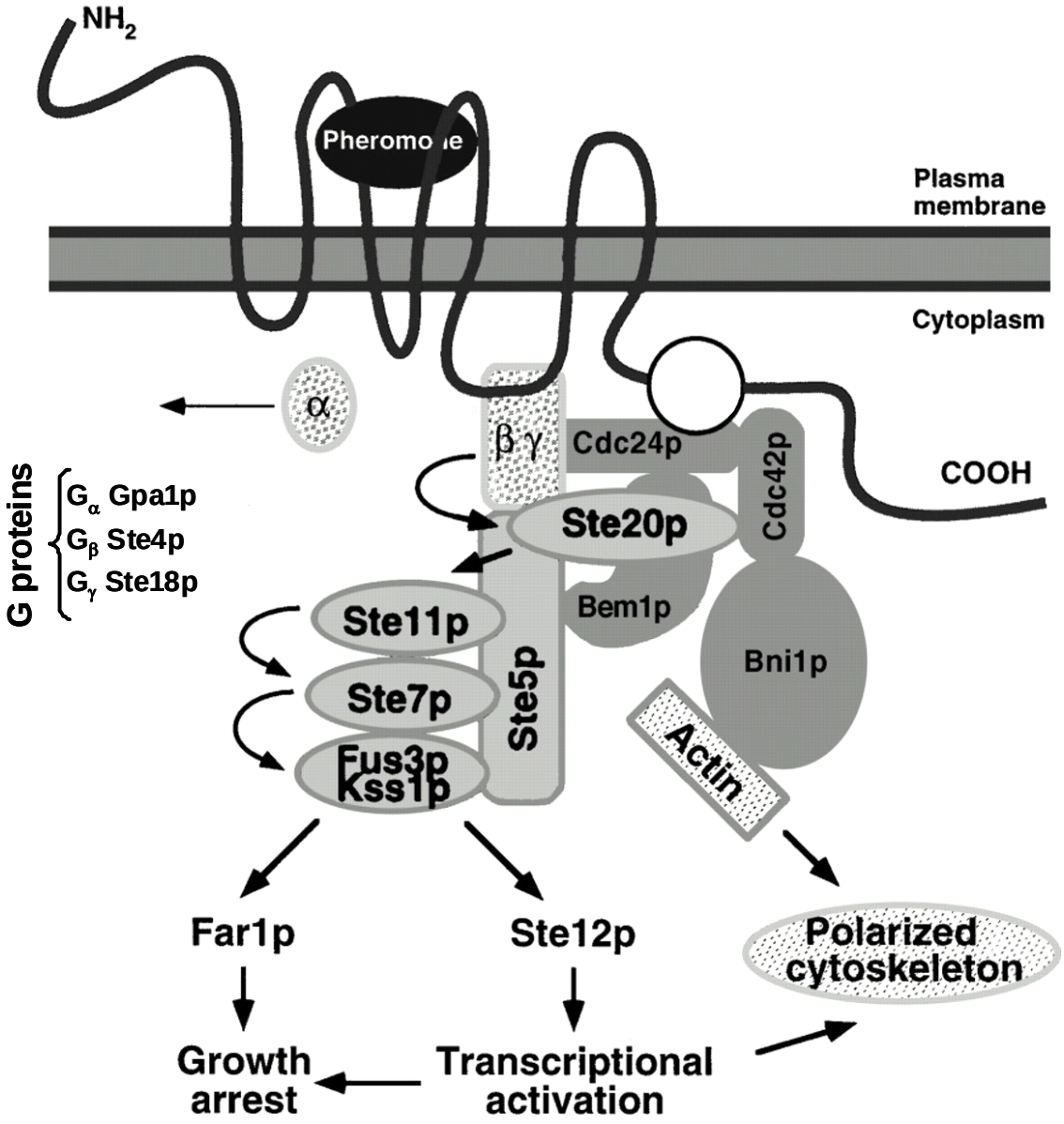
NH2
Pheromone
Plasma membrane
Cytoplasm
α
βγ
Cdc24p
Cdc42p
COOH
Ste20p
G proteins
Gα Gpa1p
Gβ Ste4p
Gγ Ste18p
Ste11p
Bem1p
Bni1p
Ste7p
Ste5p
Fus3p
Kss1p
Actin
Far1p
Ste12p
Polarized cytoskeleton
Growth arrest
Transcriptional activation
e.g. Fus1

(i.e. subunits of the G protein and/or MAPK). One of the well characterized regulators is Sst2p, a yeast homologue of regulators of G protein signaling (RGS). RGS proteins are important negative regulators of GPCR signaling. They function as GTPase-accelerating proteins (GAPs) to inactivate Gα by increasing the hydrolysis rate of GTP bound Gα. After GTP hydrolysis, the Gα subunit returns to its GDP-bound, then sequesters the Gβγ complex into a heterotrimer, which lead to down regulation of G protein signaling. So far, 37 genes have been identified that encode proteins containing an RGS or RGS-like domain within the human genome [118]. Sst2p is the first RGS protein identified in *S. cerevisiae.* Recently it was found that Sst2p can directly bind to the C-terminal tail of Ste2p via its DEP domain. In addition, binding to the receptor places Sst2p in close proximity to Gpa1p, its substrate, implicating that regulation is both rapid and specific [119].

Additionally, the phosphatases Msg5p and Mpt5p have been reported that have a role in adaptive mechanism at higher concentrations of pheromone [120]. Expression of some proteases like Bar1p (Sst1p), which specifically cleaves α-factor pheromone, adds to the complexity of the regulation of mating [121].

Structure-function analysis of α-factor pheromone

The α-factor is a tridecapeptide secreted by MATα cells and has the sequence WHWLQLKPGQPMY. Extensive analyses of α -factor analogs in combination with receptor mutagenesis have provided insights into the structural basis of α-factor activity [122-125]. Briefly, the results of these studies indicated that residues near the amine

terminus play an important role in receptor activation, the carboxyl terminus of the peptide contributes mostly to the binding affinity and the central residues of the peptide forms a β-turn around the Pro^8-Gly^9 bond aiding the orientation of the signaling and the binding domains of the pheromone (Fig. 6) [126-128]. A major experiment of this model of α-factor activity was the systematic Ala substitute creating α-factor analogs have been used to study the structure-function of the α-factor pheromone [129]. Several of the *D*-Ala series analogs, near the N-terminus, specifically [*D*-Ala^2] α-factor, [*D*-Ala^3] α-factor and [*D*-Ala^4] α-factor had no measurable biological activity [129]. However, these peptides bound relatively strongly to Ste2p and antagonized the biological activity of wild type ligand. These results were consistent with previous studies showing that antagonists discovered involved changes in residues near the amine terminus indicating that residues near this region are important for signaling. In contrast, the residues at the carboxyl terminus of α-factor strongly affected to binding to Ste2p. Mutation of these residues by either *L*- or *D*-Ala decreased affinity up to 3000-fold [129]. Removal of the carboxyl terminal residues resulted in pheromones with significantly decreased receptor affinity. Similar observations, separation of functional domains for binding and activity have been reported for other peptide receptors [130-133].

The Pro-Gly sequence is located at the central region of α-factor, which has a high probability of β-turns [134, 135]. It was suggested that a turn at this position was involved in biological activity of the pheromone [136] and this region of the peptide may create of the proper overall conformation for the pheromone [129]. Considering the multi-state conformation of receptor, the separation of a binding domain and an activation domain of α -factor suggests that there is a sequential binding of the

pheromone to its receptor. The binding domain of α -factor may interact with the receptor first, then binding of the remaining domains may occur in a sequential manner. Consistent with this hypothesis, it was demonstrated that the fluorescent alpha-factor analogue [K(7)(NBD), Nle(12)] bound to receptor via a two-step process involving an initial interaction that places the fluorophore in a hydrophobic environment, followed by a conversion to a state in which the fluorophore moves to a more polar environment [137].

One of the major goals of studies on GPCRs is understanding how ligands bind to their receptor and how this information is transferred to activation of intracellular pathway. Since yeast pheromones can be designed with chemically or photochemically active groups that promote crosslinking to the receptor, the yeast α -factor pheromone receptor was extensively used to study ligand binding. For example, a series of α-factor analogs containing *p*-benzoyl-L-phenylalanine (Bpa), a photoactivatable group, were synthesized [138]. Chemical and enzymatic fragmentation of the receptor/radio probe complex ([Bpa1, Tyr3(125I), Arg7, Phe13]α-factor-crosslinked-Ste2p) indicated that cross-linking occurred on a portion of Ste2p spanning residues 251-294 which covers a portion of TM6, the extracellular loop between TM6 and TM7, and a portion of TM7 [138]. This was the first determination of a specific contact region between a Class D GPCR and its ligand. Later, analogues of α-factor containing Bpa and biotin as a tag, were synthesized to identify the pheromone binding site to receptor [139]. The study using Bpa(1), Bpa(3), and Bpa(13) ligand suggested that the N-terminus of the pheromone interacts with a binding domain consisting of residues from the extracellular ends of TM5-TM7 and portions of EL2 and EL3 close to these TMs. It was also shown that there is a direct interaction between the position 13 side chain and a region of Ste2p

(F55-R58) at the extracellular end of TM1 in the same study [139]. In addition to the mutagenesis studies, chimeric receptors between *S. cerevisiae* and *S. kluyveri* α-factor receptors also supplied important information to understand the ligand receptor interaction(s). A substitution at residues 47-49 of the the respective GPCRs affected specificity for the respective pheromone binding but not for activation. In contrast, substitution of residues 267-269 affected pheromone specificity for activation, but not for pheromone binding. Finally substitution of residues 104-123 modestly affected both types of specificity [140, 141]. Later, it was revealed that the side chain of the tenth residue of α-factor is in close proximity with the side chains of residues 47 and/or 48 of Ste2p when the pheromone is bound to the receptor [142]. Also, our group suggested that portions of TM1 and TM6 were important for ligand interaction by using site-directed mutagenesis of Ste2p and binding assays with different α -factor analogs [143]

Taking together, a model for α-factor bound to Ste2p was proposed (Fig. 7). The model places α-factor bent around the Pro-Gly center of the peptide with the Lys side chain facing away from the transmembrane domains and interacting with a binding pocket formed by the extracellular loops. The side chain of Gln10 is proximal to residues 47 and 48 near the extracellular side of TM1, whereas the Trp1 side chain is near a pocket formed by TM6-E3-TM7. Recently it was reported the Tyr13 side chain interacts with Cys59 of Ste2p at the extracellular end of TM1 [144].

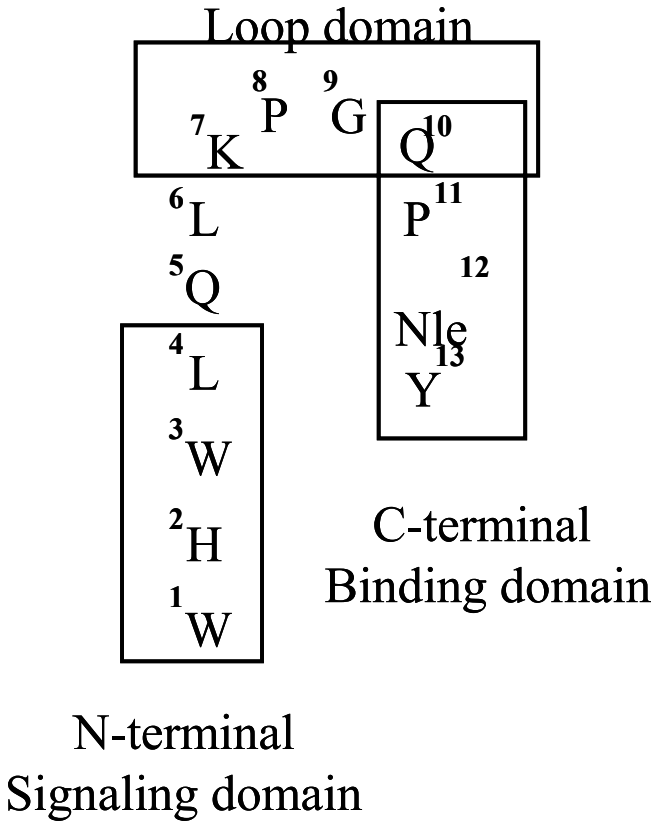

Figure 6 Functional domains of α-factor ligand

Studies of α-factor analogs have revealed two regions according to their major contributions to activity and binding affinity. The residues at the N-terminus appeared to mainly function in activation of the receptor signaling, the residues at the C-terminus strongly contribute to the binding affinity. However the two functions cannot be completely separated. The loop domain corresponds to residues of the peptide which are thought to induce a bend in the ligand structure. (Adapted from Abel *et al* [129])

Figure 7 Working model for fitting of the α-factor pheromone into a ligand binding site on its GPCR Ste2p

This schematic shows a counterclockwise orientation of TMs of the Ste2p. Two amino acid residues (Ser 47 and Thr 48), were proposed that there are in the proximity to Gln10 of bound α-factor. The Tyr13 side chain of bound α-factor interacts with Cys 59 of Ste2p at the extracellular end of TM1. The side chains of Trp1 and Trp3 bound α-factor interact with the extracellular ends of TM5-TM7. The α-factor and the receptor extracellular loops are represented by the gray curve and dotted lines, respectively. Contact residues are denoted with stars with the residue number of the pheromone (Adapted from Son *et al* [139]).

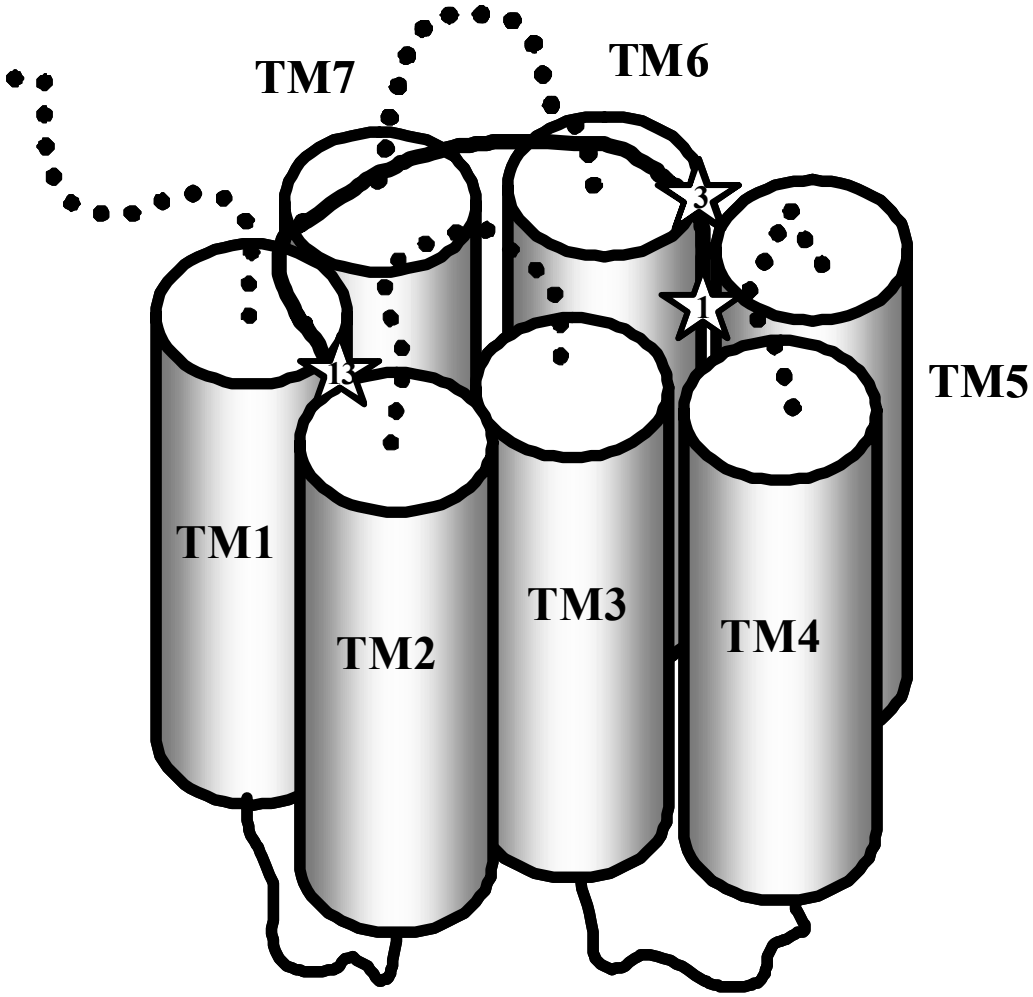
TM7
TM6
3
1
13
TM5
TM1
TM2
TM3
TM4

CHAPTER 3 Oligomerization of GPCR

An overview

Protein-protein interactions are essential to the organizational structure and function of cell signaling networks. Recently, a vast range of studies have been documented that various classes of GPCRs form dimers and/or even higher order homo-oligomers [145-148]. Dimerization is thought to be important for various aspects of GPCR function such as receptor biogenesis, formation of ligand-binding sites, signal transduction, and down-regulation (Table 4). For example, the studies of DOP receptor dimerization by Cvejic and Devi (1997) [149] provided evidence that the addition of certain agonists would inhibit or reverse receptor dimerization. They concluded that the DOP receptor was likely internalized from the cell surface as a monomer in response to agonist challenge. It was reported that inhibition of dimer in β_2-adrenoceptor by addition of a synthetic peptide corresponding to TM6 of the receptor limit agonist activation of adenylyl cyclase [150]. Thus, the study of dimerization has significance since abnormalities of dimer formation may alter the function of the receptors which results in serious disease. Indeed, many cases of dimerization is considered as a new drug targets [6].

However, specifically for G protein activation and signaling, it is not resolved whether a single GPCR molecule is sufficient or a dimer is necessary. Chabre and Maire argued that all GPCRs appear to act as monomer based on a re-assesssment of previous studies [151] while Park et al questioned the role and the existence of monomers in nature [152]. It was reported that the monomeric NTS1 receptor activates G_q more

Table 4 Proposed roles of GPCR dimerization/oligomerization

Role of dimerisation/oligomerisation	Receptor(s)
Protein folding	β_2-adrenoceptor
	CXCR1[1]
	α_2-adrenoceptors
	TSH[2] receptor
	Frizzled 4 receptor
	Calcium sensing receptor
	Melacortin-1 receptor
Efficient signal transduction	Rhodopsin
	BLT1[3] leukotriene B4 receptor

[1]CXCR, chemokine receptor; [2]TSH, thyrotropin receptor; [3]BLT2, leukotriene receptor; (Modified from Milligan [147])

efficiently than the receptor dimer in solubilized preparations [153] and monomeric rhodopsin activates transducin as fast as the rate of protein diffusion allows in detergent solution [22]. Also, rhodopsin monomers were found to activate transducin with the same efficiency as two rhodopsins in the same particle where receptors were reconstituted into lipid bilayer [154]. In contrast, it was reported that the higher-order rhodopsin oligomers are the most active species for transducin activation by using functional analyses of fractions from solubilized disk membranes [155].

Various transmembrane domains have been implicated to participate in receptor oligomerization in different receptor systems (Table 5) suggesting that the structure of oligomers formed in different GPCRs may not be the same [147]. Even within the same receptor, homo-dimer formed by different monomer-monomer interaction from inactive state to activate state [156]. The studies on class C receptors provide valuable information that the N-terminal region may also participate into oligomerization as well as transmembrane domains. The N-terminal Venus flytrap (VFT) module is one of main characteristic for class C receptors, which is structurally and functionally homologous to bacterial periplasmic proteins that bind amino acids, sugars and ions [157]. It was reported that VFTs are important for dimerization of this receptor class [158, 159, and 160]. Additionally, it is known that cysteine-rich domains (CRDs), localized between VFT and transmembrane domains, also have dimerization potential. It was demonstrated that VFT–CRD modules form disulfide-linked dimers even when expressed without the rest of the receptor from the $mGlu_1$, $mGlu_4$ and calcium-sensing (CaS) receptors [161-163].

Table 5 Structural domains reported to be involved in GPCR dimerization/oligomerization

Receptor	Implicated domains
Rhodopsin	TM[1] 4, 5
Dopamine D2	TM 4
α_{1b}-adrenoceptor	TM 1, 4, 5, 6
Complement C5a	TM 1, 2, 4
Adenosine A2a	TM 5
β_2-adrenoceptor	TM 6

[1]TM = transmembrane domain (Modified from Milligan [147])

To directly examine the physical interaction between two GPCRs, differential epitope tagging and selective immunoprecipitation have been valuable tools. Cysteine cross linking has also used to detect dimers/oligomers. In addition, a variety of reagents to cross-link two molecules have been employed [164, 165]. In order to address whether GPCR dimers exist in living cells, biophysical techniques such as bioluminescence resonance energy transfer, fluorescence resonance energy transfer have been employed to visualize dimers/oligomers. In the part III of this dissertation, the cysteine cross-linking method will be discussed in detail.

Dimer-/Oligomerization of Ste2p

Ste2p also can form a dimer. Two independent studies demonstrated that co-expression of an endocytosis-defective mutant with the wild-type receptor leads to efficient internalization of the mutant receptor, suggesting that these receptors are internalized as dimers [166, 167]. Overton and Blumer used fluorescence resonance energy transfer (FRET) between differentially tagged receptors in whole cells as an indicator for dimerization. They showed that tagged receptors lacking an endocytosis signal were able to undergo endocytosis when co-expressed with wild-type receptor. They also found the efficiencies of FRET were indistinguishable with agonist and antagonist by dose-response and time-course experiments, thus Ste2p appeared to be dimeric in the absence or presence of agonist. Using either whole cell or membrane preparation yielded a similar FRET ratio [166, 167]. The study by Yesilaltay *et al* also indicated that dimerized receptor complexes were subject to endocytosis and unoccupied

receptors could also be internalized. In addition, they found that intermolecular disulfide bonds between two intrinsic cysteines in Ste2p (C59 and C252) were unnecessary for dimer formation [166, 167].

Overton and Blumer also used FRET to identify domains of Ste2p that mediated dimerization and found TM1 was important for dimer formation. Various combinations of receptor TM fragments were expressed with YFP or CFP taggs and FRET ratios were measured. The major conclusion of the study was that TM1 has a significant role in dimerization and is possibly involved help from the N-terminal extracellular domain and TM2 to stabilize the dimer formation [168]. In a later study, it was also reported the GXXXG motif in TM1 was involved in dimerization. Mutation of this motif of Ste2p did not affect ligand binding but decreased cell signaling, indicating that dimerization is not involved in ligand binding but is important for signal transduction [169].

It was also suggested that the dimer of Ste2p functioned in a concerted fashion. Two different mutants, which were defective in promoting G protein activation were co-expressed and the ability to form a dimer *in vivo* and to correct their signaling were measured, resulting in increasing signaling significantly [170]. Analysis of dominant-negative mutants of the receptor also suggests that dimerization may be important for signal transduction. A dimer receptor formed between WT Ste2p and its dominant negative mutant (Ste2p-Y266C) failed to signal, further supporting the idea that one role for dimerization of Ste2p is efficient signaling [171].

Recently, receptors in other yeast species were found to have dimer forms that may mediate important physiological functions of GPCRs in fungi. For example, the *S. pombe* pheromone receptor Mam2 was found to form dimers during a study of a

constitutively active mutant [172]. In *C. neoformans*, domains of Gpr4 were shown to interact with another Gpr4 in a yeast two hybrid system [173]. These studies suggest that dimerization is a common phenomenon in fungi similar to GPCRs in other systems. In the part III of this dissertation, identification of dimer interfaces of Ste2p will be discussed in detail.

List of References for Part I

1. Pierce, K.L., R.T. Premont, and R.J. Lefkowitz, *Seven-transmembrane receptors.* Nat Rev Mol Cell Biol, 2002. **3**(9): p. 639-50.
2. Fredriksson, R., et al., *The G-protein-coupled receptors in the human genome form five main families. Phylogenetic analysis, paralogon groups, and fingerprints.* Mol Pharmacol, 2003. **63**(6): p. 1256-72.
3. Klabunde, T. and G. Hessler, *Drug design strategies for targeting G-protein-coupled receptors.* Chembiochem, 2002. **3**(10): p. 928-44.
4. Flower, D.R., *Modelling G-protein-coupled receptors for drug design.* Biochim Biophys Acta, 1999. **1422**(3): p. 207-34.
5. Horn, F., et al., *GPCRDB information system for G protein-coupled receptors.* Nucleic Acids Res, 2003. **31**(1): p. 294-7.
6. Jacoby, E., et al., *The 7 TM G-protein-coupled receptor target family.* ChemMedChem, 2006. **1**(8): p. 761-82.
7. Hamm, H.E., *The many faces of G protein signaling.* J Biol Chem, 1998. **273**(2): p. 669-72.
8. Karnik, S.S., et al., *Activation of G-protein-coupled receptors: a common molecular mechanism.* Trends Endocrinol Metab, 2003. **14**(9): p. 431-7.
9. George, S.R., B.F. O'Dowd, and S.P. Lee, *G-protein-coupled receptor oligomerization and its potential for drug discovery.* Nat Rev Drug Discov, 2002. **1**(10): p. 808-20.

10. Venter, J.C., et al., *The sequence of the human genome.* Science, 2001. **291**(5507): p. 1304-51.

11. Wise, A., K. Gearing, and S. Rees, *Target validation of G-protein coupled receptors.* Drug Discov Today, 2002. **7**(4): p. 235-46.

12. Hopkins, A.L. and C.R. Groom, *The druggable genome.* Nat Rev Drug Discov, 2002. **1**(9): p. 727-30.

13. Strader, C.D., et al., *Structure and function of G protein-coupled receptors.* Annu Rev Biochem, 1994. **63**: p. 101-32.

14. Kolakowski, L.F., Jr., *GCRDb: a G-protein-coupled receptor database.* Receptors Channels, 1994. **2**(1): p. 1-7.

15. Ulrich, C.D., 2nd, M. Holtmann, and L.J. Miller, *Secretin and vasoactive intestinal peptide receptors: members of a unique family of G protein-coupled receptors.* Gastroenterology, 1998. **114**(2): p. 382-97.

16. Hoon, M.A., et al., *Putative mammalian taste receptors: a class of taste-specific GPCRs with distinct topographic selectivity.* Cell, 1999. **96**(4): p. 541-51.

17. Conn, P.J. and J.P. Pin, *Pharmacology and functions of metabotropic glutamate receptors.* Annu Rev Pharmacol Toxicol, 1997. **37**: p. 205-37.

18. O'Hara, P.J., et al., *The ligand-binding domain in metabotropic glutamate receptors is related to bacterial periplasmic binding proteins.* Neuron, 1993. **11**(1): p. 41-52.

19. Arshava, B., et al., *High resolution NMR analysis of the seven transmembrane domains of a heptahelical receptor in organic-aqueous medium.* Biopolymers, 2002. **64**(3): p. 161-76.

20. Okada, T., et al., *Activation of rhodopsin: new insights from structural and biochemical studies.* Trends Biochem Sci, 2001. **26**(5): p. 318-24.

21. Filipek, S., et al., *The crystallographic model of rhodopsin and its use in studies of other G protein-coupled receptors.* Annu Rev Biophys Biomol Struct, 2003. **32**: p. 375-97.

22. Ernst, O.P., et al., *Mutation of the fourth cytoplasmic loop of rhodopsin affects binding of transducin and peptides derived from the carboxyl-terminal sequences of transducin alpha and gamma subunits.* J Biol Chem, 2000. **275**(3): p. 1937-43.

23. Cherezov, V., et al., *High-resolution crystal structure of an engineered human beta2-adrenergic G protein-coupled receptor.* Science, 2007. **318**(5854): p. 1258-65.

24. Rasmussen, S.G., et al., *Crystal structure of the human beta2 adrenergic G-protein-coupled receptor.* Nature, 2007. **450**(7168): p. 383-7.

25. Rosenbaum, D.M., et al., *GPCR engineering yields high-resolution structural insights into beta2-adrenergic receptor function.* Science, 2007. **318**(5854): p. 1266-73.

26. Hanson, M.A., et al., *A specific cholesterol binding site is established by the 2.8 A structure of the human beta2-adrenergic receptor.* Structure, 2008. **16**(6): p. 897-905.

27. Roth, C.B., M.A. Hanson, and R.C. Stevens, *Stabilization of the human beta2-adrenergic receptor TM4-TM3-TM5 helix interface by mutagenesis of Glu122(3.41), a critical residue in GPCR structure.* J Mol Biol, 2008. **376**(5): p. 1305-19.

28. Warne, T., et al., *Structure of a beta1-adrenergic G-protein-coupled receptor.* Nature, 2008. **454**(7203): p. 486-91.

29. Jaakola, V.P., et al., *The 2.6 angstrom crystal structure of a human A2A adenosine receptor bound to an antagonist.* Science, 2008. **322**(5905): p. 1211-7.

30. Park, J.H., et al., *Crystal structure of the ligand-free G-protein-coupled receptor opsin.* Nature, 2008. **454**(7201): p. 183-7.

31. Scheerer, P., et al., *Crystal structure of opsin in its G-protein-interacting conformation.* Nature, 2008. **455**(7212): p. 497-502.

32. Schwartz, T.W. and W.L. Hubbell, *Structural biology: A moving story of receptors.* Nature, 2008. **455**(7212): p. 473-4.

33. Hanson, M.A. and R.C. Stevens, *Discovery of new GPCR biology: one receptor structure at a time.* Structure, 2009. **17**(1): p. 8-14.

34. Nygaard, R., et al., *Ligand binding and micro-switches in 7TM receptor structures.* Trends Pharmacol Sci, 2009.

35. Kobilka, B., *Adrenergic receptors as models for G protein-coupled receptors.* Annu Rev Neurosci, 1992. **15**: p. 87-114.

36. Strader, C.D., et al., *The family of G-protein-coupled receptors.* Faseb J, 1995. **9**(9): p. 745-54.

37. Ji, T.H., M. Grossmann, and I. Ji, *G protein-coupled receptors. I. Diversity of receptor-ligand interactions.* J Biol Chem, 1998. **273**(28): p. 17299-302.

38. Bondensgaard, K., et al., *Recognition of privileged structures by G-protein coupled receptors.* J Med Chem, 2004. **47**(4): p. 888-99.

39. Hunyady, L., G. Vauquelin, and P. Vanderheyden, *Agonist induction and conformational selection during activation of a G-protein-coupled receptor.* Trends Pharmacol Sci, 2003. **24**(2): p. 81-6.

40. Rihakova, L., et al., *Methionine proximity assay, a novel method for exploring peptide ligand-receptor interaction.* J Recept Signal Transduct Res, 2002. **22**(1-4): p. 297-313.

41. Chorev, M., *Parathyroid hormone 1 receptor: insights into structure and function.* Receptors Channels, 2002. **8**(3-4): p. 219-42.

42. Tsomaia, N., et al., *Cooperative interaction of arginine-19 and the N-terminal signaling domain in the affinity and potency of parathyroid hormone.* Biochemistry, 2004. **43**(12): p. 3459-70.

43. Dong, M., et al., *Spatial approximation between the amino terminus of a peptide agonist and the top of the sixth transmembrane segment of the secretin receptor.* J Biol Chem, 2004. **279**(4): p. 2894-903.

44. Bellucci, F., et al., *A different molecular interaction of bradykinin and the synthetic agonist FR190997 with the human B2 receptor: evidence from mutational analysis.* Br J Pharmacol, 2003. **140**(3): p. 500-6.

45. Schroeder, C., et al., *Changes in amino-terminal portion of human B2 receptor selectively increase efficacy of synthetic ligand HOE 140 but not of cognate ligand bradykinin.* Am J Physiol Heart Circ Physiol, 2003. **284**(6): p. H1924-32.

46. Millar, R.P., et al., *Gonadotropin-releasing hormone receptors.* Endocr Rev, 2004. **25**(2): p. 235-75.

47. Janecka, A., J. Fichna, and T. Janecki, *Opioid receptors and their ligands.* Curr Top Med Chem, 2004. **4**(1): p. 1-17.

48. Judd, A.K., et al., *N-terminal modifications leading to peptide ORL1 partial agonists and antagonists.* J Pept Res, 2003. **62**(5): p. 191-8.

49. Sachon, E., et al., *Met174 side chain is the site of photoinsertion of a substance P competitive peptide antagonist photoreactive in position 8.* FEBS Lett, 2003. **544**(1-3): p. 45-9.

50. Ulfers, A.L., A. Piserchio, and D.F. Mierke, *Extracellular domains of the neurokinin-1 receptor: structural characterization and interactions with substance P.* Biopolymers, 2002. **66**(5): p. 339-49.

51. Breton, C., et al., *Direct identification of human oxytocin receptor-binding domains using a photoactivatable cyclic peptide antagonist: comparison with the human V1a vasopressin receptor.* J Biol Chem, 2001. **276**(29): p. 26931-41.

52. Wesley, V.J., et al., *Agonist-specific, high-affinity binding epitopes are contributed by an arginine in the N-terminus of the human oxytocin receptor.* Biochemistry, 2002. **41**(16): p. 5086-92.

53. Politowska, E., et al., *Docking ligands to vasopressin and oxytocin receptors via genetic algorithm.* J Recept Signal Transduct Res, 2002. **22**(1-4): p. 393-409.

54. Smith, C.J., et al., *Radiochemical investigations of [188Re(H2O)(CO)3-diaminopropionic acid-SSS-bombesin(7-14)NH2]: syntheses, radiolabeling and in vitro/in vivo GRP receptor targeting studies.* Anticancer Res, 2003. **23**(1A): p. 63-70.

55. Silvente-Poirot, S., C. Escrieut, and S.A. Wank, *Role of the extracellular domains of the cholecystokinin receptor in agonist binding.* Mol Pharmacol, 1998. **54**(2): p. 364-71.

56. Barroso, S., et al., *Identification of residues involved in neurotensin binding and modeling of the agonist binding site in neurotensin receptor 1.* J Biol Chem, 2000. **275**(1): p. 328-36.

57. Mills, J.S., et al., *Identification of a ligand binding site in the human neutrophil formyl peptide receptor using a site-specific fluorescent photoaffinity label and mass spectrometry.* J Biol Chem, 1998. **273**(17): p. 10428-35.

58. Fathy, D.B., et al., *A single position in the third transmembrane domains of the human B1 and B2 bradykinin receptors is adjacent to and discriminates between the C-terminal residues of subtype-selective ligands.* J Biol Chem, 1998. **273**(20): p. 12210-8.

59. Fanelli, F., et al., *Activation mechanism of human oxytocin receptor: a combined study of experimental and computer-simulated mutagenesis.* Mol Pharmacol, 1999. **56**(1): p. 214-25.

60. Flanagan, C.A., et al., *Multiple interactions of the Asp(2.61(98)) side chain of the gonadotropin-releasing hormone receptor contribute differentially to ligand interaction.* Biochemistry, 2000. **39**(28): p. 8133-41.

61. Kenakin, T., *Drug efficacy at G protein-coupled receptors.* Annu Rev Pharmacol Toxicol, 2002. **42**: p. 349-79.

62. Kenakin, T., *New concepts in drug discovery: collateral efficacy and permissive antagonism.* Nat Rev Drug Discov, 2005. **4**(11): p. 919-27.

63. Kobilka, B., *Agonist binding: a multistep process.* Mol Pharmacol, 2004. **65**(5): p. 1060-2.

64. Berg, K.A., et al., *Effector pathway-dependent relative efficacy at serotonin type 2A and 2C receptors: evidence for agonist-directed trafficking of receptor stimulus.* Mol Pharmacol, 1998. **54**(1): p. 94-104.

65. Vilardaga, J.P., et al., *Molecular basis of inverse agonism in a G protein-coupled receptor.* Nat Chem Biol, 2005. **1**(1): p. 25-8.

66. Wei, H., et al., *Independent beta-arrestin 2 and G protein-mediated pathways for angiotensin II activation of extracellular signal-regulated kinases 1 and 2.* Proc Natl Acad Sci U S A, 2003. **100**(19): p. 10782-7.

67. Lu, Z.L., et al., *Structural determinants for ligand-receptor conformational selection in a peptide G protein-coupled receptor.* J Biol Chem, 2007. **282**(24): p. 17921-9.

68. Keith, D.E., et al., *mu-Opioid receptor internalization: opiate drugs have differential effects on a conserved endocytic mechanism in vitro and in the mammalian brain.* Mol Pharmacol, 1998. **53**(3): p. 377-84.

69. Perez, D.M. and S.S. Karnik, *Multiple signaling states of G-protein-coupled receptors.* Pharmacol Rev, 2005. **57**(2): p. 147-61.

70. Urban, J.D., et al., *Functional selectivity and classical concepts of quantitative pharmacology.* J Pharmacol Exp Ther, 2007. **320**(1): p. 1-13.

71. Kobilka, B.K., et al., *Chimeric alpha 2-,beta 2-adrenergic receptors: delineation of domains involved in effector coupling and ligand binding specificity.* Science, 1988. **240**(4857): p. 1310-6.

72. Schoneberg, T., J. Liu, and J. Wess, *Plasma membrane localization and functional rescue of truncated forms of a G protein-coupled receptor.* J Biol Chem, 1995. **270**(30): p. 18000-6.

73. Filipek, S., et al., *G protein-coupled receptor rhodopsin: a prospectus.* Annu Rev Physiol, 2003. **65**: p. 851-79.

74. Hargrave, P.A., H.E. Hamm, and K.P. Hofmann, *Interaction of rhodopsin with the G-protein, transducin.* Bioessays, 1993. **15**(1): p. 43-50.

75. Khorana, H.G., *Rhodopsin, photoreceptor of the rod cell. An emerging pattern for structure and function.* J Biol Chem, 1992. **267**(1): p. 1-4.

76. Rao, V.R., G.B. Cohen, and D.D. Oprian, *Rhodopsin mutation G90D and a molecular mechanism for congenital night blindness.* Nature, 1994. **367**(6464): p. 639-42.

77. Yao, X., et al., *Coupling ligand structure to specific conformational switches in the beta2-adrenoceptor.* Nat Chem Biol, 2006. **2**(8): p. 417-22.

78. Kobilka, B.K. and X. Deupi, *Conformational complexity of G-protein-coupled receptors.* Trends Pharmacol Sci, 2007. **28**(8): p. 397-406.

79. Hubbell, W.L., et al., *Rhodopsin structure, dynamics, and activation: a perspective from crystallography, site-directed spin labeling, sulfhydryl reactivity, and disulfide cross-linking.* Adv Protein Chem, 2003. **63**: p. 243-90.

80. Gether, U., et al., *Structural instability of a constitutively active G protein-coupled receptor. Agonist-independent activation due to conformational flexibility.* J Biol Chem, 1997. **272**(5): p. 2587-90.

81. Gether, U., S. Lin, and B.K. Kobilka, *Fluorescent labeling of purified beta 2 adrenergic receptor. Evidence for ligand-specific conformational changes.* J Biol Chem, 1995. **270**(47): p. 28268-75.

82. Balmforth, A.J., et al., *The conformational change responsible for AT1 receptor activation is dependent upon two juxtaposed asparagine residues on transmembrane helices III and VII.* J Biol Chem, 1997. **272**(7): p. 4245-51.

83. Noda, K., et al., *The active state of the AT1 angiotensin receptor is generated by angiotensin II induction.* Biochemistry, 1996. **35**(51): p. 16435-42.

84. Groblewski, T., et al., *Mutation of Asn111 in the third transmembrane domain of the AT1A angiotensin II receptor induces its constitutive activation.* J Biol Chem, 1997. **272**(3): p. 1822-6.

85. Ward, S.D., et al., *Use of an in situ disulfide cross-linking strategy to study the dynamic properties of the cytoplasmic end of transmembrane domain VI of the M3 muscarinic acetylcholine receptor.* Biochemistry, 2006. **45**(3): p. 676-85.

86. Han, S.J., et al., *Identification of an agonist-induced conformational change occurring adjacent to the ligand-binding pocket of the M(3) muscarinic acetylcholine receptor.* J Biol Chem, 2005. **280**(41): p. 34849-58.

87. Han, S.J., et al., *Pronounced conformational changes following agonist activation of the M(3) muscarinic acetylcholine receptor.* J Biol Chem, 2005. **280**(26): p. 24870-9.

88. Cai, K., et al., *Structure and function in rhodopsin: topology of the C-terminal polypeptide chain in relation to the cytoplasmic loops.* Proc Natl Acad Sci U S A, 1997. **94**(26): p. 14267-72.

89. Struthers, M., et al., *Tertiary interactions between the fifth and sixth transmembrane segments of rhodopsin.* Biochemistry, 1999. **38**(20): p. 6597-603.

90. Yang, K., et al., *Structure and function in rhodopsin. Cysteines 65 and 316 are in proximity in a rhodopsin mutant as indicated by disulfide formation and interactions between attached spin labels.* Biochemistry, 1996. **35**(45): p. 14040-6.

91. Yu, H., et al., *A general method for mapping tertiary contacts between amino acid residues in membrane-embedded proteins.* Biochemistry, 1995. **34**(46): p. 14963-9.

92. Yu, H., M. Kono, and D.D. Oprian, *State-dependent disulfide cross-linking in rhodopsin.* Biochemistry, 1999. **38**(37): p. 12028-32.

93. Dube, P., A. DeCostanzo, and J.B. Konopka, *Interaction between transmembrane domains five and six of the alpha -factor receptor.* J Biol Chem, 2000. **275**(34): p. 26492-9.

94. Elling, C.E., S.M. Nielsen, and T.W. Schwartz, *Conversion of antagonist-binding site to metal-ion site in the tachykinin NK-1 receptor.* Nature, 1995. **374**(6517): p. 74-7.

95. Xue, C., Y.P. Hsueh, and J. Heitman, *Magnificent seven: roles of G protein-coupled receptors in extracellular sensing in fungi.* FEMS Microbiol Rev, 2008. **32**(6): p. 1010-32.

96. Seo, J.A., K.H. Han, and J.H. Yu, *The gprA and gprB genes encode putative G protein-coupled receptors required for self-fertilization in Aspergillus nidulans.* Mol Microbiol, 2004. **53**(6): p. 1611-23.

97. Srikantha, T., S.A. Lachke, and D.R. Soll, *Three mating type-like loci in Candida glabrata.* Eukaryot Cell, 2003. **2**(2): p. 328-40.

98. Paoletti, M., et al., *Evidence for sexuality in the opportunistic fungal pathogen Aspergillus fumigatus.* Curr Biol, 2005. **15**(13): p. 1242-8.

99. Muller, H., et al., *The asexual yeast Candida glabrata maintains distinct a and alpha haploid mating types.* Eukaryot Cell, 2008. **7**(5): p. 848-58.

100. Dohlman, H.G., et al., *Model systems for the study of seven-transmembrane-segment receptors.* Annu Rev Biochem, 1991. **60**: p. 653-88.

101. Lorenz, M.C., N.S. Cutler, and J. Heitman, *Characterization of alcohol-induced filamentous growth in Saccharomyces cerevisiae.* Mol Biol Cell, 2000. **11**(1): p. 183-99.

102. Lorenz, M.C., et al., *The G protein-coupled receptor gpr1 is a nutrient sensor that regulates pseudohyphal differentiation in Saccharomyces cerevisiae.* Genetics, 2000. **154**(2): p. 609-22.

103. Sprague, G.F., Jr., R. Jensen, and I. Herskowitz, *Control of yeast cell type by the mating type locus: positive regulation of the alpha-specific STE3 gene by the MAT alpha 1 product.* Cell, 1983. **32**(2): p. 409-15.

104. Thorner J., *Pheromonal regulation of development in Saccharomyces cerevisiae*, in *Molecular biology of the yeast Saccharomyces: Life cycle and inheritance*, S. J.N., Editor. 1981, Cold Spring Harbor.

105. Dohlman, H.G., *G proteins and pheromone signaling.* Annu Rev Physiol, 2002. **64**: p. 129-52.

106. Ciejek, E., J. Thorner, and M. Geier, *Solid phase peptide synthesis of alpha-factor, a yeast mating pheromone.* Biochem Biophys Res Commun, 1977. **78**(3): p. 952-61.

107. Masui, Y., et al., *Synthesis of the mating factor of Saccharomyces cerevisiae and its truncated peptides : the structure-activity relationship.* Biochem Biophys Res Commun, 1977. **78**(2): p. 534-8.

108. Anderegg, R.J., et al., *Structure of Saccharomyces cerevisiae mating hormone a-factor. Identification of S-farnesyl cysteine as a structural component.* J Biol Chem, 1988. **263**(34): p. 18236-40.

109. Marcus, S., et al., *Significance of C-terminal cysteine modifications to the biological activity of the Saccharomyces cerevisiae a-factor mating pheromone.* Mol Cell Biol, 1991. **11**(7): p. 3603-12.

110. Herskowitz, I., *MAP kinase pathways in yeast: for mating and more.* Cell, 1995. **80**(2): p. 187-97.

111. Banuett, F., *Signalling in the yeasts: an informational cascade with links to the filamentous fungi.* Microbiol Mol Biol Rev, 1998. **62**(2): p. 249-74.

112. Guo, M., et al., *The yeast G protein alpha subunit Gpa1 transmits a signal through an RNA binding effector protein Scp160.* Mol Cell, 2003. **12**(2): p. 517-24.

113. Slessareva, J.E., et al., *Activation of the phosphatidylinositol 3-kinase Vps34 by a G protein alpha subunit at the endosome.* Cell, 2006. **126**(1): p. 191-203.

114. Madden, K. and M. Snyder, *Cell polarity and morphogenesis in budding yeast.* Annu Rev Microbiol, 1998. **52**: p. 687-744.

115. Chen, Q. and J.B. Konopka, *Regulation of the G-protein-coupled alpha-factor pheromone receptor by phosphorylation.* Mol Cell Biol, 1996. **16**(1): p. 247-57.

116. Mulholland, J., et al., *Visualization of receptor-mediated endocytosis in yeast.* Mol Biol Cell, 1999. **10**(3): p. 799-817.

117. Stefan, C.J. and K.J. Blumer, *A syntaxin homolog encoded by VAM3 mediates down-regulation of a yeast G protein-coupled receptor.* J Biol Chem, 1999. **274**(3): p. 1835-41.

118. Willars, G.B., *Mammalian RGS proteins: multifunctional regulators of cellular signalling.* Semin Cell Dev Biol, 2006. **17**(3): p. 363-76.

119. Ballon, D.R., et al., *DEP-domain-mediated regulation of GPCR signaling responses.* Cell, 2006. **126**(6): p. 1079-93.

120. Zhou, J., M. Arora, and D.E. Stone, *The yeast pheromone-responsive G alpha protein stimulates recovery from chronic pheromone treatment by two mechanisms that are activated at distinct levels of stimulus.* Cell Biochem Biophys, 1999. **30**(2): p. 193-212.

121. Ballensiefen, W. and H.D. Schmitt, *Periplasmic Bar1 protease of Saccharomyces cerevisiae is active before reaching its extracellular destination.* Eur J Biochem, 1997. **247**(1): p. 142-7.

122. Eriotou-Bargiota, E., et al., *Antagonistic and synergistic peptide analogues of the tridecapeptide mating pheromone of Saccharomyces cerevisiae.* Biochemistry, 1992. **31**(2): p. 551-7.

123. Xue, C.B., et al., *Probing the functional conformation of the tridecapeptide mating pheromone of Saccharomyces cerevisiae through study of disulfide-constrained analogs.* Int J Pept Protein Res, 1996. **47**(3): p. 131-41.

124. Yang, W., et al., *Systematic analysis of the Saccharomyces cerevisiae alpha-factor containing lactam constraints of different ring size.* Biochemistry, 1995. **34**(4): p. 1308-15.

125. Liu, S., et al., *Position 13 analogs of the tridecapeptide mating pheromone from Saccharomyces cerevisiae: design of an iodinatable ligand for receptor binding.* J Pept Res, 2000. **56**(1): p. 24-34.

126. Xue, C.B., et al., *A covalently constrained congener of the Saccharomyces cerevisiae tridecapeptide mating pheromone is an agonist.* J Biol Chem, 1989. **264**(32): p. 19161-8.

127. Antohi, O., et al., *Conformational analysis of cyclic analogues of the Saccharomyces cerevisiae alpha-factor pheromone.* Biopolymers, 1998. **45**(1): p. 21-34.

128. Zhang, Y.L., et al., *Synthesis, biological activity, and conformational analysis of peptidomimetic analogues of the Saccharomyces cerevisiae alpha-factor tridecapeptide.* Biochemistry, 1998. **37**(36): p. 12465-76.

129. Abel, M.G., et al., *Structure-function analysis of the Saccharomyces cerevisiae tridecapeptide pheromone using alanine-scanned analogs.* J Pept Res, 1998. **52**(2): p. 95-106.

130. Carpenter, K.A., B.C. Wilkes, and P.W. Schiller, *The octapeptide angiotensin II adopts a well-defined structure in a phospholipid environment.* Eur J Biochem, 1998. **251**(1-2): p. 448-53.

131. Greenberg, Z., et al., *Mapping the bimolecular interface of the parathyroid hormone (PTH)-PTH1 receptor complex: spatial proximity between Lys(27) (of the hormone principal binding domain) and leu(261) (of the first extracellular loop) of the human PTH1 receptor.* Biochemistry, 2000. **39**(28): p. 8142-52.

132. Chauvin, S., et al., *Functional importance of transmembrane helix 6 Trp(279) and exoloop 3 Val(299) of rat gonadotropin-releasing hormone receptor.* Mol Pharmacol, 2000. **57**(3): p. 625-33.

133. de Gasparo, M., et al., *International union of pharmacology. XXIII. The angiotensin II receptors.* Pharmacol Rev, 2000. **52**(3): p. 415-72.

134. Venkatachalam, C.M., *Stereochemical criteria for polypeptides and proteins. V. Conformation of a system of three linked peptide units.* Biopolymers, 1968. **6**(10): p. 1425-36.

135. Chou, P.Y. and G.D. Fasman, *Prediction of beta-turns.* Biophys J, 1979. **26**(3): p. 367-73.

136. Shenbagamurthi, P., et al., *Biological activity and conformational isomerism in position 9 analogues of the des-1-tryptophan,3-beta-cyclohexylalanine-alpha-factor from Saccharomyces cerevisiae.* Biochemistry, 1985. **24**(25): p. 7070-6.

137. Bajaj, A., et al., *A fluorescent alpha-factor analogue exhibits multiple steps on binding to its G protein coupled receptor in yeast.* Biochemistry, 2004. **43**(42): p. 13564-78.

138. Henry, L.K., et al., *Identification of a contact region between the tridecapeptide alpha-factor mating pheromone of Saccharomyces cerevisiae and its G protein-coupled receptor by photoaffinity labeling.* Biochemistry, 2002. **41**(19): p. 6128-39.

139. Son, C.D., et al., *Identification of ligand binding regions of the Saccharomyces cerevisiae alpha-factor pheromone receptor by photoaffinity cross-linking.* Biochemistry, 2004. **43**(41): p. 13193-203.

140. Sen, M., A. Shah, and L. Marsh, *Two types of alpha-factor receptor determinants for pheromone specificity in the mating-incompatible yeasts S. cerevisiae and S. kluyveri.* Curr Genet, 1997. **31**(3): p. 235-40.

141. Sen, M. and L. Marsh, *Novel antagonist to agonist switch in chimeric G protein-coupled alpha-factor peptide receptors.* Biochem Biophys Res Commun, 1995. **207**(2): p. 559-64.

142. Lee, B.K., et al., *Identification of residues of the Saccharomyces cerevisiae G protein-coupled receptor contributing to alpha-factor pheromone binding.* J Biol Chem, 2001. **276**(41): p. 37950-61.

143. Abel, M.G., et al., *Mutations affecting ligand specificity of the G-protein-coupled receptor for the Saccharomyces cerevisiae tridecapeptide pheromone.* Biochim Biophys Acta, 1998. **1448**(1): p. 12-26.

144. Umanah, G.K., et al., *Cross-linking of a DOPA-containing peptide ligand into its G protein-coupled receptor.* Biochemistry, 2009. **48**(9): p. 2033-44.

145. Milligan, G., *G protein-coupled receptor dimerization: function and ligand pharmacology.* Mol Pharmacol, 2004. **66**(1): p. 1-7.

146. Milligan, G., *G-protein-coupled receptor heterodimers: pharmacology, function and relevance to drug discovery.* Drug Discov Today, 2006. **11**(11-12): p. 541-9.

147. Milligan, G., *G protein-coupled receptor dimerisation: molecular basis and relevance to function.* Biochim Biophys Acta, 2007. **1768**(4): p. 825-35.

148. Milligan, G., *G protein-coupled receptor hetero-dimerization: contribution to pharmacology and function.* Br J Pharmacol, 2009.

149. Cvejic, S. and L.A. Devi, *Dimerization of the delta opioid receptor: implication for a role in receptor internalization.* J Biol Chem, 1997. **272**(43): p. 26959-64.

150. Hebert, T.E., et al., *A peptide derived from a beta2-adrenergic receptor transmembrane domain inhibits both receptor dimerization and activation.* J Biol Chem, 1996. **271**(27): p. 16384-92.

151. Chabre, M. and M. le Maire, *Monomeric G-protein-coupled receptor as a functional unit.* Biochemistry, 2005. **44**(27): p. 9395-403.

152. Park, P.S., et al., *Oligomerization of G protein-coupled receptors: past, present, and future.* Biochemistry, 2004. **43**(50): p. 15643-56.

153. White, J.F., et al., *Dimerization of the class A G protein-coupled neurotensin receptor NTS1 alters G protein interaction.* Proc Natl Acad Sci U S A, 2007. **104**(29): p. 12199-204.

154. Bayburt, T.H., et al., *Transducin activation by nanoscale lipid bilayers containing one and two rhodopsins.* J Biol Chem, 2007. **282**(20): p. 14875-81.

155. Fotiadis, D., et al., *Structure of the rhodopsin dimer: a working model for G-protein-coupled receptors.* Curr Opin Struct Biol, 2006. **16**(2): p. 252-9.

156. Mancia, F., et al., *Ligand sensitivity in dimeric associations of the serotonin 5HT2c receptor.* EMBO Rep, 2008. **9**(4): p. 363-9.

157. Kaupmann, K., et al., *GABA(B)-receptor subtypes assemble into functional heteromeric complexes.* Nature, 1998. **396**(6712): p. 683-7.

158. Jones, K.A., et al., *GABA(B) receptors function as a heteromeric assembly of the subunits GABA(B)R1 and GABA(B)R2.* Nature, 1998. **396**(6712): p. 674-9.

159. Pin, J.P., et al., *Allosteric functioning of dimeric class C G-protein-coupled receptors.* Febs J, 2005. **272**(12): p. 2947-55.

160. Kristiansen, K., *Molecular mechanisms of ligand binding, signaling, and regulation within the superfamily of G-protein-coupled receptors: molecular modeling and mutagenesis approaches to receptor structure and function.* Pharmacol Ther, 2004. **103**(1): p. 21-80.

161. Meyer, B.H., et al., *FRET imaging reveals that functional neurokinin-1 receptors are monomeric and reside in membrane microdomains of live cells.* Proc Natl Acad Sci U S A, 2006. **103**(7): p. 2138-43.

162. Prinster, S.C., T.G. Holmqvist, and R.A. Hall, *Alpha2C-adrenergic receptors exhibit enhanced surface expression and signaling upon association with beta2-adrenergic receptors.* J Pharmacol Exp Ther, 2006. **318**(3): p. 974-81.

163. Uberti, M.A., et al., *Heterodimerization with beta2-adrenergic receptors promotes surface expression and functional activity of alpha1D-adrenergic receptors.* J Pharmacol Exp Ther, 2005. **313**(1): p. 16-23.

164. Rios, C.D., et al., *G-protein-coupled receptor dimerization: modulation of receptor function.* Pharmacol Ther, 2001. **92**(2-3): p. 71-87.

165. Breitwieser, G.E., *G protein-coupled receptor oligomerization: implications for G protein activation and cell signaling.* Circ Res, 2004. **94**(1): p. 17-27.

166. Overton, M.C. and K.J. Blumer, *G-protein-coupled receptors function as oligomers in vivo.* Curr Biol, 2000. **10**(6): p. 341-4.

167. Yesilaltay, A. and D.D. Jenness, *Homo-oligomeric complexes of the yeast alpha-factor pheromone receptor are functional units of endocytosis.* Mol Biol Cell, 2000. **11**(9): p. 2873-84.

168. Overton, M.C. and K.J. Blumer, *The extracellular N-terminal domain and transmembrane domains 1 and 2 mediate oligomerization of a yeast G protein-coupled receptor.* J Biol Chem, 2002. **277**(44): p. 41463-72.

169. Overton, M.C., S.L. Chinault, and K.J. Blumer, *Oligomerization, biogenesis, and signaling is promoted by a glycophorin A-like dimerization motif in transmembrane domain 1 of a yeast G protein-coupled receptor.* J Biol Chem, 2003. **278**(49): p. 49369-77.

170. Chinault, S.L., M.C. Overton, and K.J. Blumer, *Subunits of a yeast oligomeric G protein-coupled receptor are activated independently by agonist but function in concert to activate G protein heterotrimers.* J Biol Chem, 2004. **279**(16): p. 16091-100.

171. Gehret, A.U., et al., *Oligomerization of the yeast alpha-factor receptor: implications for dominant negative effects of mutant receptors.* J Biol Chem, 2006. **281**(30): p. 20698-714.

172. Ladds, G., et al., *A constitutively active GPCR retains its G protein specificity and the ability to form dimers.* Mol Microbiol, 2005. **55**(2): p. 482-97.

173. Xue, C., et al., *G protein-coupled receptor Gpr4 senses amino acids and activates the cAMP-PKA pathway in Cryptococcus neoformans.* Mol Biol Cell, 2006. **17**(2): p. 667-79.

PART II Study of Inter-Helical Interaction between Transmembrane domain 1 and 7 of Ste2p

CHAPTER 1 Abstract

The *S. cerevisiae* α-factor pheromone receptor, Ste2p, has been studied as a model for G protein-coupled receptor (GPCR) structure and function. Today, it is widely believed that receptors undergo conformational change(s) involving rearrangement of transmembrane domains (TMs) upon ligand binding. In this study, 36 different combinations of double Cys mutants were made by pairing six mutations on TM1 (L64 – M69) with six on TM7 (L289 – M294). Although no inter-helical interactions were found with the targeted residues under the experimental condition used, the results provided strong evidence for Ste2p homo-dimerization.

CHAPTER 2 Introduction

For about a decade from 1980 to 1990, the model for GPCR activation was proposed to be a simple bimodal conversion between inactive and active states. However, studies with various GPCRs, such as 5-HT_2-serotonin receptors [1], α_{2A}-adrenoceptors [2], AT_1 receptor [3], gonadotropin-releasing hormone receptors [4], and μ-opioid receptors [5] showed that a receptor can exist in several different conformations, suggesting a multi-state model. The multi-state model for GPCR activation proposes that the receptor alternates spontaneously between multiple active and inactive conformations [6]. Today, it is widely believed that different ligands can induce different receptor conformations [7].

Although the intracellular and extracellular loop regions play a role in receptor activation, the non-covalent interactions between TMs seem to predominate for determining the specific basal arrangement of the TM segments [8, 9, 10, 11, 12, 13] and agonist binding is thought to change the inter-helical interaction between TMs potentially leading to multiple receptor conformations. In the rhodopsin system, it was reported that TM6 undergoes large movements upon receptor activation and smaller changes were observed for TM3 [14]. Consistent with this, movements of TM3 and TM6 during agonist-induced conformational changes have been demonstrated in the β-adrenoceptor [15, 16]. The M3 muscarinic receptor is also used for studies of intramolecular interactions. It was found that the cytoplasmic end of TM6 of this receptor undergoes a rotational movement [17], and the distance between the cytoplasmic ends of TM1 and TM7 was increased during activation. In contrast the extracellular ends of TM3 and TM7

move closer to each other upon agonist binding in the M3 muscarinic receptor [18, 19]. As a method to detect interactions between residues in TMs, several different techniques, such as site-directed spin labeling, sulfhydryl reactivity studies, and disulfide cross-linking strategies have been developed and used extensively [20-24].

In Ste2p, residues and regions in transmembrane domains involved in receptor activation and signaling have been studied extensively [25-27]. For example, the studies of dominant-negative mutations in the receptor indicate that most mutants exhibiting a dominant-negative phenotype are located on the extracellular ends of the transmembrane domains, especially TM5 and TM6 [28-30]. In addition, an interaction between Val223Cys in the intracellular part of TM5 and L247C in the intracellular part of TM6 of Ste2p has been identified by a cysteine-cross-linking experiment [25]. It was also suggested that F204 in extracellular loop 2 was important for ligand binding and Y266 at the extracellular end of TM6 was involved in signal transduction [31]. Consistent with this, Yong *et al* revealed that N205 in TM5 is critical for signal transduction and interacts with Y266 in a constitutively active receptor [32].

Whereas numerous intra-molecular restraints for the inactive state conformations of GPCRs have been identified, little is known about the actual difference between the inactive and active states at the molecular level. The identification of inter-helical interactions specific to each state will provide a molecular basis for understanding mechanistic information underlying GPCR activation pathways. To identify inter-helical interactions between TM1 and TM7, we employed cysteine cross-linking. Although the anticipated inter-helical interactions were not identified from this study, the results

provided strong evidence for Ste2p dimerization which will be discussed in depth in PART III of this dissertation.

CHAPTER 3 Experimental procedures

Strains, Media, and Plasmids

Saccharomyces cerevisiae strain LM102 described by Sen and Marsh [33] was used in the growth arrest and LacZ assays. The genotype for the LM102 strain is: *MAT***a**, *bar1, his4, leu2, trp1, met1, ura3, FUS1-lacZ*::*URA3, ste2-dl* (deleted for the α-factor receptor). The protease-deficient strain BJS21 (*MAT**a**, prc1-407 prb1-1122 pep4-3 leu2 trp1 ura3-52 ste2*::*Kan*^{R}*)* was used in disulfide cross-linking and western blot assays to decrease receptor degradation during analyses [34]. The parental plasmid, pHY4 expressing the template construct used for mutagenesis, FT-HT-Xa (cys-less Ste2p, the FLAG and His epitope tags with Factor Xa cleavage cite) was generated by introducing a tandem Factor Xa cleavage site between Val192 and Thr193 into pBec2 expressing FT-HT (FLAG and His tagged Cys-less Ste2p) under a constitutive GPD promoter [35]. Twelve single Cys mutations ranging from Leu^{64} through Met^{69} on TM1 and Leu^{289} through Met^{294} on TM7 were generated in the pHY4 background by PCR based site-directed mutagenesis [36]. The sequences of constructs were verified by DNA sequence analysis completed by the Molecular Biology Resource Facility located on the campus of the University of Tennessee. Primers were purchased from Sigma Genosys or IDT (Coralville, IA). After sequence confirmation, constructs were transformed into the *ste2*-deletion strains LM102 and BJS21 by the method of Gietz et al [37]. Transformants bearing the pHY4 constructs were selected by their growth in the absence of tryptophan on MLT medium (Medium lacking tryptophan) [38]. All media components were obtained from Difco.

Growth Arrest (Halo) Assay

Growth arrest was measured as described previously [32]. Briefly, filter disks were impregnated with 10-µl portions of peptide solutions at various concentrations and placed onto the overlay containing *S. cerevisiae* LM102 cells. The plates were incubated at 30 °C for 24-36 h and then observed for clear zones (halos) around the disks. The halo measured included the diameter of the disc. The normalized activity of each mutant was determined by comparing halo size for the FT-HT-Xa receptor at 2µg of α-factor. All assays were carried out at least three times with no more than a 2-mm variation in halo size at a particular amount applied for α-factor.

FUS1-lacZ Gene Induction Assay

S. cerevisiae LM102 contains a *FUS1-lacZ* gene that is inducible by mating pheromone. Cells were grown overnight in SD (synthetic defined) medium [Yeast nitrogen base medium (Difco) without aminoacid] supplemented with the required amino acids at 30 °C to 5 x 10^6 cells/ml, washed by centrifugation, and grown for one doubling (hemocytometer count) at 30 °C. Induction was performed by adding 10^{-6} M of α-factor to 1 ml of concentrated cells (1 x 10^7 cells/ml). The mixtures were vortexed and, after incubation at 30 °C with shaking for 2 h, cells were harvested by centrifugation, and each pellet was resuspended and assayed for β-galactosidase activity (expressed as Miller units) in duplicate by using a β-galactosidase assay kit (Pierce) according to the manufacturer's instructions. The activity of each mutant was normalized by comparing β-

galactosidase activity for the wild-type strain. The standard deviation was determined from three independent experiments.

Preparation of membranes

Membrane preparation of Ste2p was carried out essentially as described previously [32]. Cells were grown to log phase, and then 1 x 10^8 cells were harvested by centrifugation and lysed by agitation with glass beads in a lysis buffer containing 50 mM Hepes, pH 7.5, 1 mM EDTA, 10 µg/ml phenylmethylsulfonyl fluoride, 2 µg/ml leupeptin, and 2 µg/ml pepstatin. The lysate was cleared by centrifugation at 2,000 x *g* for 5 min, and then membranes were harvested by centrifugation at 15,000 x *g* for 45 min. The membrane pellet was washed and then resuspended in 100 µl of a buffer (pH 7.4) containing 10% glycerol, 50mM Hepes, 0.15mM NaCl, 2mM $CaCl_2$, 5mM KCl, 5mM $MgCl_2$, 4mM EDTA [32]. The protein concentration was determined by the Lowry assay (Pierce), and the membrane preparation was stored at -20 ºC overnight and used for further assay the next day.

Disulfide Cross-linking with Cu-Phenanthroline

The 100 µg of membrane protein preparation was treated with a fresh preparation of Cu(II)-1,10-phenanthroline (CuP; final concentration, 2.5 µM CuSO4 and 7.5µM phenanthroline, pH 7.4). The treatment was carried out at room temperature for 30 min, terminated with 50 mM EDTA and kept on ice for 20 min followed by adding Laemmli sample buffer.

Factor Xa digestion

The membrane protein preparation (40 μg) was incubated with 0.4 unit of Factor Xa (Novagen) in Factor Xa cleavage buffer (0.1M NaCl, 50 mM Tris-HCl, 5 mM $CaCl_2$, pH 8.0) containing 0.1% Triton X-100 for 30min. Each sample was divided into two aliquots. The reactions were terminated by adding one-third the volume of Laemmli sample buffer (30% glycerol, 3% SDS, 0.01% bromphenol blue, 0.1875 M Tris, pH 6.8). To one aliquot β-mercaptoethanol (final 1%, v/v) was added for reducing conditions. Samples were analyzed by SDS-PAGE and Western blotting.

Western blot

Immunoblot analysis of Ste2p was carried out as described previously [32]. Each sample was incubated at room temperature and then separated on NuPAGE 10% Bis-Tris SDS-polyacrylamide gel (Invitrogen) using either non-reducing or reducing conditions and electrophoretically transferred to Immobilon™-P membrane (Millipore Corp., Bedford, MA). The blot was probed with anti-FLAG M2 antibody (Eastman Kodak Co.) or 1D4 antibody (a monoclonal antibody for rho-tag, purchased from Flintbox, BC, Canada), and the bands were visualized with the West Pico chemiluminescent detection system (Pierce).

CHAPTER 4 Results

Expression and Biological Activities of Double Cys Mutant Receptors

To identify a possible inter-helical interaction between TM1 and TM7, 36 different combinations of double Cys mutants were made by pairing the six mutations on TM1 with six on TM7. We chose twelve residues, six in TM1 (L64 – M69) and six in TM7 (L289 – M294) proximal to the cytoplasmic face of Ste2p (Fig. 8A) for mutation to Cys (Fig. 8A). These targeted residues were chosen for these reasons: (i) TM7 residues mutated (L291 – M294) are highly conserved among fungal pheromone receptors [39], (ii) TM1 and TM7 are in close proximity to one another in crystal structures of GPCRs [40, 41] and a model of Ste2p [39]. To eliminate non-specific cross-linking the template for these mutations was a Cys-less receptor. This template (FT-HT-Xa) also contained two C-terminal epitope tags (FLAG and 6XHis) and tandem Factor Xa cleavage sites (IEGRIEGR) in the second extracellular domain in order to facilitate detection of inter-domain cross-linking (Fig. 8A). Native Ste2p, FT-HT (Cys-less Ste2p with the FLAG and His epitope tags) and FT-HT-Xa (the template construct) receptors used in this study demonstrated almost identical biological activities in a growth arrest assay indicating that incorporating the protease site and the epitope tags did not alter receptor function (Fig. 8B).

The biological activities of the double Cys mutant receptors were measured and the results were summarized in Table 6. Most double mutant receptors showed similar

Figure 8 A. The two-dimensional topology of *Saccharomyces cerevisiae* Ste2p and B. Dose-response analysis of growth arrest assay

A.The cartoon indicates the location of the genetically engineered Factor Xa digestion site in EL2 and the epitope tags in the C-terminus. The two endogenous Cys residues (C59 and C252) were mutated to Ser to generate FT-HT-Xa which was the parental plasmid used to generate the cysteine mutations in positions 64 to 69 in TM1 and 289 to 294 in TM7 as indicated in the boxes. The zone of growth inhibition of strains carrying the indicated receptors was measured at various concentrations of α-factor. FT-HT-Xa is the Cys-less receptor containing C-terminal FLAG and His epitope tags and a tandem Factor Xa digestion site in EL2. FT-HT is the Cys-less receptor without the Xa digestion site containing the FLAG and His epitopes, and Native Ste2p is the wild-type receptor that has no epitope tags and has two Cys residues (C59 and C252).

A

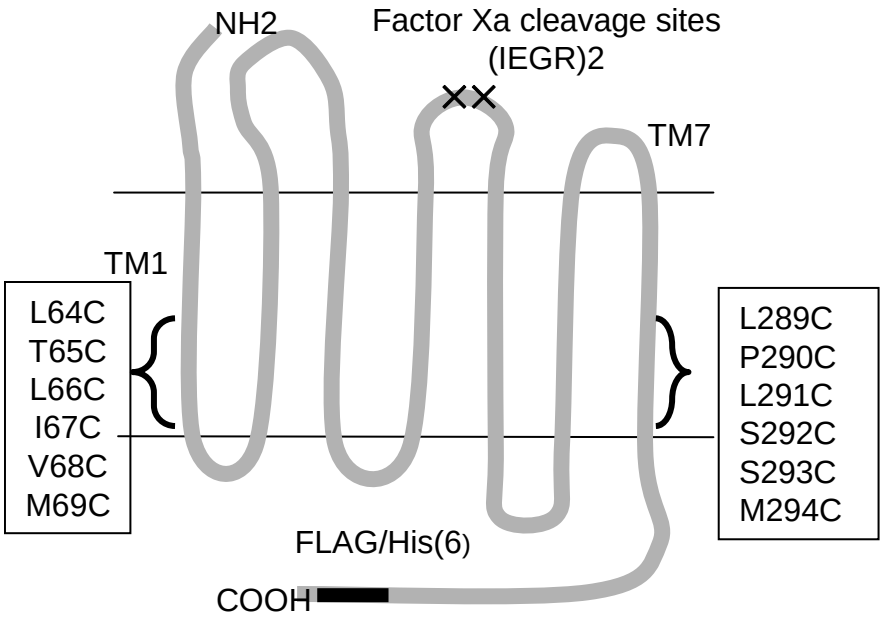
NH2
Factor Xa cleavage sites
(IEGR)2
TM7
TM1
L64C
T65C
L66C
I67C
V68C
M69C
L289C
P290C
L291C
S292C
S293C
M294C
FLAG/His(6)
COOH

B

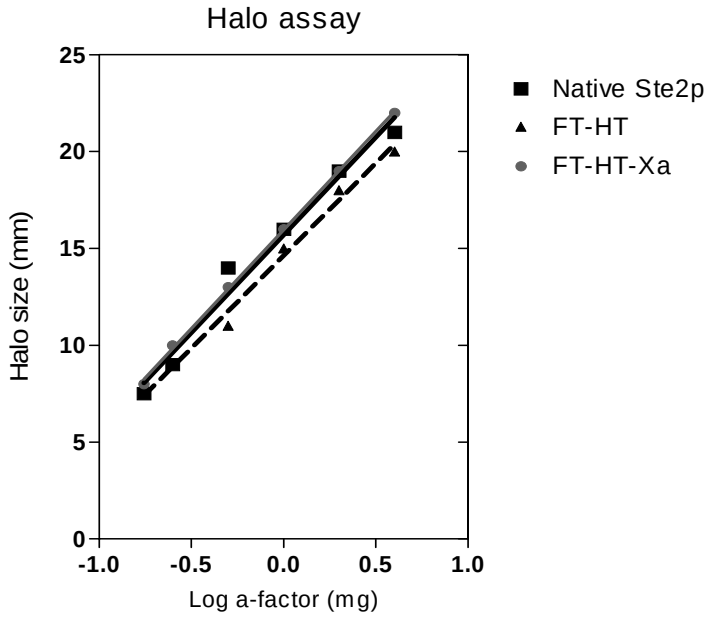
Halo assay
Halo size (mm)
Log a-factor (mg)
Native Ste2p
FT-HT
FT-HT-Xa
25
20
15
10
5
0
-1.0
-0.5
0.0
0.5
1.0

Table 6 Biological Activities of double Cys mutants

	LacZ Activity		
	Basal[1]	Induced[2]	Halo Activity[3]
FT-HT-Xa	1.0 ± 0.08 (3.7 unit)	1.0 ± 0.23 (32 unit)	1 (24mm)
L64C L289C	1.0 ± 0.13	1.0 ± 0.14	0.89
T65C L289C	1.0 ± 0.09	0.8 ± 0.03	0.92
L66C L289C	1.0 ± 0.09	0.8 ± 0.05	1.11
I67C L289C	1.1 ± 0.13	0.7 ± 0.04	1.03
V68C L289C	1.3 ± 0.16	0.8 ± 0.09	0.97
M69C L289C	1.0 ± 0.08	0.8 ± 0.08	1.03
L64C P290C	1.9 ± 0.16	1.0 ± 0.01	0.98
T65C P290C	1.9 ± 0.11	1.0 ± 0.02	0.98
L66C P290C	1.9 ± 0.15	0.9 ± 0.02	1.07
I67C P290C	2.9 ± 0.15	0.9 ± 0.01	1.05
V68C P290C	2.4 ± 0.27	1.0 ± 0.04	1.16
M69C P290C	1.7 ± 0.17	0.8 ± 0.03	1.02
L64C L291C	1.1 ± 0.04	1.7 ± 0.08	0.71
T65C L291C	1.2 ± 0.02	0.5 ± 0.06	0.00
L66C L291C	1.0 ± 0.01	1.0 ± 0.05	0.76
I67C L291C	1.5 ± 0.05	1.4 ± 0.06	1.03
V68C L291C	1.1 ± 0.03	0.5 ± 0.07	0.00
M69C L291C	1.0 ± 0.08	1.0 ± 0.05	0.98
L64C S292C	0.9 ± 0.09	1.0 ± 0.02	0.76
T65C S292C	0.9 ± 0.08	1.0 ± 0.09	0.84
L66C S292C	1.0 ± 0.12	1.4 ± 0.07	0.89
I67C S292C	0.8 ± 0.03	1.1 ± 0.16	0.97
V68C S292C	0.9 ± 0.05	0.9 ± 0.06	0.00
M69C S292C	0.7 ± 0.01	1.0 ± 0.03	1.05
L64C S293C	0.9 ± 0.03	1.0 ± 0.05	1.05
T65C S293C	1.2 ± 0.03	1.1 ± 0.03	1.08
L66C S293C	1.3 ± 0.03	1.1 ± 0.02	1.05
I67C S293C	1.1 ± 0.05	1.0 ± 0.07	1.10
V68C S293C	1.2 ± 0.05	1.2 ± 0.11	1.10
M69C S293C	1.1 ± 0.02	2.1 ± 0.04	0.90
L64C M294C	1.1 ± 0.04	1.1 ± 0.01	1.08
T65C M294C	1.1 ± 0.05	1.3 ± 0.01	1.15
L66C M294C	0.9 ± 0.03	1.1 ± 0.04	1.10
I67C M294C	0.9 ± 0.02	1.0 ± 0.02	1.00
V68C M294C	1.0 ± 0.08	0.5 ± 0.00	0.00
M69C M294C	1.1 ± 0.06	0.5 ± 0.05	0.00

[1]Relative activity (±standard deviation) compared with basal activity of FT-HT-Xa

(Table 6 continued)

[2]Relative activity (±standard deviation)compared with induced activity of FT-HT-Xa (α-factor, 1μM)

[3]Relative halo size compared with given halo size by FT-HT-Xa at 2 μg of α-factor. The standard deviation of the halo activity for all receptors was within ± 0.2 (three replicates).

n.d. = not detected

activity to FT-HT-Xa with the exception of five double mutant receptors (T65C/L291C, V68C/L291C, V68C/S292C, V68C/M294C and M69C/M294C), which exhibited partial activity as measured by the *FUS1-lacZ* assay. Moreover, the halo assay was used to measure the long term effect of receptor activation [42, 43]. For example, it is possible that conformational change introduced by specific mutations could alter coupling of the receptor with G protein or influence endocytosis of the mutant receptor such that it cannot efficiently arrest cell division.

The expression level of all double mutant receptors was similar to that of the FT-HT-Xa receptor (Representative data, Fig. 9). The multiple bands on immubolots are typical of Ste2p expression and are due probably to differences in the glycosylation state receptor, which does not influence receptor function [44]. Taken together, we conclude that Cys mutation of the targeted residues did not severely interfere with receptor expression and function, with the specific exception of the five mutants (T65C/L291C, V68C/L291C, V68C/S292C, V68C/M294C and M69C/M294C) indicated above.

Identification of Inter-molecular interaction between TMs using Factor Xa digestion

To identify inter-molecular interaction between TM1 and TM7, Factor Xa digestion was used. The Factor Xa digestion site was engineered into EL2. Digestion with Factor Xa cuts the intact receptor approximately in half. Therefore, if there is any interaction between TM1 and TM7, the disulfide bond formed between the residues will hold the receptor halves together following Factor Xa digestion (Fig. 10A) and a receptor of intact size (55 kDa) would be detected by anti-FLAG antibody on an immunoblot of

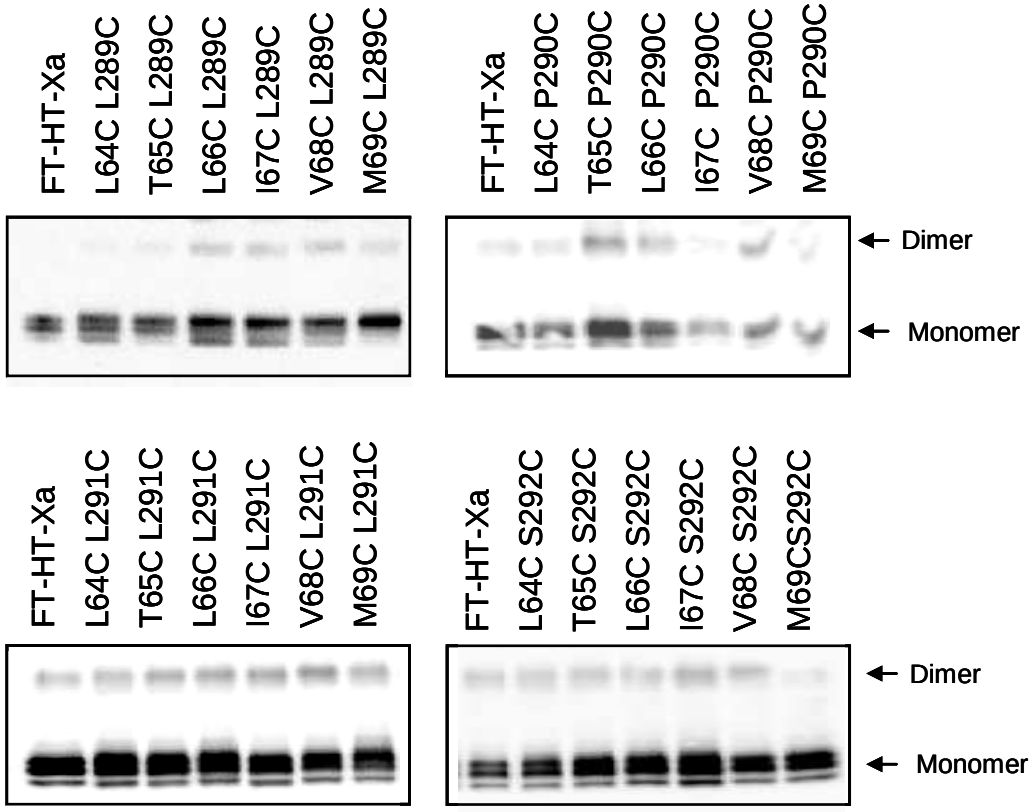

Figure 9 Expression of double Cys mutant receptors

Total membrane preparation from cells expressing each mutant receptor was analyzed by SDS-PAGE. Receptor was detected by anti-FLAG antibody. The upper band (~110 kDa) represents dimerized receptor and the lower band (~55 kDa) represents monomer.

proteins run on a gel under non-reducing condition (Fig. 10B). Under reducing gel conditions, this band would disappear and a smaller band corresponding to the C-terminal half of the receptor would be detected by anti-epitope antibodies engineered into the C-terminus (Fig. 10A and B). Before each double Cys mutant was tested, various parameters were examined to optimize the experimental conditions. Figure 11A shows the optimal concentration of Factor Xa for receptor cutting is between 0.4 and 1.6 unit for one hour incubation at 4 ºC. As expected, the C-terminal fragment of the receptor after protease digestion was detected at approximately 33 kDa using anti-FLAG antibody (Fig. 11A). An anti-Ste2p antibody, which recognizes the first 100 amino acids of the receptor, also successfully detected the N-terminal fragment of the receptor (22 kDa) following digestion. Multiple bands around 22 kDa (Fig 11B) are due to differences in glycosylation state as observed for the intact receptor.

All double Cys mutant receptors were analyzed by SDS-PAGE and western blot after Factor Xa digestion. However, no intra-molecular interaction between TM1 and TM7 was detected between the targeted residues. Instead, a band corresponding to a 66kD protein fragment (indicated by an arrow) was detected in double Cys mutant combinations involving five TM7 residues (L289C, L291C, S292C, S293C and M294C) (representative data for L291C and S293C shown in Fig. 12A and B). However, when an additional Cys mutation was made at P290 with the same mutations of TM1, the 66 kDa band was not generated (Fig. 12C). These data indicate that for specific residues in TM7, mutation to cysteine supports the formation of TM7-TM7 dimers. Interestingly, this band was detected only under non-reducing condition, and disappeared under reducing conditions. The size of the this novel 66 kDa corresponds to a dimer formed from two

fragments of C-terminal half of Ste2p joined by a disulfide bond, as would be expected to occur following Factor Xa digestion of a TM7-TM7 dimer. The fact that this band was not detected under reducing conditions supports the idea that this band was generated from cysteine cross linking. To test this, Cu (II)-1,10-phenanthroline (Cu-P) was used to treat all double Cys mutants to promote Cys-Cys disulfide bond formation. A protein band around 110 kDa was expected if Ste2p formed dimers through the engineered Cys residues in TM7. Indeed most of double cys mutants increased dimer population upon Cu-P treatment. Double mutants expressing the P290C mutation did not show an increase in dimerization, with the exception of I67C/P290C and V68C/P290C (Fig. 13). These results strongly suggested that Ste2p forms homo-dimers through introduced cysteines and led us to make single Cys mutants and further examine the capacity of these mutants to form dimers. This will be discussed in Part III in detail.

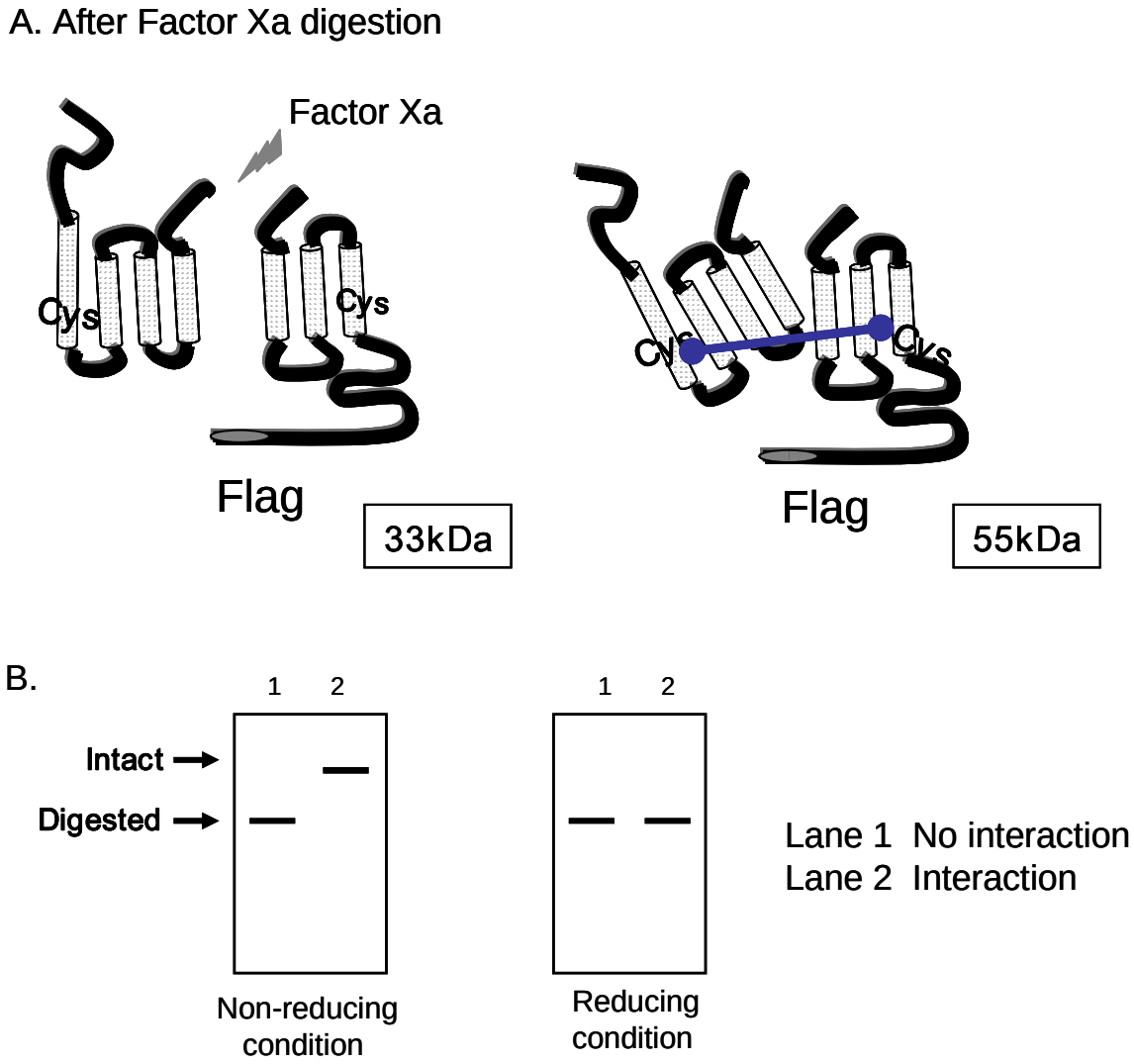

Figure 10 2D diagram illustrated expected result for interaction

A. After Factor Xa digestion, around 33kD size of receptor fragment will be detected by Anti-FLAG antibody in the absence of interaction and intact size of receptor will be detected in the presence of interaction. B. Left panel describes expected result from non-reducing condition and right panel shows expected result from reducing condition.

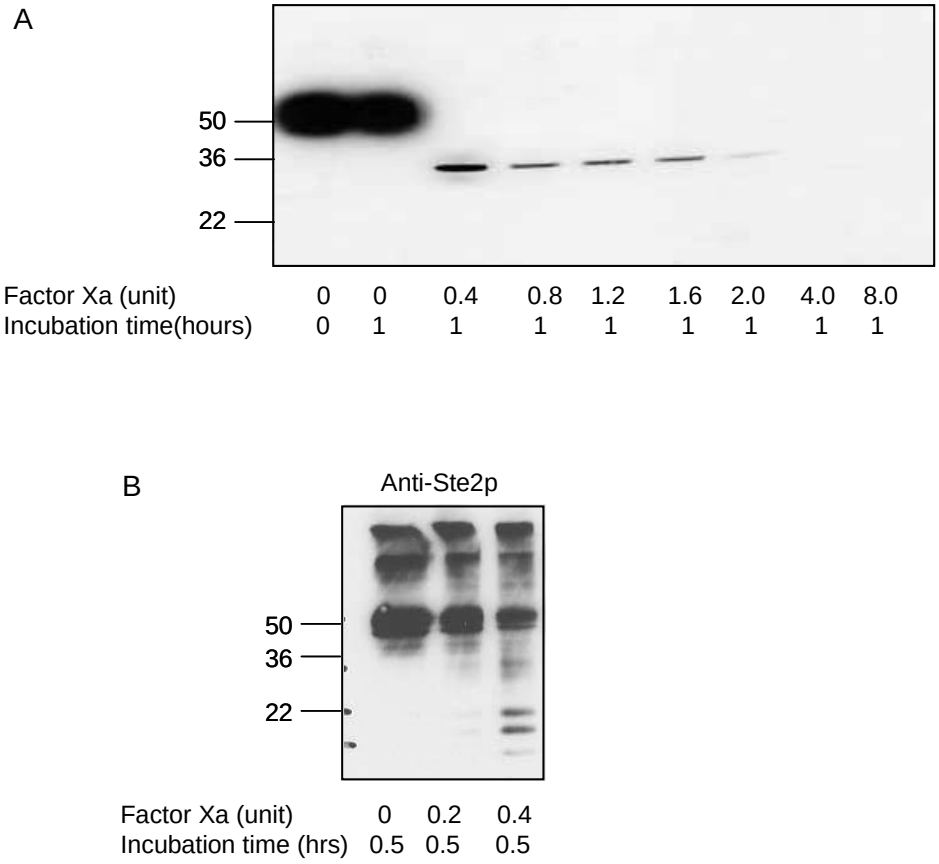

Figure 11 Factor Xa digestion of FT-HT-Xa

Total membrane was prepared from cells expressing FT-XT-Xa which is Cys-less receptor tagged with FLAG/His containing tandem Factor Xa digestion sites in the extracellular loop 2. A. Membrane was treated with different amount of Factor Xa as indicated for an hour at 4°C. Samples were analyzed on SDS-PAGE and immunoblotted with anti-FLAG antibody. B. Membrane was treated with different amount of Factor Xa as indicated for 30 min at 4°C. Samples were analyzed on SDS-PAGE and immunoblotted with anti-Ste2p antibody.

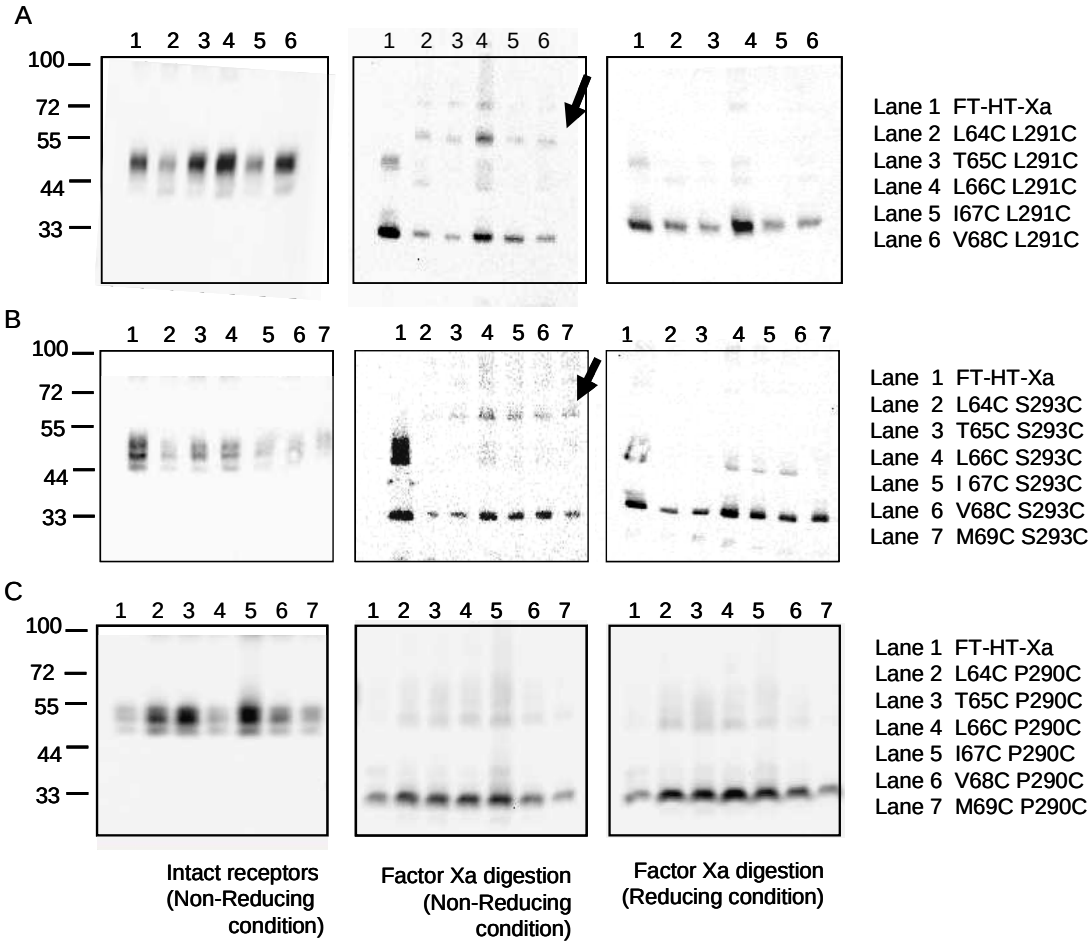

Figure 12 Factor Xa digestions of double cysteine containing Ste2p receptors

Total membrane proteins derived from cells expressing indicated receptors were digested with Factor Xa as described in the Methods. The digested samples were subjected to SDS-PAGE under non-reducing (middle panel) or reducing conditions (right panel), immunoblotted and probed by anti-FLAG antibody. Arrow indicates 66 kDa molecular bands.

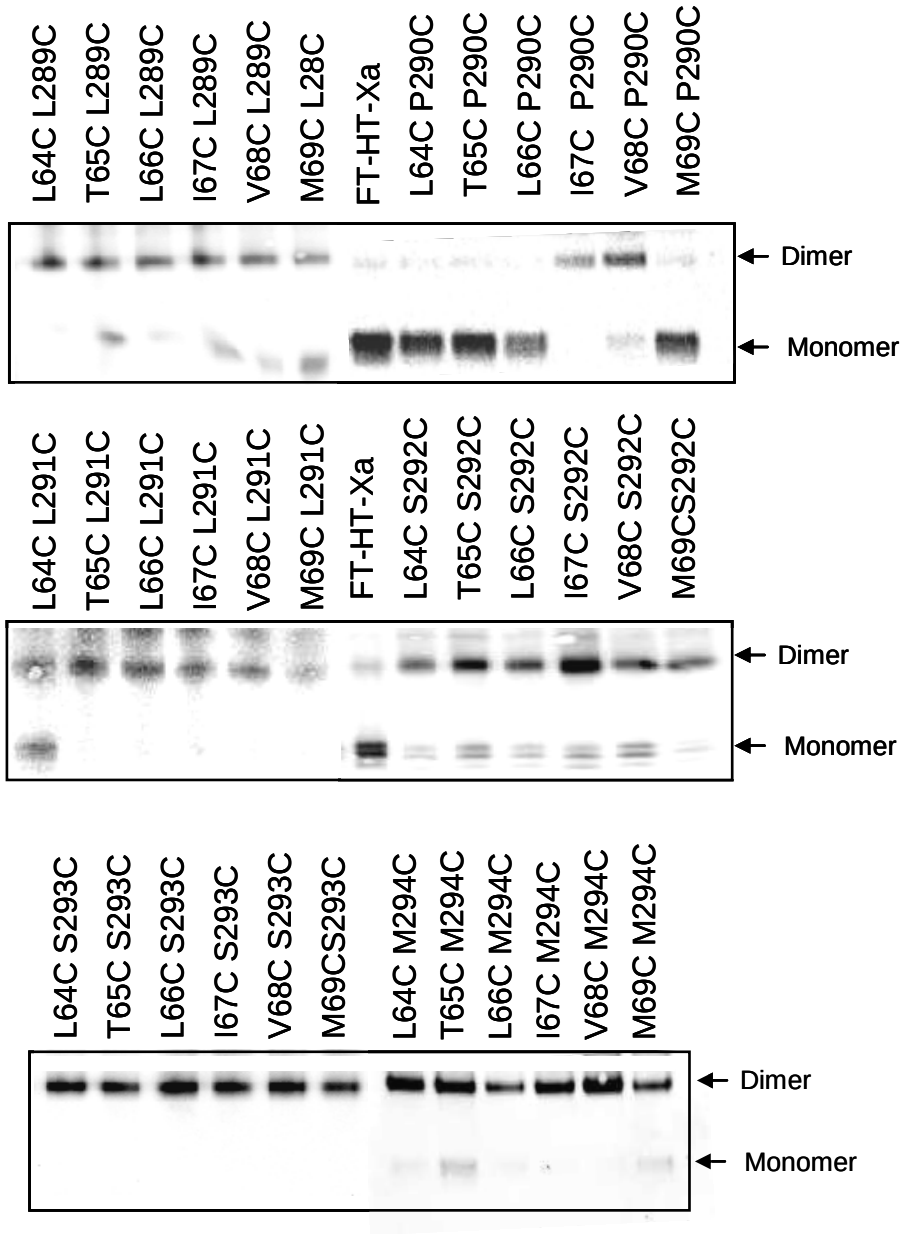
L64C L289C
T65C L289C
L66C L289C
I67C L289C
V68C L289C
M69C L28C
FT-HT-Xa
L64C P290C
T65C P290C
L66C P290C
I67C P290C
V68C P290C
M69C P290C
Dimer
Monomer
L64C L291C
T65C L291C
L66C L291C
I67C L291C
V68C L291C
M69C L291C
FT-HT-Xa
L64C S292C
T65C S292C
L66C S292C
I67C S292C
V68C S292C
M69CS292C
Dimer
Monomer
L64C S293C
T65C S293C
L66C S293C
I67C S293C
V68C S293C
M69CS293C
L64C M294C
T65C M294C
L66C M294C
I67C M294C
V68C M294C
M69C M294C
Dimer
Monomer

Figure 13 Effect of Cu-P [Cu (II)-1, 10-phenanthroline] treatment on receptors containing two cysteine replacements

Membranes were prepared, treated with Cu-P reagent, separated on SDS-PAGE. Each sample was immunoblotted and probed with anti-FLAG antibody. The upper band (~110 kDa) represents dimerized receptor and the lower band (~55 kDa) represents monomer.

CHAPTER 5 Discussion

We designed experiments to probe for inter-helical interactions between TM1 and TM7 using Cys scanning mutagenesis and cross-linking. This method has been extensively used to detect helical interactions in several GPCR systems [17, 23, 45-47]. Since our lab previously observed cysteine cross linking between N205C and Y266C without the use of an oxidizing reagent [32], we also expected to identify any interactions in TM1 and TM7 without using oxidizing reagents. However, no inter helical interactions were found with the targeted residues under the experimental condition used. It is possible that the intracellular parts of TM1 and TM7 in Ste2p are not close enough to interact, or the side chains of the targeted residues are not in the optimal orientation to form disulfide bonds, even though TM1 and TM7 are supposedly in close proximity according to established models. In contrast, we found evidence for homo-dimerization of Ste2p involving TM1 and/or TM7 which is discussed in detail in the next part of the dissertation.

Interestingly, the expression level of the single Cys mutant P290C is very much lower than for the FT-HT-Xa and Cys mutants at other positions (Fig. 15 in Part III). However, double cys mutants with P290C showed better expression (Fig. 9). Even though we could not detect any intra-molecular interaction between TM1 and TM7 with the residues targeted in this study, the fact that adding another cysteine mutation on TM1 compensates for the expression defect of P290C indicates TM1 and TM7 may somehow interact at the intra-molecular or inter-molecular level. In addition, double Cys mutant containing P290C did not produce the 66 kDa band observed for the other double Cys

mutants. This suggests that P290C may be important to maintain the proper conformation of TM7 to allow for the formation of disulfide bonds between the surrounding TM7 residues (L289C, L291C, S292C, S293C and M294C). Taken together, the results suggests that Pro 290 plays a critical role in receptor dimerization. Based on the results which will be presented in part III of this dissertation, the region of TM7 we chose to examine for potential interhelical interactions may not conform to the typical structure of a transmembrane α-helix, as this portion of TM7 may be distended and flexible, making it available for interaction with an adjacent receptor.

List of References for Part II

1. Berg, K.A., et al., *Effector pathway-dependent relative efficacy at serotonin type 2A and 2C receptors: evidence for agonist-directed trafficking of receptor stimulus.* Mol Pharmacol, 1998. **54**(1): p. 94-104.
2. Vilardaga, J.P., et al., *Molecular basis of inverse agonism in a G protein-coupled receptor.* Nat Chem Biol, 2005. **1**(1): p. 25-8.
3. Wei, H., et al., *Independent beta-arrestin 2 and G protein-mediated pathways for angiotensin II activation of extracellular signal-regulated kinases 1 and 2.* Proc Natl Acad Sci U S A, 2003. **100**(19): p. 10782-7.
4. Lu, Z.L., et al., *Structural determinants for ligand-receptor conformational selection in a peptide G protein-coupled receptor.* J Biol Chem, 2007. **282**(24): p. 17921-9.
5. Keith, D.E., et al., *mu-Opioid receptor internalization: opiate drugs have differential effects on a conserved endocytic mechanism in vitro and in the mammalian brain.* Mol Pharmacol, 1998. **53**(3): p. 377-84.
6. Kobilka, B., *Agonist binding: a multistep process.* Mol Pharmacol, 2004. **65**(5): p. 1060-2.
7. Perez, D.M. and S.S. Karnik, *Multiple signaling states of G-protein-coupled receptors.* Pharmacol Rev, 2005. **57**(2): p. 147-61.

8. Kobilka, B.K., et al., *Chimeric alpha 2-,beta 2-adrenergic receptors: delineation of domains involved in effector coupling and ligand binding specificity.* Science, 1988. **240**(4857): p. 1310-6.

9. Schoneberg, T., J. Liu, and J. Wess, *Plasma membrane localization and functional rescue of truncated forms of a G protein-coupled receptor.* J Biol Chem, 1995. **270**(30): p. 18000-6.

10. Filipek, S., et al., *G protein-coupled receptor rhodopsin: a prospectus.* Annu Rev Physiol, 2003. **65**: p. 851-79.

11. Hargrave, P.A., H.E. Hamm, and K.P. Hofmann, *Interaction of rhodopsin with the G-protein, transducin.* Bioessays, 1993. **15**(1): p. 43-50.

12. Khorana, H.G., *Rhodopsin, photoreceptor of the rod cell. An emerging pattern for structure and function.* J Biol Chem, 1992. **267**(1): p. 1-4.

13. Rao, V.R., G.B. Cohen, and D.D. Oprian, *Rhodopsin mutation G90D and a molecular mechanism for congenital night blindness.* Nature, 1994. **367**(6464): p. 639-42.

14. Hubbell, W.L., et al., *Rhodopsin structure, dynamics, and activation: a perspective from crystallography, site-directed spin labeling, sulfhydryl reactivity, and disulfide cross-linking.* Adv Protein Chem, 2003. **63**: p. 243-90.

15. Gether, U., et al., *Structural instability of a constitutively active G protein-coupled receptor. Agonist-independent activation due to conformational flexibility.* J Biol Chem, 1997. **272**(5): p. 2587-90.

16. Gether, U., S. Lin, and B.K. Kobilka, *Fluorescent labeling of purified beta 2 adrenergic receptor. Evidence for ligand-specific conformational changes.* J Biol Chem, 1995. **270**(47): p. 28268-75.

17. Ward, S.D., et al., *Use of an in situ disulfide cross-linking strategy to study the dynamic properties of the cytoplasmic end of transmembrane domain VI of the M3 muscarinic acetylcholine receptor.* Biochemistry, 2006. **45**(3): p. 676-85.

18. Han, S.J., et al., *Identification of an agonist-induced conformational change occurring adjacent to the ligand-binding pocket of the M(3) muscarinic acetylcholine receptor.* J Biol Chem, 2005. **280**(41): p. 34849-58.

19. Han, S.J., et al., *Pronounced conformational changes following agonist activation of the M(3) muscarinic acetylcholine receptor.* J Biol Chem, 2005. **280**(26): p. 24870-9.

20. Cai, K., et al., *Structure and function in rhodopsin: topology of the C-terminal polypeptide chain in relation to the cytoplasmic loops.* Proc Natl Acad Sci U S A, 1997. **94**(26): p. 14267-72.

21. Struthers, M., et al., *Tertiary interactions between the fifth and sixth transmembrane segments of rhodopsin.* Biochemistry, 1999. **38**(20): p. 6597-603.

22. Yang, K., et al., *Structure and function in rhodopsin. Cysteines 65 and 316 are in proximity in a rhodopsin mutant as indicated by disulfide formation and interactions between attached spin labels.* Biochemistry, 1996. **35**(45): p. 14040-6.

23. Yu, H., et al., *A general method for mapping tertiary contacts between amino acid residues in membrane-embedded proteins.* Biochemistry, 1995. **34**(46): p. 14963-9.

24. Yu, H., M. Kono, and D.D. Oprian, *State-dependent disulfide cross-linking in rhodopsin.* Biochemistry, 1999. **38**(37): p. 12028-32.

25. Dube, P., A. DeCostanzo, and J.B. Konopka, *Interaction between transmembrane domains five and six of the alpha -factor receptor.* J Biol Chem, 2000. **275**(34): p. 26492-9.

26. Parrish, W., et al., *The cytoplasmic end of transmembrane domain 3 regulates the activity of the Saccharomyces cerevisiae G-protein-coupled alpha-factor receptor.* Genetics, 2002. **160**(2): p. 429-43.

27. Sommers, C.M. and M.E. Dumont, *Genetic interactions among the transmembrane segments of the G protein coupled receptor encoded by the yeast STE2 gene.* J Mol Biol, 1997. **266**(3): p. 559-75.

28. Dosil, M., et al., *Dominant-negative mutations in the G-protein-coupled alpha-factor receptor map to the extracellular ends of the transmembrane segments.* Mol Cell Biol, 1998. **18**(10): p. 5981-91.

29. Dosil, M., et al., *The C terminus of the Saccharomyces cerevisiae alpha-factor receptor contributes to the formation of preactivation complexes with its cognate G protein.* Mol Cell Biol, 2000. **20**(14): p. 5321-9.

30. Leavitt, L.M., et al., *Dominant negative mutations in the alpha-factor receptor, a G protein-coupled receptor encoded by the STE2 gene of the yeast Saccharomyces cerevisiae.* Mol Gen Genet, 1999. **261**(6): p. 917-32.

31. Lin, J.C., et al., *Identification of residues that contribute to receptor activation through the analysis of compensatory mutations in the G protein-coupled alpha-factor receptor.* Biochemistry, 2005. **44**(4): p. 1278-87.

32. Lee, Y.H., F. Naider, and J.M. Becker, *Interacting residues in an activated state of a G protein-coupled receptor.* J Biol Chem, 2006. **281**(4): p. 2263-72.

33. Sen, M. and L. Marsh, *Noncontiguous domains of the alpha-factor receptor of yeasts confer ligand specificity.* J Biol Chem, 1994. **269**(2): p. 968-73.

34. Son, C.D., et al., *Identification of ligand binding regions of the Saccharomyces cerevisiae alpha-factor pheromone receptor by photoaffinity cross-linking.* Biochemistry, 2004. **43**(41): p. 13193-203.

35. Hauser, M., et al., *The first extracellular loop of the Saccharomyces cerevisiae G protein-coupled receptor Ste2p undergoes a conformational change upon ligand binding.* J Biol Chem, 2007. **282**(14): p. 10387-97.

36. Akal-Strader, A., et al., *Residues in the first extracellular loop of a G protein-coupled receptor play a role in signal transduction.* J Biol Chem, 2002. **277**(34): p. 30581-90.

37. Gietz, D., et al., *Improved method for high efficiency transformation of intact yeast cells.* Nucleic Acids Res, 1992. **20**(6): p. 1425.

38. David, N.E., et al., *Expression and purification of the Saccharomyces cerevisiae alpha-factor receptor (Ste2p), a 7-transmembrane-segment G protein-coupled receptor.* J Biol Chem, 1997. **272**(24): p. 15553-61.

39. Eilers, M., et al., *Comparison of class A and D G protein-coupled receptors: common features in structure and activation.* Biochemistry, 2005. **44**(25): p. 8959-75.

40. *Crystal structure of rhodopsin: a G protein-coupled receptor. Palczewski K,*(1) kumasaka T, hori T, behnke CA, motoshima H, fox BA, trong IL, teller DC, okada*

T, stenkamp RE, yamamoto M, miyano M. Science 2000;289:739-745. Am J Ophthalmol, 2000. **130**(6): p. 865.

41. Cherezov, V., et al., *High-resolution crystal structure of an engineered human beta2-adrenergic G protein-coupled receptor.* Science, 2007. **318**(5854): p. 1258-65.

42. McCaffrey, G., et al., *Identification and regulation of a gene required for cell fusion during mating of the yeast Saccharomyces cerevisiae.* Mol Cell Biol, 1987. **7**(8): p. 2680-90.

43. Dohlman, H.G. and J.W. Thorner, *Regulation of G protein-initiated signal transduction in yeast: paradigms and principles.* Annu Rev Biochem, 2001. **70**: p. 703-54.

44. Mentesana, P.E. and J.B. Konopka, *Mutational analysis of the role of N-glycosylation in alpha-factor receptor function.* Biochemistry, 2001. **40**(32): p. 9685-94.

45. Li, J.H., et al., *Ligand-specific changes in M3 muscarinic acetylcholine receptor structure detected by a disulfide scanning strategy.* Biochemistry, 2008. **47**(9): p. 2776-88.

46. Li, J.H., et al., *Distinct structural changes in a G protein-coupled receptor caused by different classes of agonist ligands.* J Biol Chem, 2007. **282**(36): p. 26284-93.

47. Zeng, F.Y., et al., *Use of a disulfide cross-linking strategy to study muscarinic receptor structure and mechanisms of activation.* J Biol Chem, 1999. **274**(23): p. 16629-40.

Part III Identification of Specific Transmembrane Residues and Ligand-Induced Interface Changes Involved In Homo-Dimer Formation of A Yeast G Protein-Coupled Receptor

Published as "Identification of Specific Transmembrane Residues and Ligand-Induced Interface Changes Involoved In Homo-Dimer Formation of A Yeast G Protein-Coupled Receptor", Heejung Kim, Byung-Kwon Lee, Fred Naider and Jeffrey M. Becker in *Biochemistry* 2009 Oct 28. [Epub ahead of print]]

CHAPTER 1 Abstract

The *S. cerevisiae* α-factor pheromone receptor, Ste2p, has been studied as a model for G protein-coupled receptor (GPCR) structure and function. Dimerization has been demonstrated for many GPCRs, although the role(s) of dimerization in receptor function is disputed. Transmembrane domains one (TM1) and four (TM4) of Ste2p were shown previously to play a role in dimerization. In this study, single cysteine substitutions were introduced into a Cys-less Ste2p, and disulfide-mediated dimerization was assessed. Six residues in TM1 (L64 to M69) that had not been previously investigated and nineteen residues in TM7 (T278 to A296) of which fifteen were not previously investigated were mutated to create 25 single Cys-containing Ste2p molecules. Ste2p mutants V68C in TM1 and nine mutants in TM7 (cysteine substituted into residues 278, 285, 289, and 291 to 296) showed increased dimerization upon addition of an oxidizing agent in comparison to the background dimers formed by the Cys-less receptor. The formation of dimers was decreased for TM7 mutant receptors in the presence of α-factor indicating that ligand binding resulted in a conformational change that influenced dimerization. The effect of ligand on dimer formation suggests that dimers are formed in the resting state and the activated state of the receptor by different TM interactions.

CHAPTER 2 Introduction

G protein-coupled receptors (GPCRs) are membrane proteins that form one of the largest and most diverse families of proteins in eukaryotes ranging from yeast to human. Though the primary sequences are different among the GPCRs, all GPCRs share common structural features: seven transmembrane helical domains (TMs) across the lipid bilayer, with the TMs connected by intracellular and extracellular loops, an extracellular N-terminus and an intracellular C-terminus [1]. GPCRs mediate responses to various stimuli such as hormones, odors, peptides and neurotransmitters. Binding of ligand to a GPCR triggers receptor-specific signals through a heterotrimeric G protein. Since it has been reported that genetic variation of GPCRs often alters receptor functions such as ligand binding, G protein coupling, and receptor life cycle, GPCR mutation is considered a causative agent of many of human diseases [2]. GPCRs have been the most successful molecular drug targets in clinical medicine [3].

Ste2p is the α-factor pheromone receptor in *Saccharomyces cerevisiae* and has been used as a model for the study of the molecular basis of GPCR function [4-6]. Ste2p can be replaced in yeast cells with mammalian receptors with functionality conserved [7], and Ste2p can be expressed and trigger signal transduction upon ligand binding in HEK293 cells [8]. Also, Ste2p can serve as an established model for fungal GPCRs. Recently, many more GPCRs in fungi have been identified and classified into six different categories based on sequence homology and ligand sensing [9]. Ste2p is the

most well studied receptor among fungal GPCRs, some of which are suggested to be related to fungal pathogenesis [9].

Recently, evidence has been growing that many GPCRs form homo- and/or hetero- dimeric or oligomeric complexes [9-11]. Oligomerization has been discovered by techniques such as crosslinking, bioluminescence resonance energy transfer, fluorescence resonance energy transfer, and immunoprecipitation [10]. Dimerization is thought to be important for various aspects of GPCR function such as receptor biogenesis, formation of ligand-binding sites, signal transduction, and down-regulation [11, 12]. However, the view that dimers are involved in the rhodopsin-like (Class 1A) receptor-activated signaling has been challenged [13-16].

It has been demonstrated that Ste2p is internalized as a dimer/oligomer complex [17, 18], and oligomerization-defective mutants can bind α-factor but signaling is impaired [19]. It has also been shown that the dominant/negative effect on wild-type signaling of a signaling-defective mutation in Ste2p (Ste2p-Y266C) can be partially reversed by mutations in the $G^{56}XXXG^{60}$ dimerization motif, indicating that signal transduction by oligomeric receptors requires an interaction between functional monomers [20]. Recently, dimer interfaces were identified in Ste2p near the extracellular end of TM1 and TM4 [21]. In that study it was found that dimerization was symmetric, occurring between receptors at the TM1-TM1 interface or the TM4-TM4 interface. In our current study, using the disulfide cross-linking methodology, we studied the participation of specific residues at the intracellular boundary between TM1 and intracellular loop one and the entire TM7 in Ste2p dimerization.

CHAPTER 3 Experimental procedures

Strains, Media, and Plasmids

Saccharomyces cerevisiae strain LM102 described by Sen and Marsh [22] was used in the growth arrest and LacZ assays. The genotype for the LM102 strain is: *MAT***a**, *bar1, his4, leu2, trp1, met1, ura3, FUS1-lacZ*::*URA3, ste2-dl* (deleted for the α-factor receptor). The protease-deficient strain BJS21 (*MAT**a**, prc1-407 prb1-1122 pep4-3 leu2 trp1 ura3-52 ste2*::*Kan*^{R}*)* was used in disulfide cross-linking and western blot assays to decrease receptor degradation during analyses [23]. The parental plasmid, pHY4 expressing the template construct used for mutagenesis, FT-HT-Xa (cys-less Ste2p with the FLAG and His epitope tags with Factor Xa cleavage cite, see Table 7 for description of the various receptor constructs used in this study) was generated by introducing a tandem Factor Xa cleavage site between Val192 and Thr193 into pBec2 expressing FT-HT (FLAG and His tagged Cys-less Ste2p) under a consititutive GPD promoter [24]. Twenty-five single Cys mutations ranging from Leu^{64} through Met^{69} on TM1 and Thr^{278} through Ala^{296} on TM7 were generated in the pHY4 background by PCR based site-directed mutagenesis [25]. For co-expression experiments, plasmid pHY6 was constructed from p426GPD, a 2-μm based shuttle vector with a *GPD* promoter, *CYC1* terminator, and *URA* marker for selection in yeast [26]. *STE2* containing C-terminal FLAG and His epitope tags and a tandem Factor Xa digestion site in EL2 was PCR-amplified from plasmid pHY4 using primers that introduced *BamHI* and *EcoRI* restriction sites. The resulting PCR product was subcloned into the complementary sites of

p426GPD. Also, to create pHY6 an epitope tag comprising codons encoding a 9-amino acid sequence of rhodopsin (rho-tag) was substituted for the FLAG and His epitope tags by ligation of a C-terminus part of STE2 product amplified from pBKY1[27]. Cys mutants in this template were generated as described above. The sequences of constructs were verified by DNA sequence analysis completed by the Molecular Biology Resource Facility located on the campus of the University of Tennessee. Primers were purchased from Sigma Genosys or IDT (Coralville, IA). After sequence confirmation, constructs were transformed into the *ste2*-deletion strains LM102 and BJS21 by the method of Gietz et al [28]. Transformants bearing the pHY4 or pHY6 constructs were selected by their growth in the absence of tryptophan for pHY4 on MLT medium (Medium lacking tryptophan) or in the absence of uracil for pHY6 on MLU medium (Medium lacking uracil) [29]. All media components were obtained from Difco.

Growth Arrest (Halo) Assay

Growth arrest was measured as described previously [30]. Briefly, filter disks were impregnated with 10-µl portions of peptide solutions at various concentrations and placed onto the overlay containing *S. cerevisiae* LM102 cells. The plates were incubated at 30 °C for 24-36 h and then observed for clear zones (halos) around the disks. The halo measured included the diameter of the disc. The normalized activity of each mutant was determined by comparing halo size for the FT-HT-Xa receptor at 2µg of α-factor. All

Table 7 Receptors used in this study

Receptor name	Description
Wild-type	Native Ste2p
Ste2p-FT-HT	Wild-type with FLAG /His epitope tags
FT-HT	Cys-less Ste2p-FT-HT
FT-HT-Xa	FT-HT with tandem Factor Xa cleavage sites Template for all Cys mutants generated in this study
Rho-Xa	Cys-less Ste2p with tandem Factor Xa cleavage sites and Rho tagged

assays were carried out at least three times with no more than a 2-mm variation in halo size at a particular amount applied for each peptide.

FUS1-lacZ Gene Induction Assay

S. cerevisiae LM102 contains a *FUS1-lacZ* gene that is inducible by mating pheromone. Cells were grown overnight in SD (synthetic defined) medium (Yeast nitrogen base medium (Difco) without aminoacid) supplemented with the required amino acids at 30 °C to 5 x 10^6 cells/ml, washed by centrifugation, and grown for one doubling (hemocytometer count) at 30 °C. Induction was performed by adding 10^{-6} M of α-factor to 1 ml of concentrated cells (1 x 10^7 cells/ml). The mixtures were vortexed and, after incubation at 30 °C with shaking for 2 h, cells were harvested by centrifugation, and each pellet was resuspended and assayed for β-galactosidase activity (expressed as Miller units) in duplicate by using a β-galactosidase assay kit (Pierce) according to the manufacturer's instructions. The activity of each mutant was normalized by comparing β-galactosidase activity for the wild-type strain. The standard deviation was determined from three independent experiments.

Preparation of membranes

Membrane preparation of Ste2p was carried out essentially as described previously [30]. Cells were grown to log phase, and then 1 x 10^8 cells were harvested by centrifugation and lysed by agitation with glass beads in a lysis buffer containing 50 mM

Hepes, pH 7.5, 1 mM EDTA, 10 µg/ml phenylmethylsulfonyl fluoride, 2 µg/ml leupeptin, and 2 µg/ml pepstatin. The lysate was cleared by centrifugation at 2,000 x *g* for 5 min, and then membranes were harvested by centrifugation at 15,000 x *g* for 45 min. The membrane pellet was washed and then resuspended in 100 µl of a buffer (pH 7.4) containing 10% glycerol, 50mM Hepes, 0.15mM NaCl, 2mM $CaCl_2$, 5mM KCl, 5mM $MgCl_2$, 4mM EDTA [30]. The protein concentration was determined by the Lowry assay (Pierce), and the membrane preparation was stored at -20 ºC overnight and used for further assay the next day.

Disulfide Cross-linking with Cu-Phenanthroline

The 100 µg of membrane protein preparation were treated with a fresh preparation (pH 7.4) of Cu (II)-1, 10-phenanthroline (Cu-P; final concentration, 2.5 µM CuSO4 and 7.5µM phenanthroline). The reaction was carried out at room temperature for 30 min, terminated with 50 mM EDTA and kept on ice for 20 min followed by adding Laemmli sample buffer. For study of the time course of cross-linking, Cu-P treated samples were aliquoted at 45 sec, 2 min, 5 min, 10 min, 20 min, and 30 min before termination. In experiments designed to prevent disulfide bond formation, the membranes were treated with 5mM of NEM for 20min prior to incubation with Cu-P reagent. Alpha-factor or antagonist [desW1,desH2]α-factor (10 µM final concentration) were added to the membrane preparation and incubation allowed to proceed for 30 min prior to Cu-P treatment in experiments performed to examine the influence of ligand on dimerization.

Factor Xa digestion

The membrane protein preparation (40 μg) was incubated with 0.4 unit of Factor Xa (Novagen) in Factor Xa cleavage buffer (0.1M NaCl, 50 mM Tris-HCl, 5 mM $CaCl_2$, pH 8.0) containing 0.1% Triton X-100 for 30min. Each sample was divided into two aliquots. The reactions were terminated by adding one-third the volume of Laemmli sample buffer (30% glycerol, 3% SDS, 0.01% bromphenol blue, 0.1875 M Tris, pH 6.8). To one aliquot β-mercaptoethanol (final 1%, v/v) was added for reducing conditions. Samples were analyzed by SDS-PAGE and Western blotting.

Saturation Binding assay with [^{3}H]α-Factor

Tritiated α-factor (10.2 Ci/mmol) [31] was used in saturation binding assays on total membrane preparations as described previously [29] Specific binding data were analyzed by nonlinear regression analysis for single-site binding using Prism software (GraphPad Software, San Diego, CA) to determine the B_{max} value (receptors/cell) for each mutant receptor. Each experiment was carried out at least 3 times. The close similarity among three replicates is indicated by the standard deviations shown in Table 8.

Western blot

Immunoblot analysis of Ste2p was carried out as described previously [30]. Each sample was incubated at room temperature and then separated on NuPAGE 10% Bis-Tris SDS-polyacrylamide gel (Invitrogen) using either non-reducing or reducing conditions

and electrophoretically transferred to Immobilon^{TM}-P membrane (Millipore Corp., Bedford, MA). The blot was probed with anti-FLAG M2 antibody (Eastman Kodak Co.) or 1D4 antibody (a monoclonal antibody for rho-tag, purchased from Flintbox, BC, Canada), and the bands were visualized with the West Pico chemiluminescent detection system (Pierce). Blots were imaged, and the total density of all Ste2p bands in each lane was determined using a ChemiDoc XRS photodocumentation system with Quantity One one-dimensional analysis software (Bio-Rad). The intensity of the monomer and dimer signal was measured by densitometry and the ratio of the signals was determined. The percentage of dimer was calculated as [Dimer/(Dimer+Monomer) x100]. The averages of the ratio were measured from at least three independent experiments and standard deviations are presented in Table 9.

HIS-select HC Nickel affinity

Membrane preparations (500 μg protein) from each sample were resuspended in a solubilization buffer (50 mM Tris HCl, 150 mM NaCl, 1% Triton X-100, 5 mM imidazole, pH 8.0) overnight. The solubilized proteins were then mixed with HIS-select HC Nickel affinity gel (Sigma) and incubated at 4^{O}C for 30 minutes with end-over-end mixing. The Nickel gel was separated from the mixture by centrifugation and then washed five times with buffer (50 mM sodium phosphate, pH 8.0, 0.3 M NaCl, 5 mM imidazole). Ste2p was eluted from the Nickel gel two times using elution buffer (50 mM sodium phosphate, pH 8.0, 0.3 M NaCl, 250 mM imidazole). The eluted samples were analyzed by SDS-PAGE silver staining and western blotting using antibodies against

FLAG, a 9-amino acid sequence of rhodopsin (rho-tag), or an antibody to the N-terminus of Ste2p [32].

MTSEA Labeling

Membrane preparation was performed as decribed above. The 600 µg of the total proteins in PBS buffer (1ml) were treated with MTSEA (2-[(biotinoyl)amino]ethyl methanethiosulfonate) biotin in DMSO (0.1mM) for 2 minutes. Membranes were pelleted by centrifugation at 15000 RPM for 5 minutes in cold room and resuspended in 600 µl of RIPA buffer (0.1% SDS, 1% Triton X-100, 0.5% deoxycholic acid, 1 mm EDTA in 1× PBS, pH 7.4), solubilized for 1 hour at 4 $^{\circ}$C. After addition of 150 µl of streptavidin slurry to the sample, it was incubated overnight at 4°C. The beads were then allowed to settle by gravity and supernatant was removed. The pellet was washed with RIPA buffer four times followed by washing with 2% SDS in PBS. The proteins were extracted from the beads by incubating with 40 µl of Laemmli sample buffer at 55°C for 5 minutes. The samples were separated on 10 % SDS PAGE. Westen blotting was performed and the membrane blot was probed by using anti-FLAG as decribed. Labeling was expressed as a percentage of accessibility for each individual mutant. Percent labeling was calculated by quantitating total immunoreactivity of all bands on the FLAG immunoblot, then normalized with T199C accessibility (=100%).

CHAPTER 4 Results

Expression and Biological Activities of Cys Mutant Receptors

To begin the analysis of Ste2p dimerization we chose twelve residues, six in TM1 and six in TM7 (L289 – M294) proximal to the cytoplasmic face of Ste2p (Fig. 14A) for mutation to Cys. To extend the initial cross-linking results, thirteen additional residues in TM7 were mutated (T278C – S288C, W295C, and A296C) (Fig. 14A). These targeted residues were chosen for several reasons: (i) The TM1 region chosen was one helix turn away from the sequence $G^{56}XXXG^{60}$ previously established as being involved in Ste2p dimerization [19], (ii) TM7 contains the AXXXA motif also suggested to play a role in dimerization of other proteins [33] and 20 known growth factor receptors with tyrosine kinase activity [34], (iii) eight of the TM7 residues mutated (S288-S293,W295 and A296) are conserved among fungal pheromone receptors [35], and (iv) TM1 and TM7 are in close proximity to one another in crystal structures of GPCRs [36, 37] and a model of Ste2p [35]. To eliminate non-specific cross-linking the template for these mutations was a Cys-less receptor. This template (FT-HT-Xa) also contained two C-terminal epitope tags (FLAG and 6XHis) and tandem Factor Xa cleavage sites (IEGRIEGR) in the second extracellular domain in order to facilitate detection of inter-domain cross-linking (Fig. 14A). Wild-type, FT-HT (Cys-less Ste2p with the FLAG and His epitope tags) and FT-HT-Xa (the template construct) receptors used in this study demonstrated almost identical biological activities in a growth arrest assay indicating that incorporating the protease site

and the epitope tags did not alter receptor function (Fig. 8B in Part II). In addition, FT-HT-Xa and Ste2p-FT-HT showed identical expression (Fig. 14B).

The expression level of each single-Cys mutant receptor was determined by western blot analysis. All mutants except P290C showed several bands between 44kDa and 55kDa and expression levels similar to that of FT-HT-Xa (Fig. 15A and Fig. 18A). The multiple bands are typical of Ste2p expression and are due to differences in its glycosylation state, which does not influence receptor function [38]. Although two intrinsic Cys residues have been substituted, a weak band at 110 kDa, corresponding to a dimerized form of Ste2p, was observed for the FT-HT receptor (Fig. 15B). This band is likely a native, non-covalent dimer which was not disrupted by membrane protein preparation or SDS-PAGE. Such dimers have been observed on SDS-PAGE gels by other investigators working with Ste2p [20, 39, 40] and are also seen with the FT-HT-Xa receptor (Fig. 20A; Lane 1). This weak dimer observed in the Cys-less receptor is consistent with immunoprecipition results showing that the two intrinsic Cys are not involved in dimerization [18].

Membrane expression of P290C receptor was very low when judged by western blot (Fig.15A). It is known that one of the roles of the conserved proline in TM7 in GPCRs is correct folding [41]. The reduced expression of P290C was observed previously when it was shown that this receptor was primarily defective in plasma membrane localization using a P290C-GFP receptor, but the P290C-GFP construct did not demonstrate a defect in signaling [42].

Figure 14 The two-dimensional topology of *Saccharomyces cerevisiae* Ste2p

A.The cartoon indicates the location of the genetically engineered Factor Xa digestion site in EL2 and the epitope tags in the C-terminus. The two endogenous Cys residues (C59 and C252) were mutated to Ser to generate FT-HT-Xa which was the parental GPCR used to generate the TM1 and TM7 cysteine mutations in positions 64 to 69 in TM1 and 278 to 296 in TM7 as indicated in the boxes. B. Expression of FT-HT-Xa. Membrane proteins were analyzed by SDS-PAGE, then immunoblotted and probed with anti-FLAG antibody

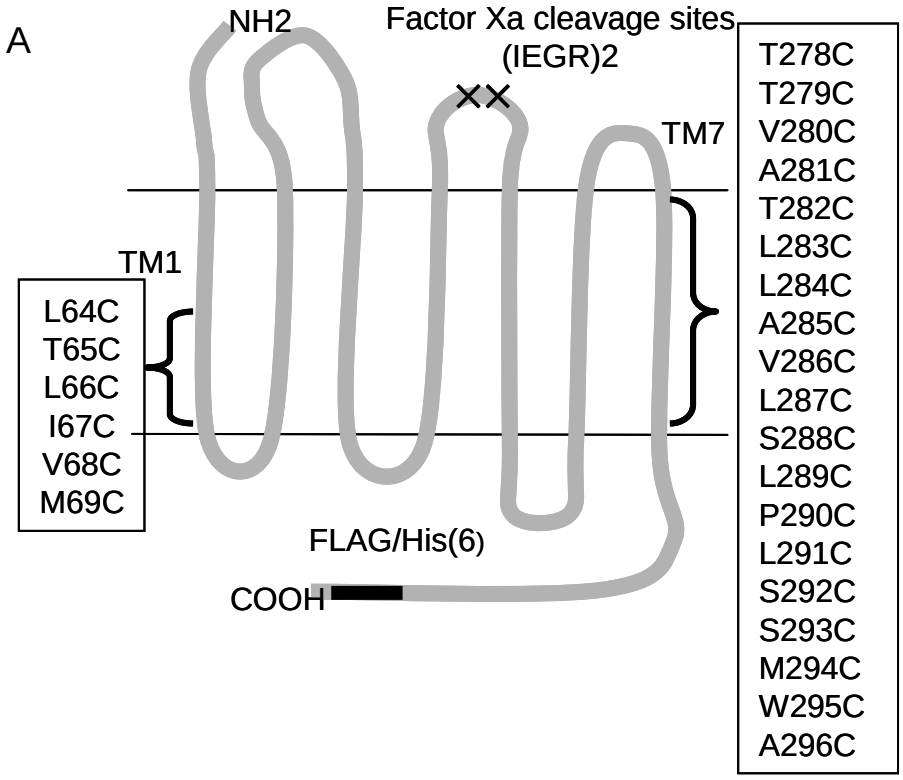
A
NH2
Factor Xa cleavage sites
(IEGR)2
TM7
TM1
L64C
T65C
L66C
I67C
V68C
M69C
T278C
T279C
V280C
A281C
T282C
L283C
L284C
A285C
V286C
L287C
S288C
L289C
P290C
L291C
S292C
S293C
M294C
W295C
A296C
FLAG/His(6)
COOH

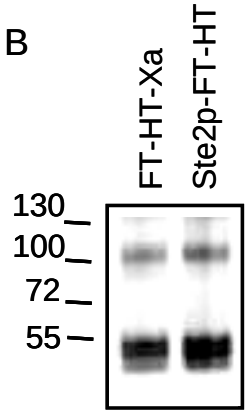
B
FT-HT-Xa
Ste2p-FT-HT
130
100
72
55

Figure 15 Effect of Cu-P (Cu (II)-1, 10-phenanthroline) treatment on the dimerization of Ste2p containing single cysteine mutations

Membrane proteins were treated with Cu-P or left untreated, followed by SDS-PAGE, then immunoblotted and probed with anti-FLAG antibody. The upper band (~110 kDa) represents dimerized receptor and the lower band (~55 kDa) represents monomer. A. Receptors with Cys in TM1 or TM7 were treated with Cu-P (Right panel) or were untreated (Left Panel). Receptors indicated in bold exhibited a shift in signal from monomeric to dimeric form. B. Controls with Cys-less Ste2p-FT-HT and Ste2p-FT-HT. C. V68C and S292C receptors were untreated or treated with Cu-P in the presence or absence of NEM (N-ethylmaleimide) added prior to Cu-P treatment. D. Each indicated receptors were treated with Cu-P in the presence of NEM (N-ethylmaleimide) added prior to Cu-P treatment.

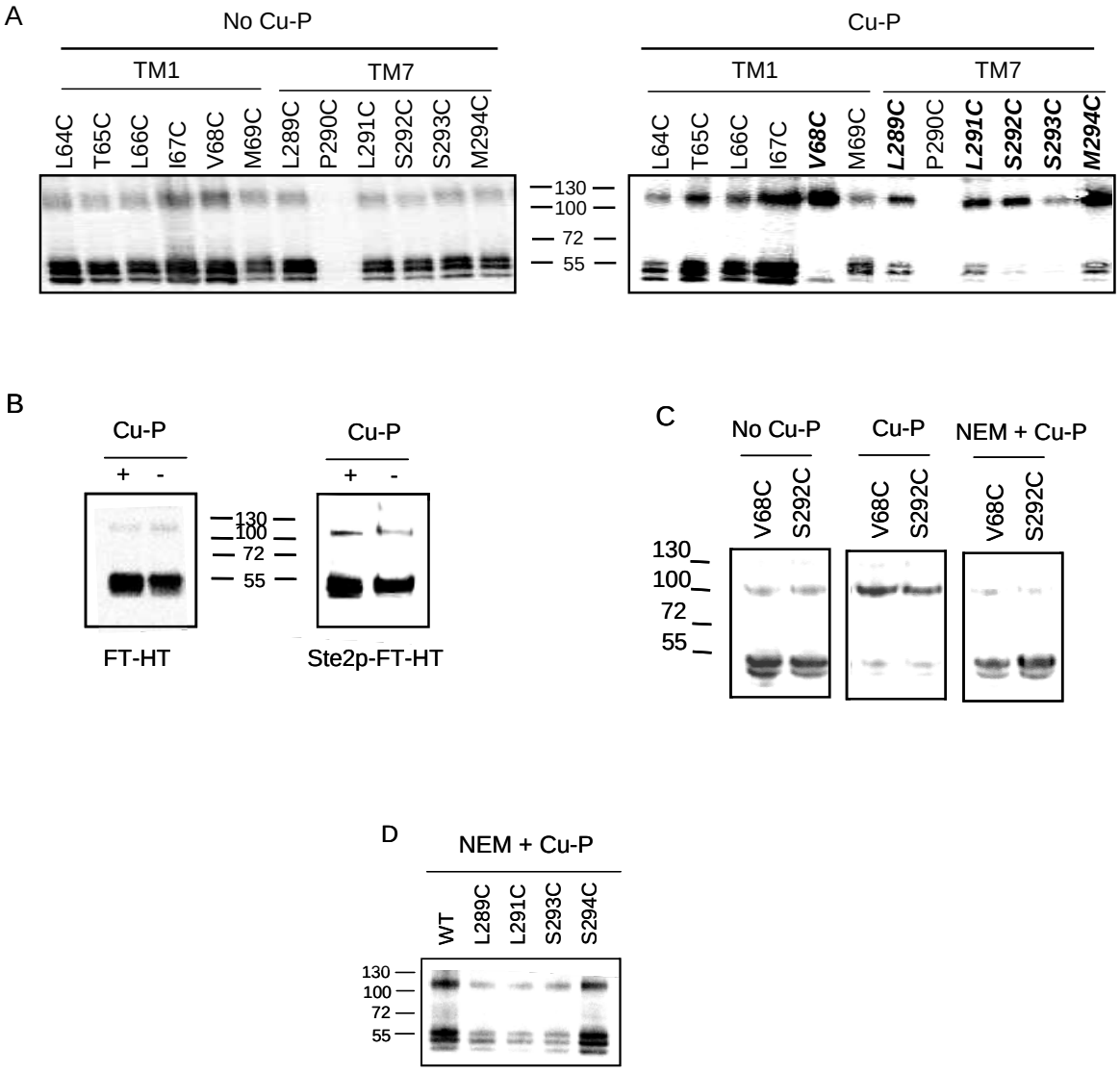
A
No Cu-P
Cu-P
TM1
TM7
L64C
T65C
L66C
I67C
V68C
M69C
L289C
P290C
L291C
S292C
S293C
M294C
130
100
72
55
B
Cu-P
+ -
FT-HT
Ste2p-FT-HT
C
No Cu-P
Cu-P
NEM + Cu-P
V68C
S292C
D
NEM + Cu-P
WT
L289C
L291C
S293C
S294C

Biological activity of each mutant was measured by growth arrest, β-galactosidase activity and binding assays and is normalized relative to the parent receptor (Table 8). Most mutant receptors showed similar β-galactosidase activity and growth arrest activity as compared to FT-HT-Xa. Two mutants (M69C and L283C) showed slightly lower induced β-galactosidase activities and A281C did not show growth arrest activity which is consistent with a previous study [43]. The difference between β-galactosidase activity and cell division arrest has been observed in many mutagenic studies of Ste2p [44-46]. It has been proposed that a short term signaling effect is measured by the β-galactosidase assay, whereas the long term effect is measured by the halo assay.

The α-factor binding affinities of most Cys mutants were the same and within the experimental error range (± 2.5 fold), with the exceptions of the S292C, receptor which showed an increase in binding affinity (5 fold lower Kd value), and the L283C and S288C which showed a decrease in binding affinity (up to 4.7 fold higher Kd values) as compared to that of FT-HT-Xa. B-Max values determined by a saturation binding assay indicated that the numbers of binding sites were similar to FT-HT-Xa for most mutant receptors, with the exceptions of T279C V280C, A281C and T282C, which showed expression about 50% lower than that of FT-HT-Xa. The P290C receptor showed no detectable α-factor binding, consistent with lack of measureable expression in the western blot analysis. Nonetheless, this receptor exhibited comparable growth arrest and β-galactosidase activities, suggesting that there were sufficient receptors expressed on the cell surface to elicit these biological responses upon ligand treatment (Table 8), albeit below detectable levels as measured by binding or western blots. Previous studies have

Table 8 Biological activities of Cys mutant receptors

Receptor		β-galactosidase Activity		Growth Arrest activity[3]	Binding Assay[4]	
		Basal Activity[1]	Induced Activity[2]		B-Max	Kd(nM)
FT-HT-Xa		1.0 ± 0.1	1.0 ± 0.1	1.00	1.0 ± 0.3	1.0 ± 0.3
TM1	L64C	1.0 ± 0.1	0.9 ± 0.2	1.00	1.7 ± 0.2	2.5 ± 0.7
	T65C	0.9 ± 0.1	0.9 ± 0.1	1.08	1.2 ± 0.2	1.5 ± 0.7
	L66C	1.0 ± 0.1	1.3 ± 0.5	1.00	0.5 ± 0.1	0.5 ± 0.2
	I67C	1.0 ± 0.1	1.1 ± 0.3	1.04	1.5 ± 0.1	2.2 ± 0.5
	V68C	1.0 ± 0.1	0.9 ± 0.3	1.00	0.9 ± 0.2	1.1 ± 0.4
	M69C	1.1 ± 0.1	0.7 ± 0.2	1.00	0.7 ± 0.1	1.0 ± 0.4
TM7	T278C	0.7 ± 0.1	0.9 ± 0.2	0.88	0.7 ± 0.1	0.7 ± 0.3
	T279C	1.1 ± 0.2	0.9 ± 0.1	1.08	0.4 ± 0.1	0.4 ± 0.1
	V280C	0.8 ± 0.1	1.3 ± 0.5	1.00	0.3 ± 0.1	0.5 ± 0.1
	A281C	0.5 ± 0.1	1.1 ± 0.3	n.d	0.4 ± 0.1	0.8 ± 0.2
	T282C	1.8 ± 0.5	0.9 ± 0.3	1.00	0.4 ± 0.1	0.9 ± 0.2
	L283C	1.6 ± 0.3	0.7 ± 0.2	0.96	1.7 ± 0.7	4.7 ± 1.3
	L284C	1.0 ± 0.1	0.8 ± 0.2	0.92	0.6 ± 0.1	1.1 ± 0.3
	A285C	1.4 ± 0.1	1.0 ± 0.1	0.88	0.7 ± 0.2	0.9 ± 0.2
	V286C	1.3 ± 0.1	1.0 ± 0.3	1.12	0.7 ± 0.1	1.9 ± 0.7
	L287C	1.7 ± 0.1	1.0 ± 0.3	1.01	0.8 ± 0.1	1.1 ± 0.1
	S288C	1.1 ± 0.1	1.0 ± 0.3	1.00	0.7 ± 0.1	4.1 ± 1.5
	L289C	1.4 ± 0.1	0.8 ± 0.2	0.92	1.3 ± 0.2	2.1 ± 0.6

(Table 8 continued)

P290C	1.4 ± 0.1	1.0 ± 0.1	0.88	n.d.	n.d.
L291C	1.3 ± 0.1	1.0 ± 0.3	0.88	0.6 ± 0.1	1.7 ± 0.8
S292C	1.4 ± 0.1	1.0 ± 0.3	1.04	0.6 ± 0.1	0.2 ± 0.1
S293C	1.5 ± 0.1	1.0 ± 0.3	1.00	1.2 ± 0.1	2.5 ± 0.4
M294C	1.2 ± 0.1	1.2 ± 0.4	0.94	0.8 ± 0.1	0.9 ± 0.2
W295C	1.7 ± 0.3	1.5 ± 0.3	1.01	1.3 ± 0.1	1.3 ± 0.1
A296C	1.7 ± 0.4	2.5 ± 0.8	1.00	0.7 ± 0.1	0.4 ± 1.5

[1]Relative activity (±standard deviation) compared with basal activity of FT-HT-Xa (Miller unit of FT-HT-Xa was 3.9)

[2]Relative activity (±standard deviation) compared with induced activity of FT-HT-Xa at 1μM of α-factor (Miller unit of FT-HT-Xa was 31.7)

[3]The relative halo size (growth arrest) was compared to the halo size of the FT-HT-Xa receptor at 2μg of α-factor applied to a disc (the halo size of FT-HT-Xa was 24 mm). The standard deviation of the halo activity for all receptors was within ± 0.2 (three replicates). n.d. = not detected

[4]The Bmax and Kd values are presented relative to those of the FT-HT-Xa receptor. The Bmax and the Kd were determined by saturation binding of radioactive α-factor according to the protocol in Methods. n.d. = not detected, as the binding was not greater than background (B-Max of FT-HT-Xa was 3491 and Kd was 10.7nM).

shown that remarkably low levels of Ste2p at the cell surface are sufficient to manifest the biological responses [47]. Taken together, we conclude that Cys mutation of the targeted residues did not severely interfere with receptor expression and function. We did not use the P290C receptor further in this study as it was expressed at a very low level.

Dimerization of Some Cys Mutants in TM1 and TM7 Is Markedly Enhanced by the Oxidizing Reagent Cu (II)-1, 10-Phenanthroline

Initially we tested the involvement of twelve TM residues, six on TM1 and six on TM7 (L289 – M294) proximal to the cytoplasmic face of Ste2p (Fig. 14), in dimerization. As stated above, FT-HT-Xa and virtually all of the single Cys containing Ste2p mutants exhibited weak bands at about 110 kDa consistent with a small amount of dimerized Ste2p. However, in all cases the predominant band was near 55 kDa, the molecular mass of monomeric Ste2p. When these same receptors were treated with Cu (II)-1, 10-phenanthroline (Cu-P), a reagent that has been used as an oxidizing reagent to drive disulfide bond formation in membrane proteins [48-51], many of the Cys mutated receptors showed marked increases in the 110 kDa band and a concomitant decrease in the monomer band (Fig 15A, Table 9). Notably, V68C, a TM1 mutant and five mutants on TM7 (L289C, L291C, S292C, S293C and M294C) showed strong (>60%) dimerization upon Cu-P treatment (Fig. 15A, Table 9). When FT-HT (epitope tagged Cys-less receptor) and Ste2p-FT-HT (epitope tagged receptor with intrinsic cysteine residues at C59 in TM1 and C252 in TM5) receptors were tested, there was no difference in dimerization in the presence and absence of Cu-P treatment (Fig. 15B) indicating that increased dimerization of mutant receptors was due to the specific cysteine residues

Table 9 Effect of ligand binding on Cu-P (Cu (II)-1, 10-phenanthroline) stimulated disulfide bond formation[1]

Receptor		No treatment	Cu –P[2]	α, Cu-P[3]	A, Cu-P[4]
FT-HT-Xa		15.0 ± 4.4	12.0 ± 0.1	13.1 ± 0.2	12.2 ± 0.1
TM1	L64C	15.8 ± 0.1	11.3 ± 0.4	14.6 ± 1.0	13.6 ± 0.8
	T65C	16.2 ± 0.1	14.4 ± 0.1	15.9 ± 0.3	12.8 ± 0.3
	L66C	12.3 ± 0.4	11.9 ± 1.0	13.2 ± 0.4	11.9 ± 0.8
	I67C	19.3 ± 4.5	17.0 ± 0.1	17.4 ± 4.1	18.0 ± 2.0
	V68C	28.5 ± 3.2	99.2 ± 0.1	98.3 ± 0.8	98.8 ± 0.1
	M69C	17.7 ± 6.9	14.2 ± 5.0	17.0 ± 6.4	28.9 ± 10.2
TM7	T278C	15.1 ± 0.8	65.8 ± 8.8	12.5 ± 0.1	12.4 ±0.1
	T279C	17.3 ± 0.3	10.1 ± 2.3	15.8 ± 0.2	10.9 ± 2.7
	V280C	15.3± 2.1	14.7± 1.5	16.3 ± 0.6	12.4 ± 0.1
	A281C	16.8± 0.5	11.9± 0.6	14.3 ± 1.5	11.3 ± 0.1
	T282C	11.7± 0.3	15.4± 0.1	12.0 ± 0.8	11.7 ± 0.1
	L283C	16.6± 0.4	15.7± 0.2	13.3 ± 0.1	10.7± 3.5
	L284C	15.2± 0.1	12.0 ± 0.2	17.7 ± 3.0	15.3 ± 0.1
	A285C	16.5 ± 0.8	53.5 ± 8.3	16.5 ± 2.1	17.7 ±0.5
	V286C	15.6 ± 0.4	17.0 ± 0.3	13.2 ± 2.0	15.9 ±0.4
	L287C	16.0 ± 0.1	14.3 ± 1.3	11.3 ± 1.7	16.0 ±1.8
	S288C	14.7 ± 1.0	14.7 ± 1.5	11.5 ± 0.6	12.6 ±0.2
	L289C	26.8 ± 2.0	61.0 ± 9.8	50.2 ± 12.9	40.9 ±8.2
	L291C	31.8 ± 0.4	66.4 ± 0.1	52.0 ± 8.8	44.5 ± 5.6
	S292C	30.2 ± 8.3	82.3 ± 0.4	75.5 ± 11.4	65.9 ±0.2
	S293C	21.1 ± 0.7	70.2 ± 5.3	38.5 ± 8.3	44.0 ±0.1

(Table 9 continued)

M294C	27.0 ± 7.6	75.6 ± 1.0	57.8 ± 0.7	50.8 ± 1.0
W295C	15.7 ± 0.2	95.2 ± 0.7	76.2 ± 0.6	86.3 ±0.1
A296C	14.8 ± 2.1	91.1 ± 1.0	73.6 ± 1.5	82.1 ±0.8

[1]The intensity of the monomer and dimer signal was measured by densitometry and the ratio of the signals was determined. The intensity of the monomer and dimer signal was measured by densitometry and the ratio of the signals was determined. The percentage of dimer was calculated as [Dimer/(Dimer+Monomer) x100].

[2]Cu-P = Cu-P (Cu (II)-1, 10-phenanthroline) treatment.

[3]α, Cu-P = membranes treated with alpha-factor and Cu-P(Cu (II)-1, 10-phenanthroline).

[4]A, Cu-P = membranes treated with antagonist and Cu-P(Cu (II)-1, 10-phenanthroline).

engineered into Ste2p. To further test whether dimerization was mediated by disulfide bond formation involving cysteine residues, NEM (N-ethylmaleimide) pre-treatment was used. NEM alkylates the free –SH group of cysteine irreversibly, so that disulfide bond formation cannot occur after NEM treatment. As shown in Figure 15C and D, pretreatment of receptors, which increased dimer upon Cu-P, with NEM completely, eliminated the Cu-P mediated dimerization (Fig. 15C, and D). In addition, in all cases where a high level of crosslinking was observed the membranes were treated with Cu-P and the reaction terminated by EDTA only and by EDTA and NEM to prevent crosslinking that might occur upon subsequent manipulation of the sample. No differences were found in the extent of crosslinking with the additional NEM treatment (Table 10). In contrast to these six residues, placement of cysteine at positions 64, 65, 66, 67 and 69 followed by Cu-P treatment did not result in a dimer population that exceeded 20% (Fig. 15A, right panel). Taken together, the results indicate that insertion of cysteine residues at position 68 on TM1 and positions 289, 291, 292, 293 or 294 on TM7 led to high levels of Ste2p dimerization through disulfide formation.

Although the studies described above provided evidence for Cu-P catalyzed Ste2p dimerization, it was possible that the single Cys mutant Ste2p is cross-linking with other proteins with similar molecular weight to yield the observed high molecular weight bands. To confirm that the observed dimer band in the western blot was a Ste2p-Ste2p homo-dimer, we took advantage of the protease (Factor Xa) digestion site engineered into EL2 of Ste2p. Cross-linking between two Cys residues in TM7 followed by Factor Xa digestion would yield a homodimeric complex of 66 kDa (Fig. 16A). Indeed TM7 mutants (L289C, L291C, S292C, S293C and M294C) digested with Factor Xa led to

Table 10 Effect of NEM on Cu-P(Cu (II)-1, 10-phenanthroline) stimulated disulfide bond formation[1]

Receptor		No treatment	EDTA[2]	EDTA and NEM[3]
FT-HT-Xa		16 ± 2.3	17 ± 2.3	16 ± 0.1
TM1	V68C	22 ± 10.3	99 ± 0.3	99± 0.1
TM7	T278C	22 ± 13.5	61 ± 1.7	54 ± 0.3
	A285C	15 ± 4.5	58 ± 0.6	54 ± 0.2
	L289C	11 ± 5.0	59± 2.5	53 ± 0.9
	L291C	26 ± 8.8	64 ± 3.5	57 ± 0.1
	S292C	17 ± 3.2	76 ± 0.8	70 ± 6.5
	S293C	19 ± 5.5	75 ± 4.8	69 ± 4.8
	M294C	26 ± 1.1	72 ± 6.3	76 ± 3.7
	W295C	32 ± 8.3	80 ± 4.2	81 ± 3.5
	A296C	39 ± 0.9	66 ± 8.3	79 ± 5.2

[1] The intensity of the monomer and dimer signal was measured by densitometry and the ratio of the signals was determined. The percentage of dimer was calculated as Dimer/(Dimer+Monomer) *100.

[2] Sample was treated with Cu-P(Cu (II)-1, 10-phenanthroline) and the reaction was terminated by EDTA only

[3] Sample was treated with Cu-P(Cu (II)-1, 10-phenanthroline) and the reaction was terminated by EDTA and NEM

the appearance of a band near 66 kDa when SDS-PAGE was run under non-reducing conditions (Fig. 16B; left panel). This band was markedly reduced when the gel was run in the presence of β-mercaptoethanol, a potent disulfide reducing agent. The 66 kDa band was specific for dimerized receptors with a disulfide connection between monomers as the band was not observed for FT-HT-Xa (Cys-less) and a TM1 mutant (M69C) in which there was no disulfide-mediated dimer formation (Fig. 16B). The monomer bands (~55 kDa) are due to an incomplete Factor Xa digestion. We performed partial digestion because a longer incubation led to the degradation of all bands. Bands at ~33 kD are Factor Xa digestion products of the monomeric receptor species (remaining in the samples). The generation of this band from the S292C and S293C mutant receptors, in which the majority of receptors formed dimers (Fig. 15A, right panel), is likely the result of detergent induced (Triton X-100 in Factor Xa digestion buffer) dissociation of background dimers. Indeed, the presence of background dimers from all the receptors tested including FT-HT-Xa (Cys-less) and M69C were reduced in the presence of Triton X-100.

Further support for the disulfide bond induced dimer formation was provided when differentially tagged receptors were co-expressed. M294C mutants and FT-XT-Xa were chosen for this experiment. Membranes from cells co-expressing receptors tagged with the FLAG/His epitopes and receptors tagged with the Rho epitope were precipitated using the HIS-select HC Nickel affinity column and immunoblotted with anti-Ste2p antibody and anti-Rho antibody. The total amount of receptors present following immune precipitation was determined using an antibody directed against the N-terminus of the receptor (left panel, Fig. 17). For both the FT-HT-Xa/Rho-Xa and M294C/M294C-Rho

receptors, bands corresponding to monomeric and dimeric forms were detected in both the presence and absence of Cu-P treatment. The dimerized form was more abundant than the monomer for the M294C/M294C-Rho receptor due to the presence of the engineered cysteines which form disulfide bond thus increasing the dimer population. In contrast, the FT-HT-Xa/Rho-Xa receptor showed a prominent monomer band and weak dimer signal, as observed for FT-HT-Xa expressed alone. As seen in right panel of figure 17, using the anti-Rho antibody, only dimerized receptors were observed for the M294C-Rho receptor, which indicates that Ste2p did indeed homo-dimerize. These results and the cross-linking results demonstrate the proximal location of the residues (L289-M294) on the intracellular parts of the TM7 domains of two Ste2p molecules, and provide evidence for homo-dimerization of Ste2p involving TM7 as well as TM1. The finding that six consecutive residues in TM7, with the exception of P290C, showed an increase in dimerization was unexpected since this region is believed to be α-helical. To see whether dimerization would occur throughout TM7, we expanded Cys replacement to include the full TM7 by generating eleven additional cysteine mutants N-terminal to the L289 residue (T278C, T279C, V280C, A281C, T282C, L283C, L284C, A285C, V286C, L287C, and S288C) and two cysteine mutants C-terminal to the M294 residue (W295C and A296C). Membranes from each mutant were prepared and processed with or without Cu-P treatment. Compared to the Cys-less FT-HT-Xa receptor, the T278C and A285C receptors exhibited at least a 3-fold increase in dimerization (Fig. 18). Though dimer formation on T278C mutant was not observed in a recent study [21], this mutant showed strong dimer formation with Cu-P treatment in our study. The difference observed for this

Figure 16 Protease Factor Xa digestions of single cysteine containing Ste2p receptors

A. Diagram showing possible explanation for ~66 kDa band from TM7-TM7 interaction. B. Total membrane proteins derived from cells expressing indicated receptors. Cu-P treated membranes with Ste2p containing single Cys mutations at various positions as indicated were treated with Factor Xa as described in the Methods. The digests were subjected to SDS-PAGE under reducing or non-reducing conditions, immunoblotted and probed by anti-FLAG antibody.

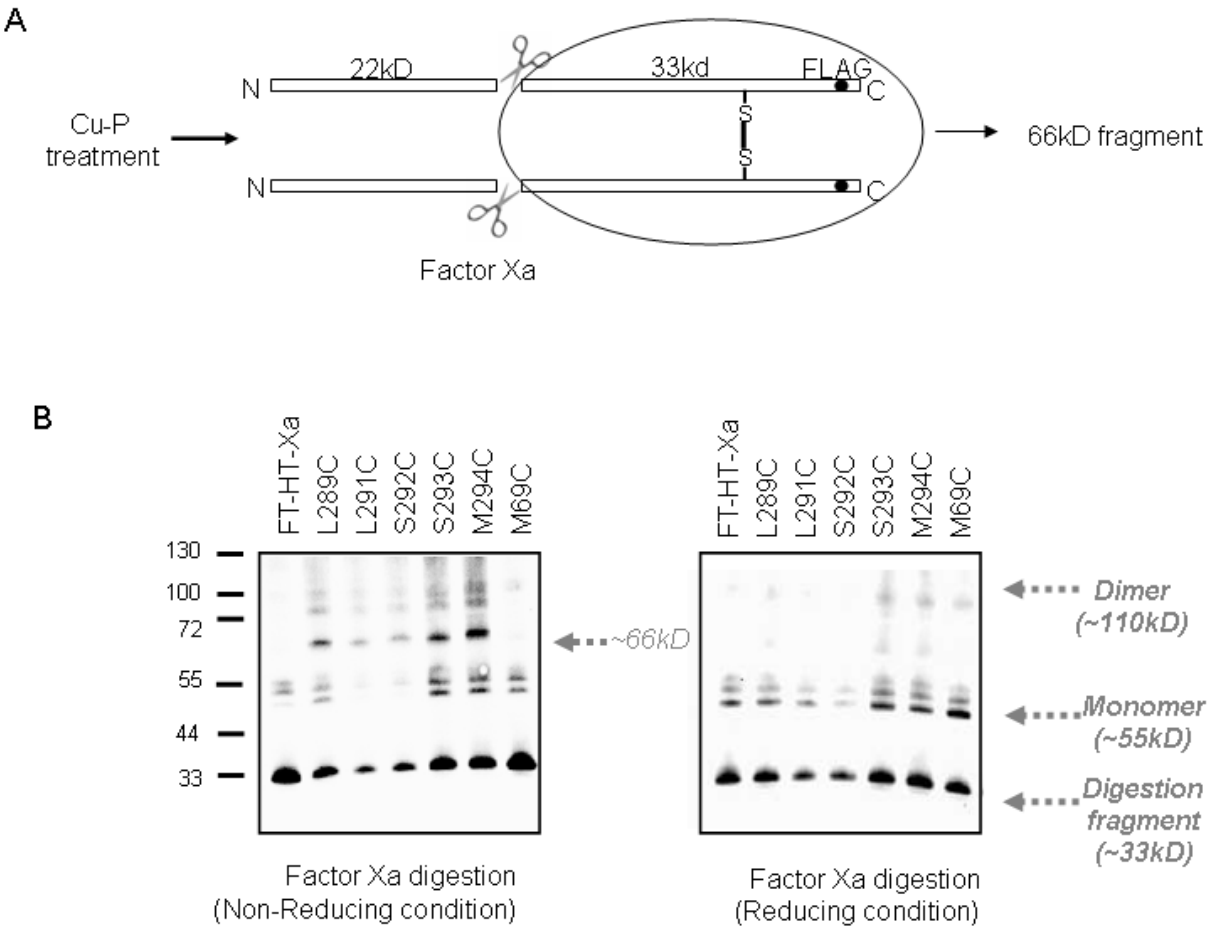
A
22kD
33kd
FLAG
N
C
Cu-P
treatment
66kD fragment
Factor Xa
B
FT-HT-Xa
L289C
L291C
S292C
S293C
M294C
M69C
130
100
72
55
44
33
~66kD
Dimer
(~110kD)
Monomer
(~55kD)
Digestion
fragment
(~33kD)
Factor Xa digestion
(Non-Reducing condition)
Factor Xa digestion
(Reducing condition)

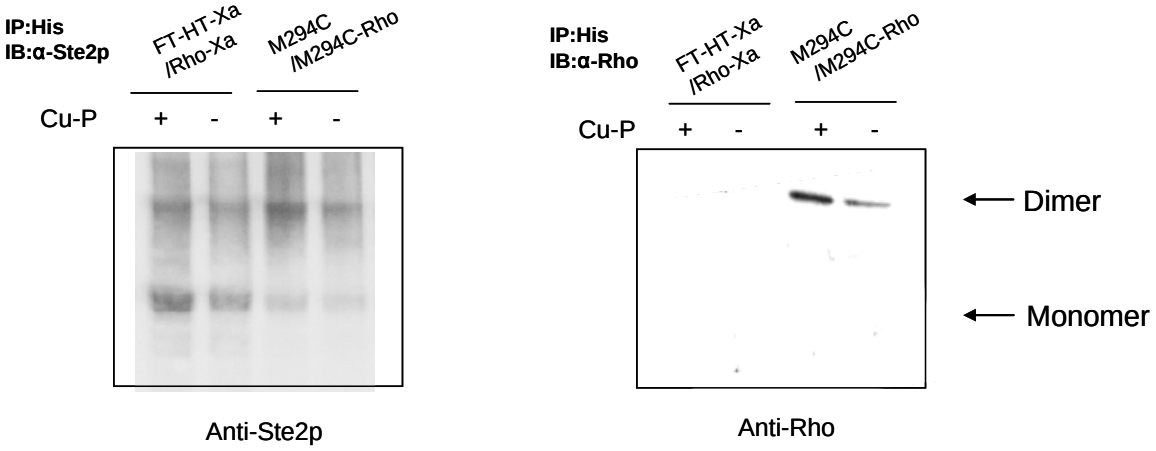

Figure 17 Pull-down assay

Total membrane was prepared from cells co-expressing differentially tagged receptors as indicated. Following treatment with or without Cu-P, samples were immunobloted with anti-Ste2p antibody (Left panel) or anti-Rho antibody (Right panel). The upper band (~110 kDa) represents dimerized receptor and the lower band (~55 kDa) represents monomer.

one residue is likely the result of variations in experimental design. In our current study Cu-P was used at a final concentration of 2.5 μM, while in the previous study the concentration was 500 μM. In addition, in our study we used membrane preparations whereas whole cells were used by Wang et al [21]. Receptors W295C and A296C showed a large increase in dimerization upon treatment with Cu-P compared to FT-HT-Xa, (Fig 18; Table 9). In contrast, nine mutants (T279C-L284C, V286C, L287C and S288C) gave virtually identical dimerization results in the presence and absence of the oxidizing agent (Fig. 18; Table 9). Again NEM (N-ethylmaleimide) pre-treatment completely eliminated the Cu-P mediated dimerization (Fig. 18C). These results indicate that unlike the residues C-terminal to Pro290, residues located N-terminal to Pro290 exhibit a periodicity with respect to dimer formation of Cys mutants which is consistent with the α-helical structure predicted for typical transmembrane domains of GPCRs. Because of a concern that disulfide crosslinking might trap and thereby favor the accumulation of dimer during the 30 min oxidization reaction, we analyzed the efficiency of the dimer formation at different times (Fig. 19). The results indicated that L291C, S292C, S293C, M294C, and W295C started to form dimers after 45 seconds of Cu-P incubation and reached half maximum levels within 5 minutes. Previously, the relative distance between TM residues in rhodopsin was estimated by the reaction time for disulfide formation between to Cys residues on different TMs [52]. Thus, our data indicate that TM7 C-terminal to P290 is highly flexible allowing all of the residues in this part of TM7 to form disulfide bonds with more or less the same rapidity.

Effect of Ligand Addition on Dimerization

It is generally believed that activation of GPCRs upon ligand binding results in a conformational change involving rearrangement of transmembrane domains [53-56]. To ascertain whether this conformational change would affect Ste2p dimerization, we investigated the changes in the dimerization pattern of Ste2p receptors in the presence and absence of ligand. The membranes expressing each mutant receptor were incubated with agonist (α-factor) or an antagonist ([desW1, desH2] α -factor) and then treated with Cu-P. Dimer and monomer formation were monitored by western blots (Fig. 20A and 20B) and the ratio of dimer to monomer was determined (see Methods, Table 9). Dimer formation of the Cys-less FT-HT-Xa receptor in the presence or absence of Cu-P was not affected by agonist or antagonist (Fig.20A and Table 9). Also, the ratio of dimer to monomer formed by Cu-P mediated cross-linking of the TM1 cysteine mutants did not change significantly after incubation with α-factor or α-factor antagonist (representative results for V68C is shown in Fig. 20B and Table 9). A time course of crosslinking at 0.75, 2, 5, 10, 20, and 30 min was also performed with the V68C receptor incubated with either α-factor or antagonist. The reaction was complete at 45 seconds (0.75 min) and no change in crosslinking relative to that observed in the absence of ligand was observed (Fig. 21). TM7 mutants which did not exhibit increased levels of dimerization upon Cu-P treatment (T279C-L284C, V286C, L287C and S288C), also showed no difference in dimer formation in the presence of α -factor or antagonist (representative results for S288C is shown in Fig. 20B Table 9). However, for those TM7 receptors which exhibited significant increase in dimer formation upon Cu-P treatment (A285C, L289C, L291C, S292C, S293C, M294C, W295C, and A296C), α-factor treatment decreased the relative

amount of dimer formation (representative results for T278C and W295C are shown in Fig. 20B and Table 9). Taken together, the dimer interface of TM7 of Ste2p changed in response to either agonist or antagonist binding.

Figure 18 Effect of Cu-P (Cu (II)-1, 10-phenanthroline) treatment on FT-HT-Xa containing cysteine replacements in TM7

Membranes were prepared, treated without (A) or with (B) Cu-P reagent, solubilized and separated on SDS-PAGE. Each sample was immunoblotted and probed with anti-FLAG antibody. The upper band (~110 kDa) represents dimerized receptor and the lower band (~55 kDa) represents monomer. C. Each indicated receptors were treated with Cu-P in the presence of NEM (N-ethylmaleimide) added prior to Cu-P treatment.

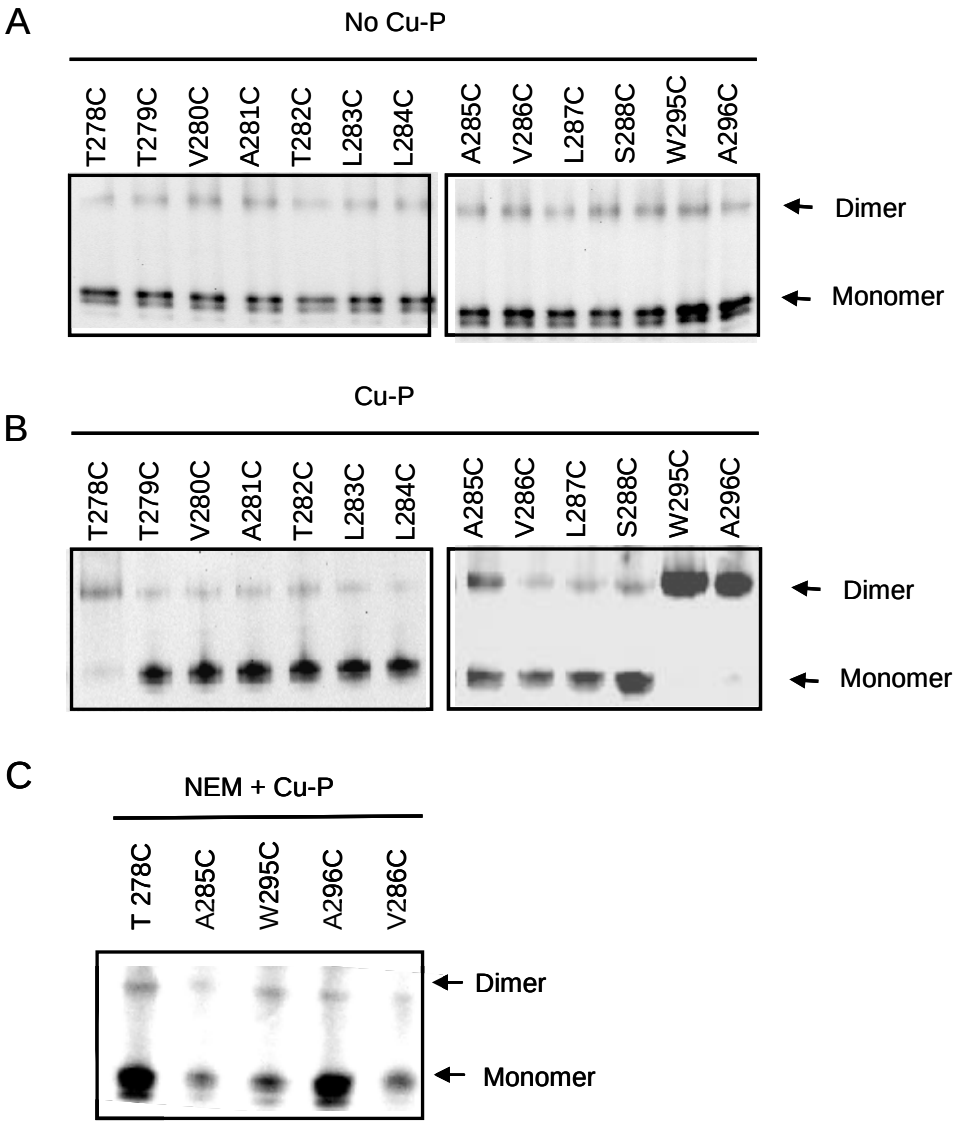
A
No Cu-P
T278C
T279C
V280C
A281C
T282C
L283C
L284C
A285C
V286C
L287C
S288C
W295C
A296C
Dimer
Monomer
B
Cu-P
T278C
T279C
V280C
A281C
T282C
L283C
L284C
A285C
V286C
L287C
S288C
W295C
A296C
Dimer
Monomer
C
NEM + Cu-P
T 278C
A285C
W295C
A296C
V286C
Dimer
Monomer

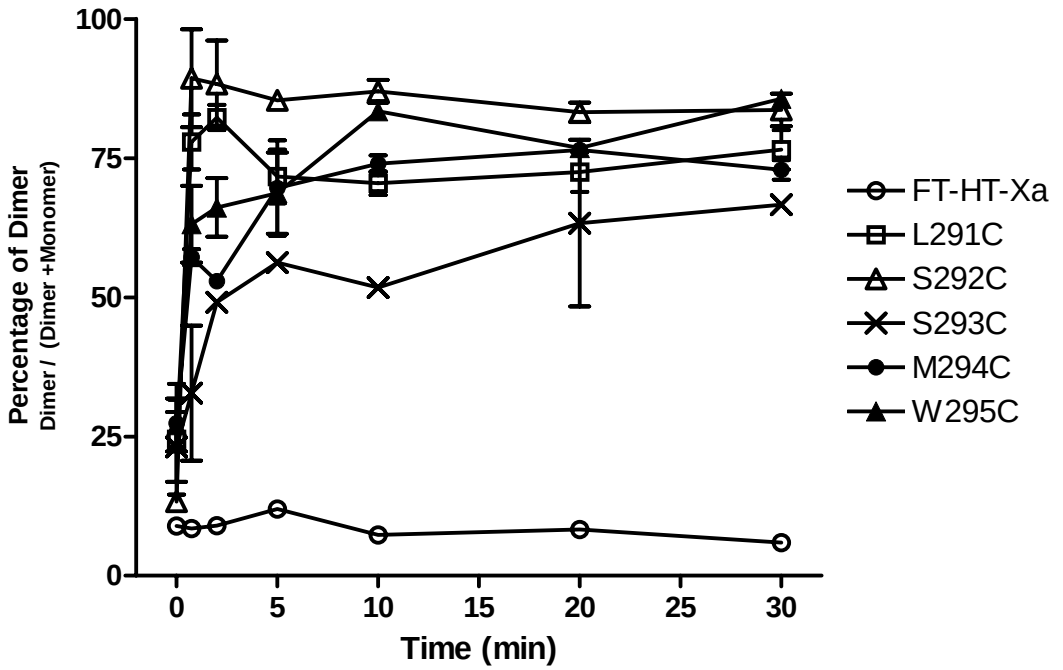

Figure 19 Time course analysis of dimer formation at the residues C-terminal to P290 of TM7

Total membranes were prepared from cells expressing each receptors and treated with Cu-P (Cu (II)-1, 10-phenanthroline) for 45 sec, 2 min, 5 min, 10 min, 20 min, and 30 min. The samples were analyzed by SDS-PAGE, following by immunoblotting with anti-FLAG antibody. The average percentage of dimer population from three independent experiments was calculated and plotted.

Figure 20 Effect of ligand binding on Cu-P (Cu (II)-1, 10-phenanthroline) stimulated disulfide bond formation

A, B. Total membrane protein was derived from cells expressing indicated receptors. Each sample was immunoblotted and probed with anti-FLAG antibody. FT-HT-Xa receptor was treated as indicated. B '-' indicates no treatment, '+' indicates Cu-P treated samples, 'α +' indicates samples incubated with α-factor followed by Cu-P treatment and 'A+' indicates samples incubated with the antagonist, [desW1, desH2]α-factor, followed by Cu-P treatment.

A

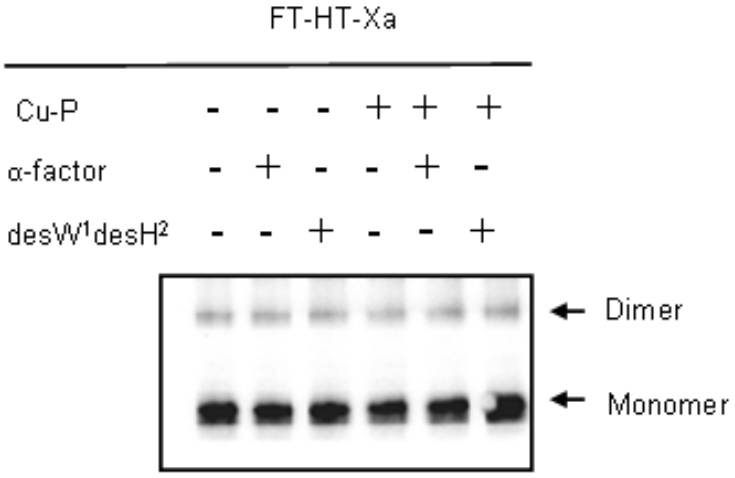
FT-HT-Xa
Cu-P - - - + + +
α-factor - + - - + -
desW1desH2 - - + - - +
Dimer
Monomer

B

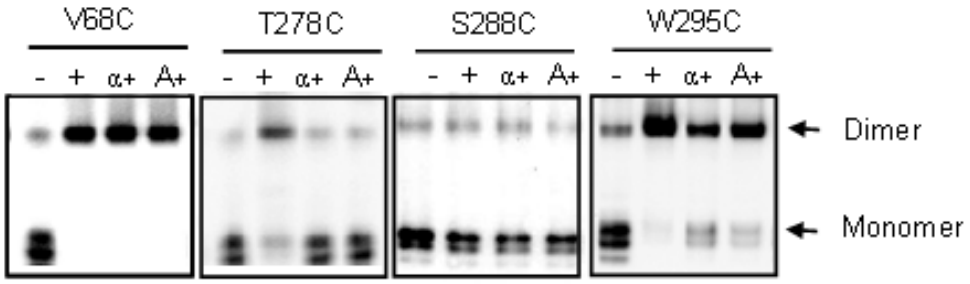
V68C
T278C
S288C
W295C
- + α+ A+
Dimer
Monomer

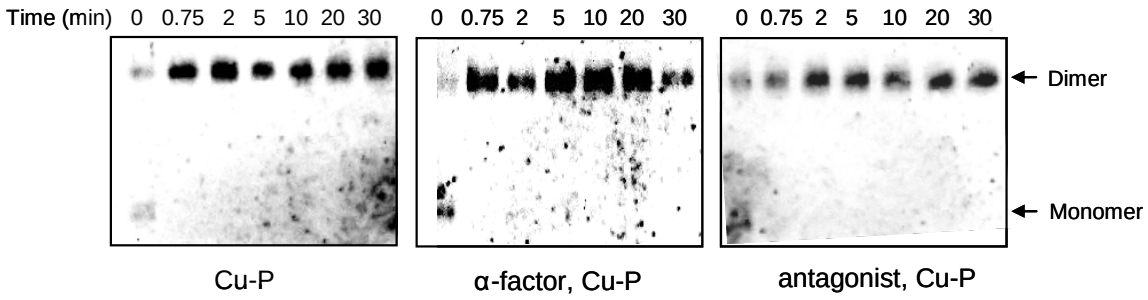

Figure 21 Time course cross-linking of V68C

Total membranes were prepared from cells expressing V68C receptor and treated as indicated. 'Cu-P' indicates Cu (II)-1, 10-phenanthroline (Cu-P) treated samples, 'α-factor, Cu-P' indicates samples incubated with α-factor followed by Cu-P treatment and 'antagonist, Cu-P' indicates samples incubated with the antagonist [desW1, desH2] α -factor followed by Cu-P treatment. Cross-linking was terminated at 45 sec, 2 min, 5 min, 10 min, 20 min, and 30 min. The samples were analyzed by SDS-PAGE, following by immunoblotting with anti-FLAG antibody. The upper band (~110 kDa) represents dimerized receptor and the lower band (~55 kDa) represents monomer.

CHAPTER 5 Discussion

In this study, using a disulfide cross-linking methodology, we identified a specific residue in TM1 that interacts with itself in Ste2p dimers, and we present the first evidence that residues in TM7 of this receptor participate in its dimerization. All of our studies were conducted with Ste2p in its membrane-bound state. Previously, it was shown that the maximum distance between α-carbons linked by disulfide bonds is about 7Å [57]. Thus, cross-linking experiments should identify amino acid side chains that are in close proximity when using the Cu-P oxidation reagent, which facilitates oxidation of sulfhydryl groups in cysteine residues. In analyzing our data, it is important to note that disulfide crosslinking might trap transient intermediates. Depending on the time of cross-linking relative to the rates of interconversion of the monomeric and dimeric states of the receptor, covalent cross-linking might affect the equilibrium and bias the sample to yield more dimeric species than are present in the native population of the receptor. However, by comparing the cross-linked population of a receptor mutated in a specific region we believe we can learn about the relative tendencies of individual residues to participate in receptor-receptor contacts. Cross-linking between cysteine residues engineered into GPCRs and the use of Cu-P as an oxidizing reagent to facilitate disulfide bond formation between TMs in GPCRs has been used extensively by the Wess and Oprian laboratories [48, 51, 55, 58, 59] and was recently applied to Ste2p dimerization [21].

It had been suggested that TM1 formed a component of the interface between the two receptors in the Ste2p dimer [19, 21, 60]. Our results support these findings and furthermore provide direct evidence for the involvement of V68 in TM1 in Ste2p

dimerization. The mutant receptor V68C showed markedly increased dimerization over that of the FT-HT-Xa after Cu-P treatment, while under identical conditions all of the remaining TM1 Cys receptors showed at most a minor increase in dimer formation (Fig. 15A; Table 9). The ability of V68C to form dimers is in good agreement with the recently published finding of a V45C-V45C cross-linking [21] since V45 and V68 are both located on the same face of TM1 and on opposite ends of TM1 (Fig. 22A). It was previously proposed that $G^{56}XXXG^{60}$ residues in TM1 of one GPCR monomer interacted with a hydrophobic-rich surface of TM1 (perhaps involving residues I53, V57, A61, and L64), on the second monomer by a kind of "groove-in-ridge" association with Gly being the "groove" residues and the hydrophobic residues acting as the "ridges" [19]. In this study, we found that V68C formed a disulfide bond. The fact that only one residue in the sequence ($L^{64}T^{66}L^{67}I^{67}V^{68}M^{69}$) formed this linkage suggests that the Ste2p-Ste2p interactions involving this region of the TM1 helix have significant spatial restrictions and that the TM1 helix at the carboxyl side of the $G^{56}XXXG^{60}$ sequence may be relatively rigid. We note that a biophysical analysis of TM1 in micelles indicates that the $G^{56}XXXG^{60}$ motif itself is flexible [[61] and unpublished results] and may facilitate TM-TM interactions between proximal helical elements. In any event our mutational analysis of the TM1 domain defines a specific residue (V68) that appears to be involved in Ste2p dimerization. In a previous FRET analysis, Overton and Blumer [60] analyzed the transmembrane domains of Ste2p that are involved in dimerization by expressing various combinations of Ste2p fragments. They concluded that TM1 is necessary and probably

Figure 22 Dimerization interfaces of Ste2p

A. V68 (red), a dimer contact found in the current study, is located on the same plane with V45 (green) a dimer contact at the extracelluar end of TM1 [21]. The backbones of two glycine residues (blue) known to play a role in Ste2p dimerization are shown. Two residues (F55, R58) involved in ligand binding are presented as a stick model located on the opposite side of the dimer interface. B. TM7/TM7 dimer interface. The backbones of three dimer contacts identified from the current study (T278, A285 and L289, from top to bottom) are colored green. A281 (light gray) and T282 (red) would appear to be candidates for dimer contact based on a sideview of TM7 (Fig. 23A), but the model here shows that alignments of these two residues are not favorable for disulfide bond formation. C. Proposed oligomerization interfaces of Ste2p. Dimerization of Ste2p involving TM1/TM1 (magenta) and/or TM7/TM7 (yellow) interface allows TM4/TM4 interface (dark grey) to mediate a new dimerization contact enabling oligomerization. An extracellular view of a representative trimer is shown.

A

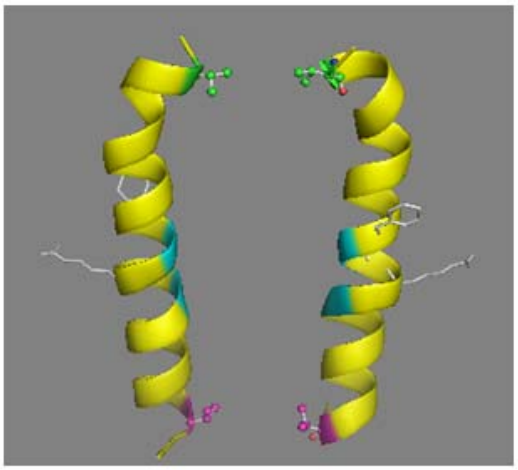

B

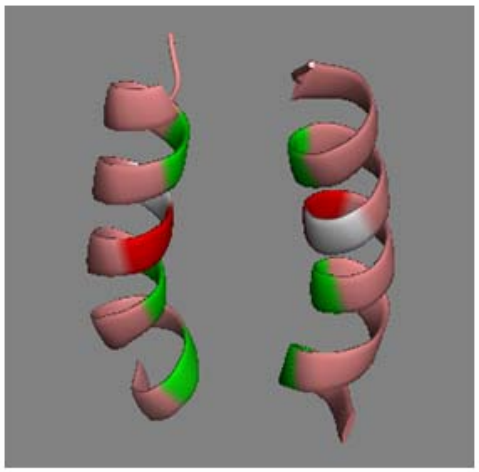

C

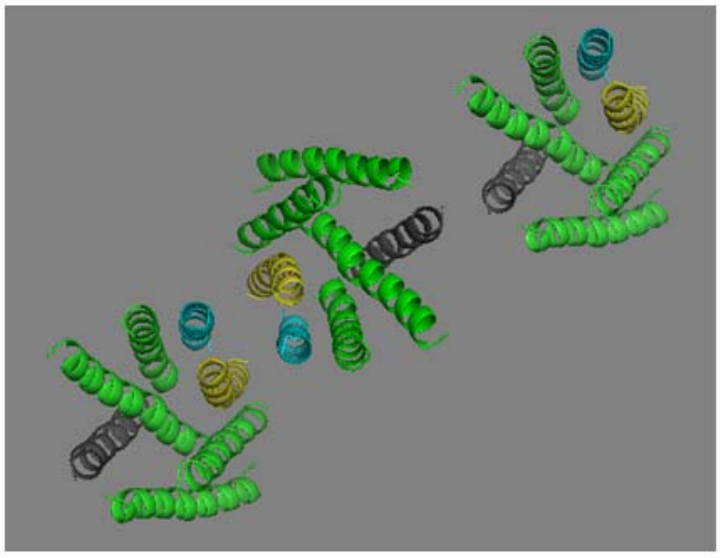

sufficient for dimerization, although they speculated that the N-terminus and TM2 may contribute to stabilize the dimers. However, our disulfide cross-linking data demonstrated that TM7 is also involved in the interface for dimerization of Ste2p. In the present study we have analyzed full-length receptors and it is possible that the fusion of fluorescent protein at the C-terminal of truncated receptors in the previous FRET studies hampered the interactions between TM7 domains. The involvement of TM7 in dimer formation is consistent with our previous observation that a TM6-TM7 fragment of Ste2p runs as a dimer in SDS-PAGE gel [62].

The finding that TM7 residues are involved in Ste2p dimerization leads us to propose that at least three dimerization interfaces can exist in Ste2p. In addition to the TM1 and TM4 interfaces previously found [21, 60], our data suggests that TM7-TM7 interactions are also involved in direct contacts in the Ste2p dimer. Since TM1-TM1 and TM4-TM4 contacts have been previously suggested to be involved in higher order oligomers [21] and a Ste2p trimer was demonstrated by crosslinking in a gel and by atomic force microscopy [40] it is possible that in a single receptor can interact simultaneously with two additional receptors with different interfaces between the monomers: TM7 and/or TM1 can interact with TM7 and/or TM1 of a second receptor, while TM4 can interact with TM4 of a third receptor to form oligomers. A representation of a trimer is shown in Fig. 22C. With higher oligomers envisaged to contain additional interactions. Based on the existing experimental data it is not possible to conclude whether TM1-TM1 and TM7-TM7 dimers can be formed simultaneously in the cell. The results described in this study show that cysteine residues introduced in positions T278, A285 and L289 on the extracellular half of TM7 form a disulfide bond with their

counterpart in another Ste2p monomer (Fig. 23A). This finding provides valuable information relating to the arrangement of the TM bundles of Ste2p and allow us to present a helical wheel projection of TM7 (Fig. 23B) in which these three residues are oriented outward instead of facing inside the TM bundles as proposed previously in the Ste2p model based on rhodopsin [35]. A281 and T282, which in a two dimensional representation (Fig. 23A, 23B) appear to lie on the same helix face, do not form dimers. However, our 3D model suggests that A281 and T282 are not close enough to form disulfide bonds when replaced by Cys as illustrated in the modified model (Fig. 22B). Therefore, the dimerization mediated by T278, A285, and L289 is consistent with the alpha-helical periodicity in TM7 that continues up to Pro 290. In the absence of a crystal structure for Ste2p, the disulfide crosslinking results contributes to understanding structural features of the functional receptor such as inter-helical interactions that may be involved in oligomerization.

In contrast to the specific pattern of residues which could participate in cross-linking in the portion of TM7 most adjacent to the extracellular surface, when the engineered cysteine residues were located at the intracellular end of the TM7, C-terminal to Pro290 which creates a kink in TM7, all residues were able to form disulfide bonds (Fig. 23A) implying an absence of an ordered structure. We do not believe that the experimental protocol, specifically the use of the oxidizing agent, leads to a global denaturation of Ste2p because native cysteine residues in TM1 (C59) and TM5 (C252) did not form an inter-GPCR disulfide linkage under the same experimental conditions

Figure 23 Representation of cross-linking results of TM7 and helical wheel presentation of TM1 and TM7 in Ste2p

A. Summary of TM7 cysteine cross-linking results. The horizontal lines represent the boundary of the cell membrane. Residues indicated by a circle filled in gray when mutated to Cys are involved in dimer formation, whereas those residues shown in a box do not form disulfide bonds. Residues marked by an * compensate for the non-functional Y266C mutation. B. Helical wheel presentation of TM1 and TM7. Residues indicated by a circle filled in gray are involved in dimer formation as found in this study. Residues marked by an X are important for ligand binding.

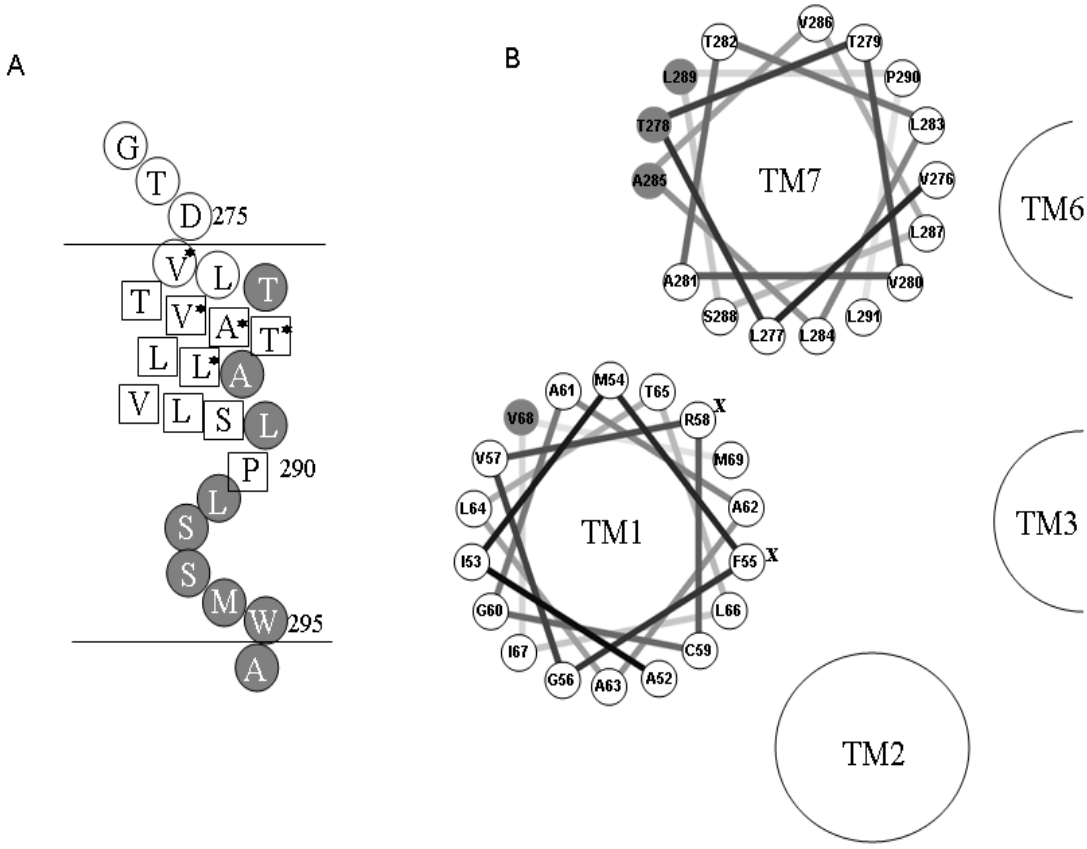
A
G
T
D
275
V
L
T
T
V
A
T
L
L
A
V
L
S
L
P
290
L
S
S
M
W
295
A
B
V286
T282
T279
L289
P290
T278
L283
A285
TM7
V276
TM6
L287
A281
V280
S288
L277
L284
L291
A61
M54
T65
V68
R58
X
V57
M69
L64
TM1
A62
TM3
I53
F55
X
G60
L66
I67
C59
G56
A63
A52
TM2

(Fig. 15B). Additionally, only one of the TM1 cysteine mutants formed Ste2p dimers and only three residues out of twelve in the extracellular part of the TM7 showed increased dimerization. Rather we propose that the L291-W295 region of Ste2p may be flexible enough to allow these residues to be exposed for disulfide bond formation with their counterpart in a second Ste2p monomer. Proline residues disrupt hydrogen bonding and have been shown to twist the standard structure of helices by introducing a kink between the segments contiguous with each other and to form molecular hinges [41, 63]. The dynamic nature of the residues at the carboxyl side of Pro290 is consistent with the results of a high resolution analysis of a 73 residue fragment of Ste2p in DPC micelles which indicated that the Pro290 resulted in a kinked helix in this membrane mimetic environment [64]. An irregular helical structure in part of a TM has been documented in the crystal structures of other GPCRs. In rhodopsin, TM7 contains a helical segment near the extracellular face of the receptor, followed by a non-helical segment in the vicinity of P303 [36]. The crystal structure of the beta-adrenergic receptor also indicates the presence of a short extended area in TM7 [65]. In addition, it has been proposed, using computational simulations of the NPXXY motif, that this region was not an ideal alpha helical structure [66]. Thus, there is precedent to propose that the part of TM7 in Ste2p that is near the cytoplasmic membrane interface is not helical in structure. Although there is a possibility that the residues C-terminal to Pro290 are not in the transmembrane domain, this is unlikely because a previous study [42] and our cysteine accessibility results for these residues, strongly suggested that W295 and A296 are the boundary between TM7 and the intracellular space (Fig. 24 and Table 11). Obviously, non-hydrogen bonded elements of a peptide in a membrane represent a high energy state

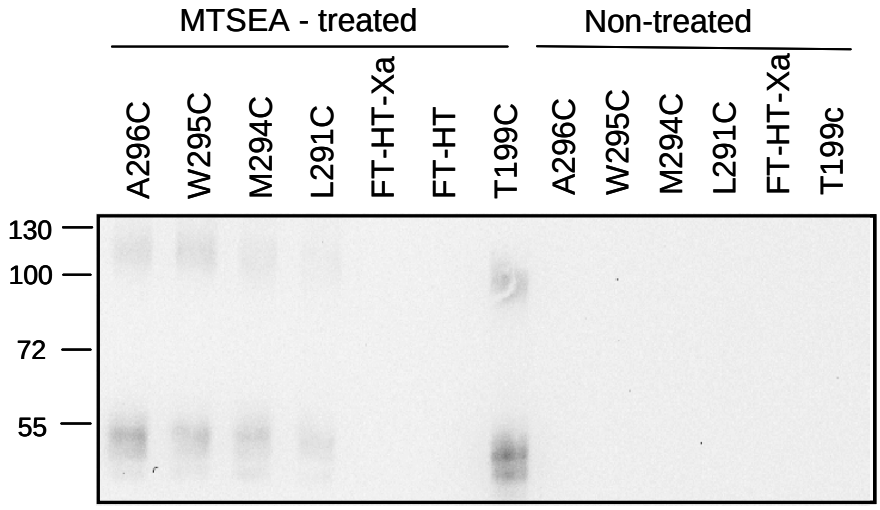

Figure 24 Cysteine labeling of selected mutants

Membranes were prepared from cells expressing each receptors and treated with MTSEA-biotin or non-treated as indicated. Then, the samples were analyzed by SDS-PAGE, following by immunoblotting with anti-FLAG antibody.

Table 11 Cysteine labeling of selected mutants

Residue	% of MTSEA biotin labeling[1]
T199C	100
L291C	22.5
M294C	37
W295C	40
A296C	63

[1]Labeling was expressed as a percentage of accessibility for each individual mutant after normalization with T199C accessibility (=100%) as described in the Experimental Procedures

and it is possible that critical water molecules satisfy some of the required interactions for Ste2p. Water molecules that bridge various receptor regions have been implicated in the crystal structure of other GPCRs [36, 65]. Their involvement in the structure of Ste2p must await a high resolution structure of this GPCR.

It has been observed that the homo-dimer interface of the dopamine D2 receptor can be altered upon ligand binding [50]. To monitor possible ligand-induced conformational changes in Ste2p dimerization, membrane samples were incubated with either agonist or antagonist followed by Cu-P treatment. TM1 mutants showed similar degrees of dimer formation in the presence or absence of ligand, which is consistent with a recent study showing that dimer formation of V45C at TM1 was insensitive to α-factor treatment [21]. In contrast, both agonist and antagonist treatment led to a decrease in the level of dimer formed by TM7-TM7 interaction indicating that ligand binding caused a conformational change in this region. In addition to a conformational change inTM7 induced by ligand binding, we can not rule out changes elsewhere in Ste2p upon ligand binding that affects dimer formation.

The effect of ligand binding on TM7-mediated dimer formation suggests that resting state dimers and activated state dimers involve different TM arrangements. Previously it was shown that the ratio of monomer to dimer did not change in the presence of ligand in Ste2p as tested by FRET [17]. Thus, it is possible that the equilibrium distribution between monomer-dimer is maintained during receptor activation, even while the dimer interface may differ. In addition, a recent study of the serotonin 5HT2c receptor demonstrated that ligand binding induces a differential effect

on the dimer interfaces. While the TM1/TM1 interface was insensitive to ligand treatment, the TM4/5 interface changed during receptor activation [67].

Interestingly, a number mutations of residues (V276, V280, A281, T282, and L284) which compensated for the activity of the signaling defective mutant receptor Y266C are clustered at the extracellular portion of the TM7 (Fig. 23A, TM7 residues labeled as *)[68]. The cluster of compensatory mutations at the extracellular part of TM7 indicates that this region is important for receptor activation. The decrease in dimer formation at TM7 after ligand binding that we showed for T278C and A285C, both located in the extracellular part of TM7, also suggest a conformational change in this portion of Ste2p. In addition, two residues in TM1 (M54 and F55) were also identified [68] as compensatory mutations for Y266C. Residues F55 and R58 are known to be ligand contact sites and M54 is adjacent to F55 [23, 69]. Therefore, the extracellular ends of TM1 and TM7 may play a key role in initiating receptor activation after ligand binding to TM1 and the subsequent conformational change of TM7 may facilitate the receptor to adopt a fully activated state. Thus, the regions of the receptor that experience changes in the formation of dimers upon ligand binding might be important for the activation mechanism. Many GPCRs assume different conformations in their active and inactive states, and it is widely accepted that GPCRs sample many states even when occupied by ligand [for review see [70]]. Under our experimental conditions Cu-P mediated disulfide formation appears to distinguish these different conformations, possibly implicating a change of the dimer interface as part of the receptor activation mechanism.

The similar effects of agonist and antagonist binding on disulfide formation involving residues in the TM7 dimer interface can be understood in terms of distinct

binding and signaling domains for α-factor [71]. Extensive structure-function analysis of α-factor and Ste2p has revealed that the N-terminus of α-factor has a role in activating the receptor while the C-terminus is critical for receptor binding. Since agonist (WHWLQLKPGQPNleY) and antagonist (WLQLKPGQPNleY) are very similar (10 identical residues out of 13), and both ligands compete with each other with high affinity in binding to Ste2p, it is reasonable to suppose that the binding sites of both ligands in the receptor are highly overlapping especially at the C-terminal end of the ligands. Moreover, we believe that ligand binding is a multi-step process in which the carboxyl terminus of α-factor and α-factor antagonists bind first and then several conformational changes occur along the activation pathway [72, 73]. Finally, the carboxyl terminus has been shown to interact with residues in TM1 [23, 73]. Based on this understanding it is not unreasonable that both agonists and antagonists first bind to TM1 promoting changes in the conformation of both TM1 and of TM7, which is next to TM1 in the tertiary structure of Ste2p. These conformational changes apparently restrict disulfide formation at the TM7 dimerization interface between Ste2p monomers except the region between the boundary of TM7 and cytoplasmic tail.

Much remains to be understood concerning the significance of GPCR dimerization in the signaling process. The residues in TM7 examined in this study, $S^{288}LPLSSMWA^{296}$, are highly conserved in Class D receptors and are considered to have a similar function to the NPXXY residues in Class A receptors [35]. In Class A receptors, the NPXXY motif is regarded to be important for receptor activation. For example, mutations in this motif affected receptor expression, ligand affinity, receptor sequestration, and heterotrimeric G protein coupling [74-77]. It is possible that TM7

plays an important role in both receptor activation and dimerization in Ste2p and in other GPCRs as well, and that dimerization is linked to signaling by these ubiquitous proteins. The results presented herein provide residue level information concerning the proximity of different sites on two Ste2p monomers in their native membrane environment. The physiological relevance of this information and of dimerization in GPCRs continues to be an intriguing area of GPCR biology.

List of References for Part III

1. Lefkowitz, R.J., *The superfamily of heptahelical receptors.* Nat Cell Biol, 2000. **2**(7): p. E133-6.
2. Sadee, W., et al., *Genetic variations in human G protein-coupled receptors: implications for drug therapy.* AAPS PharmSci, 2001. **3**(3): p. E22.
3. Insel, P.A., et al., *Impact of GPCRs in clinical medicine: monogenic diseases, genetic variants and drug targets.* Biochim Biophys Acta, 2007. **1768**(4): p. 994-1005.
4. Dohlman, H.G., et al., *Model systems for the study of seven-transmembrane-segment receptors.* Annu Rev Biochem, 1991. **60**: p. 653-88.
5. Dohlman, H.G. and J.W. Thorner, *Regulation of G protein-initiated signal transduction in yeast: paradigms and principles.* Annu Rev Biochem, 2001. **70**: p. 703-54.
6. Naider, F. and J.M. Becker, *The alpha-factor mating pheromone of Saccharomyces cerevisiae: a model for studying the interaction of peptide hormones and G protein-coupled receptors.* Peptides, 2004. **25**(9): p. 1441-63.
7. Dirnberger, D. and K. Seuwen, *Signaling of human frizzled receptors to the mating pathway in yeast.* PLoS ONE, 2007. **2**(9): p. e954.
8. Yin, D., et al., *Successful expression of a functional yeast G-protein-coupled receptor (Ste2) in mammalian cells.* Biochem Biophys Res Commun, 2005. **329**(1): p. 281-7.

9. Xue, C., Y.P. Hsueh, and J. Heitman, *Magnificent seven: roles of G protein-coupled receptors in extracellular sensing in fungi.* FEMS Microbiol Rev, 2008. **32**(6): p. 1010-32.

10. Rios, C.D., et al., *G-protein-coupled receptor dimerization: modulation of receptor function.* Pharmacol Ther, 2001. **92**(2-3): p. 71-87.

11. Milligan, G., *G protein-coupled receptor dimerisation: molecular basis and relevance to function.* Biochim Biophys Acta, 2007. **1768**(4): p. 825-35.

12. Milligan, G., *G protein-coupled receptor dimerization: function and ligand pharmacology.* Mol Pharmacol, 2004. **66**(1): p. 1-7.

13. Bayburt, T.H., et al., *Transducin activation by nanoscale lipid bilayers containing one and two rhodopsins.* J Biol Chem, 2007. **282**(20): p. 14875-81.

14. Chabre, M. and M. le Maire, *Monomeric G-protein-coupled receptor as a functional unit.* Biochemistry, 2005. **44**(27): p. 9395-403.

15. White, J.F., et al., *Dimerization of the class A G protein-coupled neurotensin receptor NTS1 alters G protein interaction.* Proc Natl Acad Sci U S A, 2007. **104**(29): p. 12199-204.

16. Whorton, M.R., et al., *A monomeric G protein-coupled receptor isolated in a high-density lipoprotein particle efficiently activates its G protein.* Proc Natl Acad Sci U S A, 2007. **104**(18): p. 7682-7.

17. Overton, M.C. and K.J. Blumer, *G-protein-coupled receptors function as oligomers in vivo.* Curr Biol, 2000. **10**(6): p. 341-4.

18. Yesilaltay, A. and D.D. Jenness, *Homo-oligomeric complexes of the yeast alpha-factor pheromone receptor are functional units of endocytosis.* Mol Biol Cell, 2000. **11**(9): p. 2873-84.

19. Overton, M.C., S.L. Chinault, and K.J. Blumer, *Oligomerization, biogenesis, and signaling is promoted by a glycophorin A-like dimerization motif in transmembrane domain 1 of a yeast G protein-coupled receptor.* J Biol Chem, 2003. **278**(49): p. 49369-77.

20. Gehret, A.U., et al., *Oligomerization of the yeast alpha-factor receptor: implications for dominant negative effects of mutant receptors.* J Biol Chem, 2006. **281**(30): p. 20698-714.

21. Wang, H.X. and J.B. Konopka, *Identification of Amino Acids at Two Dimer Interface Regions of the alpha-Factor Receptor (Ste2).* Biochemistry, 2009.

22. Sen, M. and L. Marsh, *Noncontiguous domains of the alpha-factor receptor of yeasts confer ligand specificity.* J Biol Chem, 1994. **269**(2): p. 968-73.

23. Son, C.D., et al., *Identification of ligand binding regions of the Saccharomyces cerevisiae alpha-factor pheromone receptor by photoaffinity cross-linking.* Biochemistry, 2004. **43**(41): p. 13193-203.

24. Hauser, M., et al., *The first extracellular loop of the Saccharomyces cerevisiae G protein-coupled receptor Ste2p undergoes a conformational change upon ligand binding.* J Biol Chem, 2007. **282**(14): p. 10387-97.

25. Akal-Strader, A., et al., *Residues in the first extracellular loop of a G protein-coupled receptor play a role in signal transduction.* J Biol Chem, 2002. **277**(34): p. 30581-90.

26. Mumberg, D., R. Muller, and M. Funk, *Yeast vectors for the controlled expression of heterologous proteins in different genetic backgrounds.* Gene, 1995. **156**(1): p. 119-22.

27. Lee, B.K., et al., *Affinity purification and characterization of a G-protein coupled receptor, Saccharomyces cerevisiae Ste2p.* Protein Expr Purif, 2007. **56**(1): p. 62-71.

28. Gietz, D., et al., *Improved method for high efficiency transformation of intact yeast cells.* Nucleic Acids Res, 1992. **20**(6): p. 1425.

29. David, N.E., et al., *Expression and purification of the Saccharomyces cerevisiae alpha-factor receptor (Ste2p), a 7-transmembrane-segment G protein-coupled receptor.* J Biol Chem, 1997. **272**(24): p. 15553-61.

30. Lee, Y.H., F. Naider, and J.M. Becker, *Interacting residues in an activated state of a G protein-coupled receptor.* J Biol Chem, 2006. **281**(4): p. 2263-72.

31. Raths, S.K., F. Naider, and J.M. Becker, *Peptide analogues compete with the binding of alpha-factor to its receptor in Saccharomyces cerevisiae.* J Biol Chem, 1988. **263**(33): p. 17333-41.

32. Konopka, J.B., D.D. Jenness, and L.H. Hartwell, *The C-terminus of the S. cerevisiae alpha-pheromone receptor mediates an adaptive response to pheromone.* Cell, 1988. **54**(5): p. 609-20.

33. Kleiger, G., et al., *GXXXG and AXXXA: common alpha-helical interaction motifs in proteins, particularly in extremophiles.* Biochemistry, 2002. **41**(19): p. 5990-7.

34. Sternberg, M.J. and W.J. Gullick, *A sequence motif in the transmembrane region of growth factor receptors with tyrosine kinase activity mediates dimerization.* Protein Eng, 1990. **3**(4): p. 245-8.

35. Eilers, M., et al., *Comparison of class A and D G protein-coupled receptors: common features in structure and activation.* Biochemistry, 2005. **44**(25): p. 8959-75.

36. Palczewski, K., et al., *Crystal structure of rhodopsin: A G protein-coupled receptor.* Science, 2000. **289**(5480): p. 739-45.

37. Cherezov, V., et al., *High-resolution crystal structure of an engineered human beta2-adrenergic G protein-coupled receptor.* Science, 2007. **318**(5854): p. 1258-65.

38. Mentesana, P.E. and J.B. Konopka, *Mutational analysis of the role of N-glycosylation in alpha-factor receptor function.* Biochemistry, 2001. **40**(32): p. 9685-94.

39. Blumer, K.J., J.E. Reneke, and J. Thorner, *The STE2 gene product is the ligand-binding component of the alpha-factor receptor of Saccharomyces cerevisiae.* J Biol Chem, 1988. **263**(22): p. 10836-42.

40. Shi, C., et al., *In vitro characterization of ligand-induced oligomerization of the S. cerevisiae G-protein coupled receptor, Ste2p.* Biochim Biophys Acta, 2009. **1790**(1): p. 1-7.

41. Sansom, M.S. and H. Weinstein, *Hinges, swivels and switches: the role of prolines in signalling via transmembrane alpha-helices.* Trends Pharmacol Sci, 2000. **21**(11): p. 445-51.

42. Choi, Y. and J.B. Konopka, *Accessibility of cysteine residues substituted into the cytoplasmic regions of the alpha-factor receptor identifies the intracellular residues that are available for G protein interaction.* Biochemistry, 2006. **45**(51): p. 15310-7.

43. Lin, J.C., K. Duell, and J.B. Konopka, *A microdomain formed by the extracellular ends of the transmembrane domains promotes activation of the G protein-coupled alpha-factor receptor.* Mol Cell Biol, 2004. **24**(5): p. 2041-51.

44. McCaffrey, G., et al., *Identification and regulation of a gene required for cell fusion during mating of the yeast Saccharomyces cerevisiae.* Mol Cell Biol, 1987. **7**(8): p. 2680-90.

45. Dube, P., A. DeCostanzo, and J.B. Konopka, *Interaction between transmembrane domains five and six of the alpha -factor receptor.* J Biol Chem, 2000. **275**(34): p. 26492-9.

46. Parrish, W., et al., *The cytoplasmic end of transmembrane domain 3 regulates the activity of the Saccharomyces cerevisiae G-protein-coupled alpha-factor receptor.* Genetics, 2002. **160**(2): p. 429-43.

47. Shah, A. and L. Marsh, *Role of Sst2 in modulating G protein-coupled receptor signaling.* Biochem Biophys Res Commun, 1996. **226**(1): p. 242-6.

48. Li, J.H., et al., *Distinct structural changes in a G protein-coupled receptor caused by different classes of agonist ligands.* J Biol Chem, 2007. **282**(36): p. 26284-93.

49. Han, S.J., et al., *Pronounced conformational changes following agonist activation of the M(3) muscarinic acetylcholine receptor.* J Biol Chem, 2005. **280**(26): p. 24870-9.

50. Guo, W., et al., *Crosstalk in G protein-coupled receptors: changes at the transmembrane homodimer interface determine activation.* Proc Natl Acad Sci U S A, 2005. **102**(48): p. 17495-500.

51. Yu, H., et al., *A general method for mapping tertiary contacts between amino acid residues in membrane-embedded proteins.* Biochemistry, 1995. **34**(46): p. 14963-9.

52. Struthers, M., et al., *Tertiary interactions between the fifth and sixth transmembrane segments of rhodopsin.* Biochemistry, 1999. **38**(20): p. 6597-603.

53. Bukusoglu, G. and D.D. Jenness, *Agonist-specific conformational changes in the yeast alpha-factor pheromone receptor.* Mol Cell Biol, 1996. **16**(9): p. 4818-23.

54. Farrens, D.L., et al., *Requirement of rigid-body motion of transmembrane helices for light activation of rhodopsin.* Science, 1996. **274**(5288): p. 768-70.

55. Zeng, F.Y., et al., *Use of a disulfide cross-linking strategy to study muscarinic receptor structure and mechanisms of activation.* J Biol Chem, 1999. **274**(23): p. 16629-40.

56. Luo, X., D. Zhang, and H. Weinstein, *Ligand-induced domain motion in the activation mechanism of a G-protein-coupled receptor.* Protein Eng, 1994. **7**(12): p. 1441-8.

57. Srinivasan, N., et al., *Conformations of disulfide bridges in proteins.* Int J Pept Protein Res, 1990. **36**(2): p. 147-55.

58. Li, J.H., et al., *Ligand-specific changes in M3 muscarinic acetylcholine receptor structure detected by a disulfide scanning strategy.* Biochemistry, 2008. **47**(9): p. 2776-88.

59. Ward, S.D., et al., *Use of an in situ disulfide cross-linking strategy to study the dynamic properties of the cytoplasmic end of transmembrane domain VI of the M3 muscarinic acetylcholine receptor.* Biochemistry, 2006. **45**(3): p. 676-85.

60. Overton, M.C. and K.J. Blumer, *The extracellular N-terminal domain and transmembrane domains 1 and 2 mediate oligomerization of a yeast G protein-coupled receptor.* J Biol Chem, 2002. **277**(44): p. 41463-72.

61. Arshava, B., et al., *High resolution NMR analysis of the seven transmembrane domains of a heptahelical receptor in organic-aqueous medium.* Biopolymers, 2002. **64**(3): p. 161-76.

62. Cohen, L.S., et al., *Expression and biophysical analysis of two double-transmembrane domain-containing fragments from a yeast G protein-coupled receptor.* Biopolymers, 2008. **90**(2): p. 117-30.

63. Cordes, F.S., J.N. Bright, and M.S. Sansom, *Proline-induced distortions of transmembrane helices.* J Mol Biol, 2002. **323**(5): p. 951-60.

64. Neumoin, A., et al., *NMR studies in dodecylphosphocholine of a fragment containing the seventh transmembrane helix of a G-protein-coupled receptor from Saccharomyces cerevisiae.* Biophys J, 2007. **93**(2): p. 467-82.

65. Rosenbaum, D.M., et al., *GPCR engineering yields high-resolution structural insights into beta2-adrenergic receptor function.* Science, 2007. **318**(5854): p. 1266-73.

66. Konvicka, K., et al., *A proposed structure for transmembrane segment 7 of G protein-coupled receptors incorporating an asn-Pro/Asp-Pro motif.* Biophys J, 1998. **75**(2): p. 601-11.

67. Mancia, F., et al., *Ligand sensitivity in dimeric associations of the serotonin 5HT2c receptor.* EMBO Rep, 2008. **9**(4): p. 363-9.

68. Lin, J.C., et al., *Identification of residues that contribute to receptor activation through the analysis of compensatory mutations in the G protein-coupled alpha-factor receptor.* Biochemistry, 2005. **44**(4): p. 1278-87.

69. Abel, M.G., et al., *Mutations affecting ligand specificity of the G-protein-coupled receptor for the Saccharomyces cerevisiae tridecapeptide pheromone.* Biochim Biophys Acta, 1998. **1448**(1): p. 12-26.

70. Park, P.S., D.T. Lodowski, and K. Palczewski, *Activation of G protein-coupled receptors: beyond two-state models and tertiary conformational changes.* Annu Rev Pharmacol Toxicol, 2008. **48**: p. 107-41.

71. Abel, M.G., et al., *Structure-function analysis of the Saccharomyces cerevisiae tridecapeptide pheromone using alanine-scanned analogs.* J Pept Res, 1998. **52**(2): p. 95-106.

72. Bajaj, A., et al., *A fluorescent alpha-factor analogue exhibits multiple steps on binding to its G protein coupled receptor in yeast.* Biochemistry, 2004. **43**(42): p. 13564-78.

73. Lee, B.K., et al., *Identification of residues of the Saccharomyces cerevisiae G protein-coupled receptor contributing to alpha-factor pheromone binding.* J Biol Chem, 2001. **276**(41): p. 37950-61.

74. Barak, L.S., et al., *The conserved seven-transmembrane sequence NP(X)2,3Y of the G-protein-coupled receptor superfamily regulates multiple properties of the beta 2-adrenergic receptor.* Biochemistry, 1995. **34**(47): p. 15407-14.

75. Fritze, O., et al., *Role of the conserved NPxxY(x)5,6F motif in the rhodopsin ground state and during activation.* Proc Natl Acad Sci U S A, 2003. **100**(5): p. 2290-5.

76. Prioleau, C., et al., *Conserved helix 7 tyrosine acts as a multistate conformational switch in the 5HT2C receptor. Identification of a novel "locked-on" phenotype and double revertant mutations.* J Biol Chem, 2002. **277**(39): p. 36577-84.

77. Wess, J., et al., *Functional role of proline and tryptophan residues highly conserved among G protein-coupled receptors studied by mutational analysis of the m3 muscarinic receptor.* Embo J, 1993. **12**(1): p. 331-8.

Part IV Participation of the Ste2p N-terminus in Homo-Dimer Formation and the Effect of Ligand Binding on this Interaction

CHAPTER 1 Introduction

The structural hallmark of GPCRs is their seven membrane-spanning domains connected by extracellular and intracellular loops, oriented such that the N terminus is outside of the cell and the C terminus is inside. As discussed in the part I, GPCRs sense signals in the extracellular environment. Ligand binding to its cognate GPCR promotes a conformational change in the receptor and triggers signal transduction. As the receptor goes through the activation mechanism, it is well known that movement of the transmembrane domains are involved in the change of conformation [1], [2-6]. It is expected that concurrent changes in conformation also occur in the N-terminus and extracellular loops of the receptor, though limited structural information is available for these regions.

Using the substituted cysteine accessibility method (SCAM) [7] our lab found that the first extracellular loop (EL1) of the α-factor receptor has a tertiary structure that limits solvent accessibility to some residues, and this accessibility changes in a ligand-dependent manner presumably through induced conformation changes. SCAM analysis is being used currently in our lab to study the accessibility of residues of the N-terminus of Ste2p. During these analyses it was noted that the N-terminal mutant Y26C promotes receptor dimerization under both reducing and non-reducing conditions. This observation stimulated the investigation into whether other N-terminal residues participate in the dimerization of Ste2p, as was observed for residues in TM1 and TM7 (Part 3, Dissertation). In the Class C group of GPCRs, it has been established that a motif known as the Venus fly trap (VFT) at the N-terminus, and cysteine-rich domains (CRDs),

localized between VFT and transmembrane domains are important for dimerization of this receptor class [8, 9] [10-13]. Thus there is a precedent for the involvement of N-terminal residues in GPCR dimerization.

CHAPTER 2 Experimental procedures

Strains, Media, and Plasmids

The Saccharomyces cerevisiae strain BJS21 was used in all assays [7]. The relevant genotype is *MAT**a**, prc1-407 prb1-1122 pep4-3 leu2 trp1 ura3-52 ste2::Kan*^{R}. For disulfide cross-linking, yeast strain BJS21 (ste2-deletion strain) bearing each fifteen different single cys mutants ranging from Gln^{20} through Ser^{34} of N-terminus of Ste2p were given from Seraj Uddin (at UT knoxville). Cells were grown in the absence of tryptophan on MLT medium [7]. All media components were obtained from Difco and were of the highest quality available.

Preparation of membranes

Membrane preparation of Ste2p was carried out essentially as described previously [14]. Cells were grown to log phase, and then 1 x 10^8 cells were harvested by centrifugation and lysed by agitation with glass beads in a lysis buffer containing 50 mM Hepes, pH 7.5, 1 mM EDTA, 10 µg/ml phenylmethylsulfonyl fluoride, 2 µg/ml leupeptin, and 2 µg/ml pepstatin. The lysate was cleared by centrifugation at 2,000 x *g* for 5 min, and then membranes were harvested by centrifugation at 15,000 x *g* for 45 min. The membrane pellet was washed and then resuspended in 100 µl of a buffer (pH 7.4) containing 10% glycerol, 50mM Hepes, 0.15mM NaCl, 2mM $CaCl_2$, 5mM KCl, 5mM $MgCl_2$, 4mM EDTA [14]. The protein concentration was determined by the Lowry assay (Pierce), and the membrane preparation was stored at -20 ºC overnight and used for further assay the next day.

Disulfide Cross-linking with Cu-Phenanthroline

The 100 μg of membrane protein preparation were treated with a fresh preparation (pH 7.4) of Cu (II)-1,10-phenanthroline (CuP; final concentration, 2.5 μM CuSO4 and 7.5μM phenanthroline). The reaction was carried out at room temperature for 30 min, terminated with 50 mM EDTA and kept on ice for 20 min followed by adding Laemmli sample buffer. In experiments designed to prevent disulfide bond formation, the membranes were treated with 5mM of NEM for 20min prior to incubation with Cu-P reagent. α-factor or antagonist,[desW1,desH2]α-factor (10 μM final concentration), were added to the membrane preparation and incubation allowed to proceed for 30 min prior to Cu-P treatment in experiments performed to examine the influence of ligand on dimerization

Western blot

Immunoblot analysis of Ste2p was carried out as described previously [14]. Each sample was incubated at room temperature and then separated on NuPAGE 10% Bis-Tris SDS-polyacrylamide gel (Invitrogen) using either non-reducing or reducing conditions and electrophoretically transferred to Immobilon^{TM}-P membrane (Millipore Corp., Bedford, MA). The blot was probed with anti-FLAG M2 antibody (Eastman Kodak Co.) and the bands were visualized with the West Pico chemiluminescent detection system (Pierce).

CHAPTER 3 Results

Cells expressing each of the different Cys mutants were grown and membranes were prepared. The samples were analyzed by SDS-PAGE and probed with anti-FLAG antibody (Fig. 25). In general, all mutants showed higher dimer formation than WT under non-reducing conditions without Cu-P treatment (Fig. 25A and Fig. 26). About 20% of the WT receptor was in the dimer form under conditions that we showed previously (Part III, Dissertation) was due to non-disulfide mediated, inter-molecular interactions, whereas from 30 to 90 % of the mutant receptors were in the dimer form (Fig. 26). Nine mutants (G21C, T23C, N25C, T27C, I29C, G31C, N32C, G33C, and S34C) showed a small increase in dimerization (ranging from 1.3 ~ 1.8 fold) in comparison to WT (Fig. 25A and Fig. 26). Six Cys mutants, Q20C, S22C, I24C, Y26C, S28C, and Y30C, showed a large increase in the dimer population relative to the monomer receptor (Fig. 25A and Fig 26).

Under reducing conditions (data not shown, results from Seraj Uddin, a student in the Becker Lab), the percentage of dimer for all Cys mutants, except Y26C, dropped to that of WT indicating that these dimers were formed via disulfide bonds between the mutated Cys residues. The fact that the Y26C dimer was not affected by reducing conditions indicated that this unique dimer was formed by a non-disulfide interaction. Mutation of the residue might lead to increased non-covalent interactions between residues on two Ste2p molecules resulting in dimerization of the receptor.

N25C and T27C receptors showed different band patterns compared to WT (Fig. 25A). When analyzed by SDS-PAGE, WT Ste2p migrates as a group of three bands,

consisting of the two major glycosylated forms of Ste2p along with the lower molecular weight unglycosylated form (see WT lane, Fig. 25A). N25 and T27 are known to be within the motif of N-linked glycosylation (Asn-X-Ser/Thr) of the receptor [15]. Thus, substitution of these residues to Cys decreased heterogeneity of the glycosylated receptors leading to a more prominent lower molecular weight band which is the non-glycosylated form of Ste2p and a concomitant lesser amount of higher molecular weight band(s). While N32C and S34C also are within an N-linked glycosylation motif, there were no readily observable differences with these two mutants with respect to WT (Fig. 25A).

It was possible that disulfide bonds were prevented from forming in some mutants due to the environment of the Cys residue. Addition of Cu-P to provide a more oxidative environment that facilitates Cys cross-linking has been used in many experiments to determine Cys-Cys disulfide formation in membrane proteins [16-20]. Treatment of Cu-P was performed with all fifteen N-terminal Cys mutants (Fig 25B). Nine mutants (Q20C, G21C, T23C, Y26C, and from Y30C through S34C) were not affected by Cu-P treatment (Fig. 25A, B, Fig. 27). However, three mutants (S22C, I24C, and S28C) exhibited increased dimerization upon Cu-P treatment. In addition, three mutants (N25C, T27C, and I29C) which in the previous experiment did not form dimers without Cu-P addition, did dimerize in the presence of Cu-P.

To verify that this increase was due to disulfide bond formation, NEM pretreatment was performed with the N25C, T27C and I29C mutants. NEM pretreatment blocked dimerization for all three mutants (Fig. 25E), showing that the dimers were indeed formed via a disulfide bond. These data suggest that the α-carbons of the two Cys

residues are located close to each other, within 7 Å, the maximum distance to form a Cu-P mediated disulfide bond [21]. We did not observe any change in dimer ratio upon Cu-P addition with the five mutants spanning residues Y30C to S34C, indicating that those residues are not in close proximity (Fig 25A, B and Fig. 27).

It has been observed that ligand binding can induce a change in the receptor dimer interface (this Dissertation, Part III) and [22, 23]. To examine the ligand effect on Cys-mediated dimerization at the N-terminus, membranes were incubated with either α-factor or [desW^{1}desH^2] α-factor (an antagonist) prior to Cu-P treatment. The dimerization of the Q20C and Y26C mutants was not influenced by the presence of either ligand. In contrast, the S22C mutant increased dimerization in the presence of Cu-P and α-factor or the antagonist. While pre-incubation with α-factor did not affect the ratio of dimer for the G21C, T23C and I24C mutants, antagonist pre-treatment of these three mutants resulted in increased Cu-P dependent dimer formation (Fig.25 and Fig 27A).

The presence of ligand also altered the dimer population for the N25C, T27C, and I29C mutants. These three mutants exhibited an increase in dimerization stimulated by the presence of Cu-P. However, pre-treatment with α-factor prior to Cu-P treatment blocked the formation of dimers for these mutants. In contrast, Cu-P stimulated dimerization did occur with antagonist treatment. (Fig. 25C, D and Fig. 27B). These results suggest that the N-terminus dimer interface is changed by ligand binding, with different effects of agonist and antagonist. Once again, no change was observed in the dimer ratio in the presence of agonist or antagonist for the five mutants spanning Y30C to S34C, suggesting that these residues are not components of the dimer interface in the resting or activated receptor (Fig. 25C, D and Fig. 27C).

Figure 25 Dimer formation of Cys mutants

Membrane proteins untreated (A), treated with Cu-P (B), incubated with α-factor followed by Cu-P (C), incubated with antagonist followed by Cu-P (D) or NEM added prior to Cu-P (E) were analyzed by SDS-PAGE, then immunoblotted and probed with anti-FLAG antibody. The upper band (~110 kDa) represents dimerized receptor (indicated by a D) and the lower band (~55 kDa) represents monomer (indicated by a M).

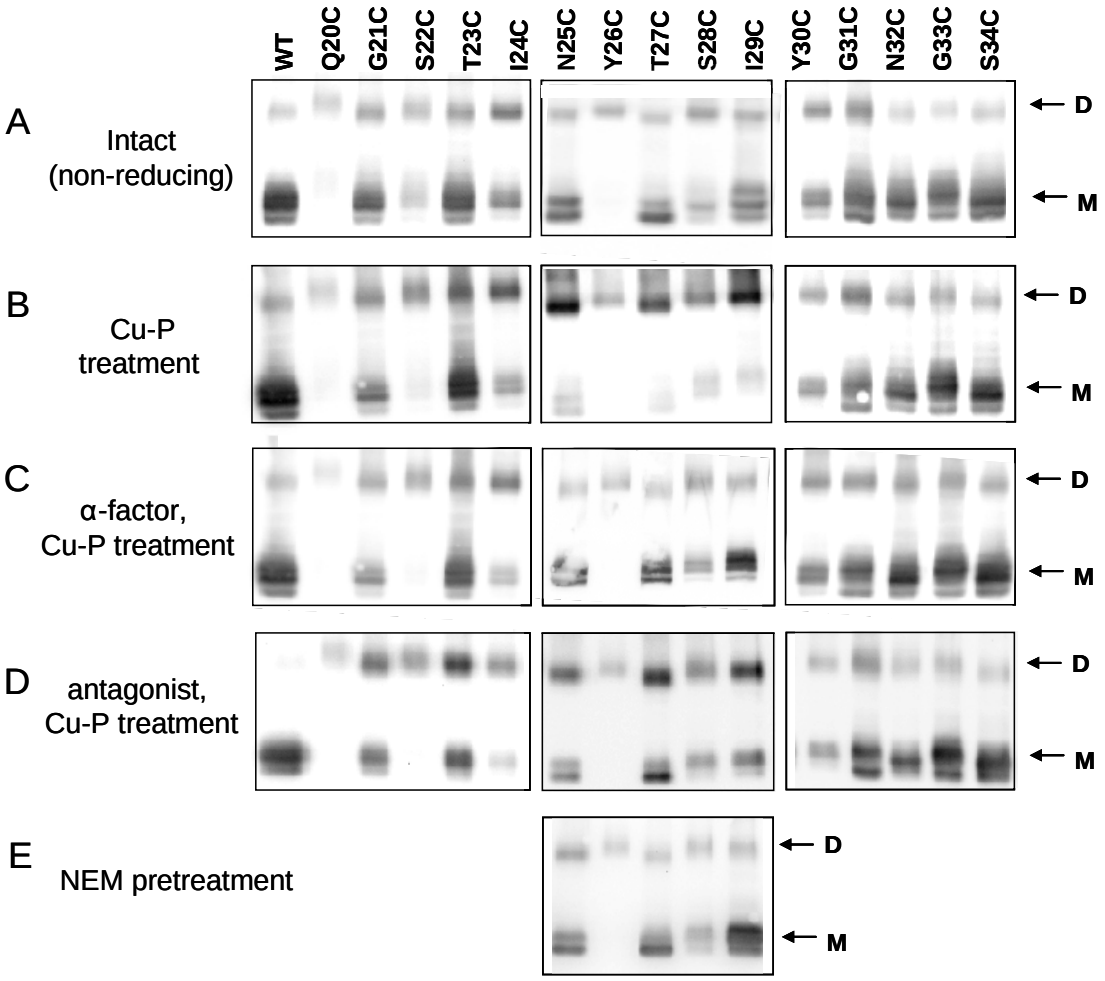
WT
Q20C
G21C
S22C
T23C
I24C
N25C
Y26C
T27C
S28C
I29C
Y30C
G31C
N32C
G33C
S34C
A
Intact
(non-reducing)
B
Cu-P
treatment
C
α-factor,
Cu-P treatment
D
antagonist,
Cu-P treatment
E
NEM pretreatment
D
M

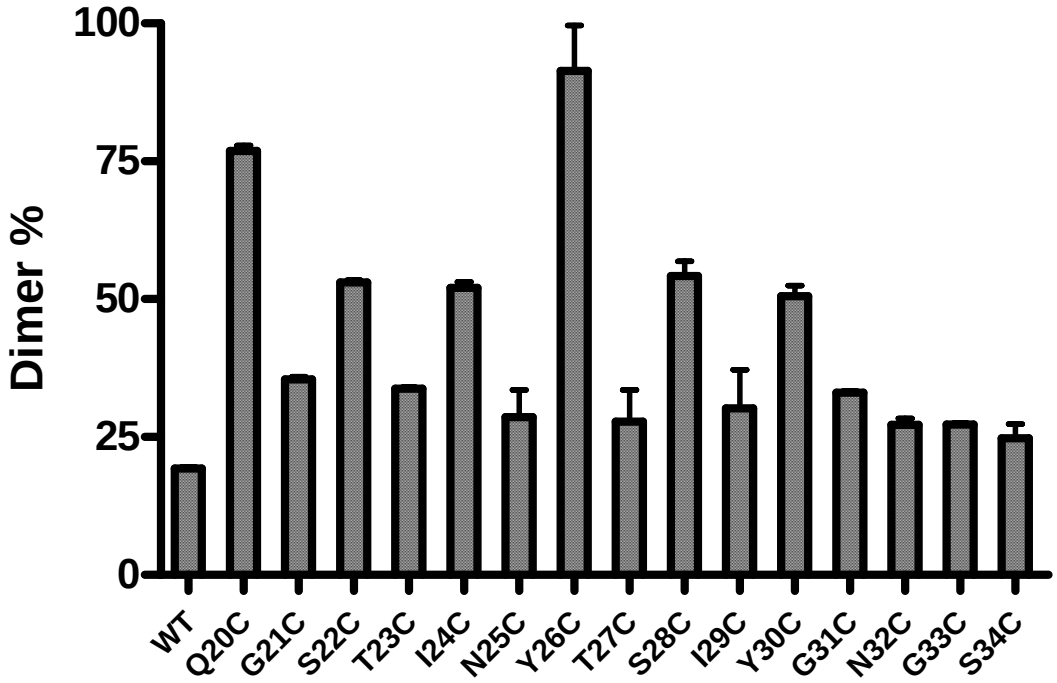

Figure 26 The percent of dimer formed by each Cys mutant

Membrane proteins were analyzed by SDS-PAGE, then immunoblotted and probed with anti-FLAG antibody. The intensity of the monomer and dimer signal was measured by densitometry and the ratio of the signals was determined. The percentage of dimer was calculated as [Dimer/(Dimer+Monomer) x100].

Figure 27 Effect of ligand binding on Cu-P [Cu (II)-1, 10-phenanthroline] stimulated disulfide bond formation

Total membrane protein was prepared from cells expressing the indicated receptors: (A) Q20C-I24C, (B) N25C-I29C. Each sample was immunoblotted and probed with anti-FLAG antibody. Receptors were treated as indicated. '(-)' indicates no treatment, 'Cu-P' indicates Cu-P treated samples, 'α Cu-P' indicates samples incubated with α-factor followed by Cu-P treatment and 'A Cu-P' indicates samples incubated with the antagonist [desW1, desH2]α-factor followed by Cu-P treatment. The intensity of the monomer and dimer signal was measured by densitometry and the ratio of the signals was determined. The percentage of dimer was calculated as [Dimer/(Dimer+Monomer) x100].

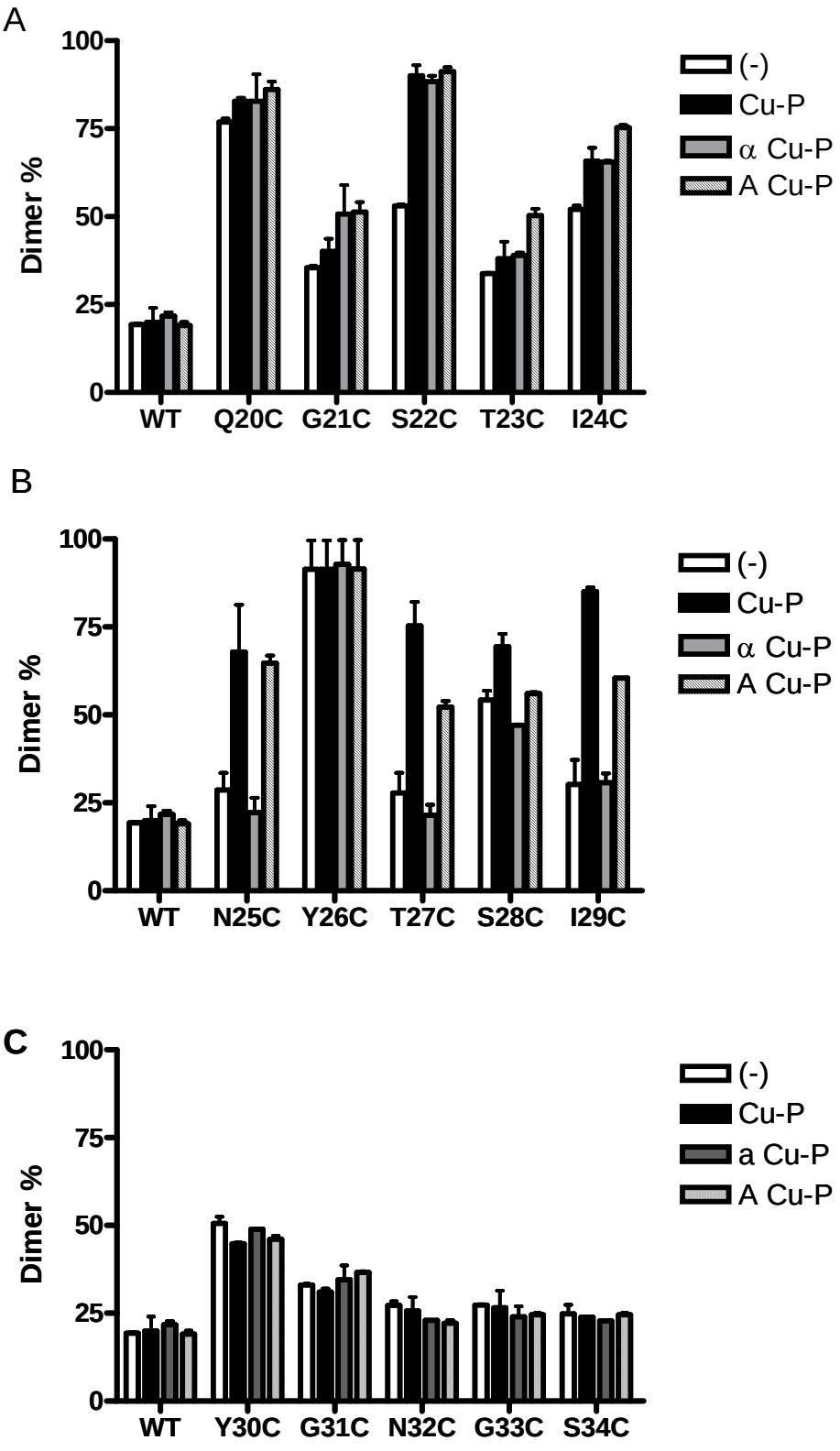
A
100
75
50
25
0
Dimer %
WT
Q20C
G21C
S22C
T23C
I24C
(-)
Cu-P
α Cu-P
A Cu-P
B
100
75
50
25
0
Dimer %
WT
N25C
Y26C
T27C
S28C
I29C
(-)
Cu-P
α Cu-P
A Cu-P
C
100
75
50
25
0
Dimer %
WT
Y30C
G31C
N32C
G33C
S34C
(-)
Cu-P
a Cu-P
A Cu-P

CHAPTER 4 Discussion

In this study, we found that a part of the N-terminus participates in the formation of a dimer interface. Within the N-terminus the sequence between residues 19 to 31 was predicted to form a beta strand [24]. In this dissertation, residues were found that increased dimerization in the absence of Cu-P upon mutation to Cys (Q20C, S22C, I24C, Y26C, S28C, and Y30C). If these residues are localized on one side of the predicted beta strand in the native Ste2p, then this may place them in position to interact with a corresponding beta strand on a second Ste2p molecule. Residues G21, T23, N25, T27, I29, and G31 are expected to be located on other side of the beta strand, and these residues when replaced by Cys do not form dimers in the absence of Cu-P. As the collision rate between the two thiols is dependent on the inter-residue distance [25, 26], the odd-numbered residues may not be in close enough proximity to each other to form effective disulfide bonds in the absence of Cu-P. However, dimers are formed in the presence of Cu-P with N25C, T27C, and I29C. We believe that Cu-P functioned to enhance dimerization by providing a more oxidative environment that facilitated disulfide bond formation. We postulate that these receptors are impaired in their glycosylation due to mutation (N25c and T27C) in the N-X-T/S motif or a mutation (I29C) that affected glycosylation. The lowered glycosylation allows these residues to be in close enough proximity to react when Cu-P is present. This hypothesis needs to be tested by determination of the glycosylation state of these mutant receptors. We did not observe high levels of dimerization for residues N32C, G33C, or S34C in either the presence or

absence of Cu-P. Residues N32, G33, and S34 are not part of the predicted beta strand, therefore the region containing these residues might not be in close enough proximity to cross-link well. They showed only a small increase (1.5 fold or less) in dimer population with or without Cu-P.

Prior incubation with α-factor prevented the Cu-P induced increase in dimerization for the N25C, T27C, and I29C mutants, indicating a ligand-dependent change occurred in this region. In contrast, treatment with antagonist, which binds but does not activate the receptor, did not prevent the Cu-P-mediated dimer increase. Alpha-factor binding to the receptor may alter the position of this region of the N-terminus, or cause a distortion in the beta strand which makes the residues unable to interact and form a disulfide bond. Interestingly, the G21C and T23C receptors, which do not form dimers in the presence or absence of α-factor, did display an increased dimer formation in the presence of antagonist. This indicates that the receptor adopts an intermediate conformation between active and inactive state upon antagonist binding, which shifts the G21 and T23 residues into a position favorable for dimer formation. Thus, although phenotypically the antagonist binding maintains the receptor in the inactive state, antagonist can still influence receptor conformation. Taken together, the ligand dependent change of the dimer interface provided significant evidence that the N-termimus of Ste2p is structured and that this structure can be altered either directly in response to ligand binding or indirectly as part of the receptor activation mechanism.

CHAPTER 5 Summary and Future direction

Summary

This dissertation reports the identification of homo-dimer interfaces for Ste2p, the yeast α-factor receptor, a model system for mammalian GPCR peptide hormone receptors. Information regarding ligand-induced change at the dimer interface is reported as well. To identify the dimer interfaces, single cysteine substitutions were introduced into Ste2p, and disulfide-mediated dimerization was assessed. It was determined that one specific residue was involved in dimerization in transmembrane domain 1 (TM1) and 9 residues were involved in dimers formed via TM7. Interestingly, for the TM7 mutant receptors the formation of dimers decreased in the presence of α-factor, indicating that ligand binding resulted in a conformational change in this domain. Based on these results, it was proposed that the dimer interfaces may differ in the resting and the activated states of the receptor. Furthermore, the pattern of dimer formation resulted in a re-evaluation of the structure of TM7, indicating that the full TM7 did not behave as a perfect α-helix as predicted by modeling. In addition, residues at N-terminus of Ste2p were also found to participate in dimer formation and surprisingly, dimerization mediated through some of these residues was influenced by the presence of ligands. Future experiments, suggested below, are proposed to provide further details on the dimer structure-function relationship.

Whole cell, In vivo, cross-linking

The study of dimer formation in this dissertation was done with receptors in membrane preparations. While the receptors in membrane preparations still maintain their native conformation, as determined by receptor binding affinity, whole cell cross-linking would be useful. For these experiments, cross-linking could be assessed in a native, intact cell for residues that are exposed to the extracellular surface. Since we found residues that form dimers at the N-terminus, which is external to the cell membrane, it should be feasible to do *in vivo* cross-linking with Cu-P by using whole cells expressing those mutants. Such an approach was used recently by Wang and Konopka to identify residues involved in dimerization of Ste2p via the extracellular extracellular surface of the receptor, although N-terminal residues were not investigated [27]. The effect of whole cell cross-linking on the physiological function of the receptor has not been examined in this dissertation and might shed new light on the biological relevance of receptor dimerization. However, when testing the biological activity of the receptor in an intact cell, the metal toxicity of Cu-P must be considered since copper is toxic at high concentration [28]. We observed an orange discoloration of the cells after prolonged incubation (1-2 hrs) with Cu-P at 2.5 μM. Thus, a future experiment should be determination of concentration of Cu-P which allows cross-linking without toxicity. Alternatively, a chemical cross-linker can be used for the *in vivo* studies in lieu of Cu-P. Currently, many cross-linkers with a variety of characteristics are commercially available. For example, Shi et al used succinimidyl *trans*-4-(maleimidylmethyl) cyclohexane-1-carboxylate (SMCC) to demonstrate Ste2p dimer and trimer formation [29]. Another common reagent used to explore protein-protein interactions are the bismaleimide

crosslinkers, BMOE, BMB and BMH, used to specifically connect the thiol groups between two Cys residues (Fig. 28) [30-32]. The use of cross-linkers to detect and stabilize protein-protein interactions at the dimer interface in intact cells will contribute to our understanding of dimer structure-function relationships. Furthermore, comparison of results using whole cells with those obtained from membrane preparations will be useful to determine how accurately results obtained with membrane preparations reflect those obtained with the intact cell.

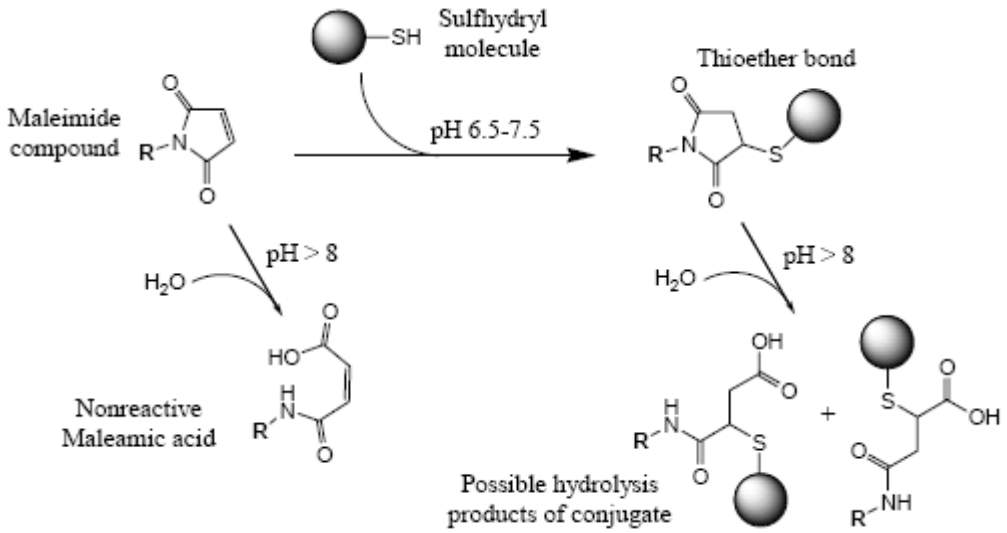

Figure 28 Reaction of maleimide-activated compounds to sulfhydryls

(http://www.piercenet.com/Objects/View.cfm?type=File&ID=0796)

Study of receptor function and dimer relationship

N-terminal mutants that spontaneously dimerize upon introduction of Cys are good candidates to test for the relationship between dimer formation and receptor function. We can compare the biological activities of those mutants to WT without adding oxidizing reagents, which might affect the physiological function of the yeast cell itself. Recently, Shi et al suggested that the N-terminal tail of Ste2p may have a role in modulation of mating, specifically the fusion of the MATa and MATα cells [24]. They found that deletion of the first 20 amino acids (ΔN20) of Ste2p led to a decrease in mating efficiency, but had little impact on receptor mediated G1growth arrest. Thus the mutant cells responded properly in the growth arrest assay, indicating that the signal was transduced by the receptor, but the cells failed to physically fuse to form diploids. They also performed targeted scanning mutagenesis and cysteine accessibility studies to investigate the site specific functional contributions of N-terminus. In that study, they identified two highly conserved hydrophobic residues, I24 and I29, involved in the mating process. The mating activity associated with these sites was shown to be independent of receptor mediated G1 arrest signaling. Interestingly, mutation of either I24 or I29 to Cys dramatically dropped mating abilities of the mutants compared to mutation to Ala. In our study I24C and I29C were found to dimerize more readily than WT. It is possible that disulfide bond formation at these residues may inhibit the proper conformational change necessary for mating ability but not growth arrest. Indeed, it has been observed that the functions of the receptor can be separated. For example, Ste2p-Y266A mutant can bind ligand without triggering the MAPK pathway [33]. Though all Cys mutants (of residues Q20C- S34C of the N-terminus) were found to retain normal

function in the growth arrest assay (personal communication with Seraj Uddin at UT), the mating ability of the dimerized mutants have not yet been tested. A comparison of mating competence in WT Ste2p with the N-terminal Cys mutants will contribute to the understanding of the possible roles for dimerization in this GPCR.

Relationship of Dimers to Glycosylation State of Ste2p

The two residues, N25 and T27, at the N-terminus, which form dimers upon Cu-P treatment, are known to be within the motif for N-linked glycosylation (Asn-X-Ser/Thr) of Ste2p. The role of N-glycosylation in the dimerization of GPCRs has been described previously. In the β1-adrenergic receptor, the mutant N15A, which results in the elimination of a glycosylation site, is functional but deficient in dimerization relative to the wild-type receptor [34]. The roles of N-glycosylation in the dimerization of the human Bradykinin B2 receptor were also examined. It was determined that N-glycosylation participated in stabilization of dimers [35]. For the epidermal growth factor receptor, receptor-receptor self-association was also reported to be highly dependent on a conformation induced by N-linked glycosylation [36].

While most GPCRs are known to be N-glycosylated, the functional effects of glycosylation vary significantly from receptor to receptor [37], in Ste2p, the nonglycosylated receptor (N25Q/N32Q) displayed normal growth arrest activity and subcellular localization, indicating that glycosylation is not important for wild-type receptor signaling activity [15]. To test whether N-glycosylation has any effect on dimer formation of Ste2p, three forms of the receptor having zero, one or two N-glycosylation

sites can be used as templates to carry residue-specific Cys mutations. Dimer formation of the mutants in the glycosylation deficient and WT backgrounds can be compared via Western blot analysis. Alternatively, Cys mutant and WT Ste2p can be compared with respect to disulfide bond formation following treatment with enzymes, such as Endoglycosidase H or PNGase F, which deglycosylate proteins.

Study for higher order oligomer of Ste2p

Recently, many studies have documented that various classes of GPCRs form dimers and/or even higher order oligomers [38-41]. Consistent with this, TM1, TM4, TM7 and the N-terminus were found to serve as dimer interfaces for Ste2p [27, 42] leading us to propose the existence of higher-order oligomerization for Ste2p. It is possible that a single receptor can interact simultaneously with two additional receptors, by utilizing different dimer interfaces between the monomers: TM7 and/or TM1 can interact with TM7 and/or TM1 of a second receptor, while TM4 can interact with TM4 of a third receptor to form oligomers. Dimerization via the N-terminus can also occur with either TM1 and/or TM7 interaction to form oligomers. To test this, double Cys mutants containing one Cys in either TM1 or TM7 and another Cys in TM4 can be used. Cross-linking of receptors with Cys substituted simultaneously into both TM1/or TM7 and TM4 should lead to the formation higher order species that can be identified by 4-12% gradient SDS-gels (personal communication, George Umanah of the Becker lab).

Another method that might be used to identify the intrinsic (non-disulfide mediated) oligomerization of Ste2p is perfluoro-octanoic acid (PFO)-PAGE [43-46]. PFO

is a mild detergent. Thus, it maintains interactions within protein oligomers and permits assessment of the native quaternary structure of membrane proteins when it is used to replace SDS in gel electrophoresis.

For *in vivo* testing, biophysical assays such as FRET and protein fragment complementation assay [47] also can be used. Split fluorescent proteins are not fluorescent when expressed alone, but when fused to proteins in close proximity, they assemble, fluoresce and thus serve to report on molecular proximity. This method has been applied to find higher oligomerization of D2 dopamine receptor. Taken together, all of the methods described above may be used to document and understand further the nature of dimer/ higher order oligomerization of Ste2p.

Investigation of dimer formation pattern of TM7 mutants in C-terminal tail truncated Ste2p

It was observed that consecutive six TM7 residues (from L291 to A296) were all involved in dimer formation of Ste2p in this study and we proposed that this cytoplasmic end of TM7 may not be a typical α-helical structure. It is possible the junction between TM7 and C- terminal tail may be loosend due to the protein interactions with the C-terminal tail of Ste2p which contains around 160 amino acids (~18.5 kDa). To test this, Ste2p truncated at residue 304 can be used. Previously, it was shown that truncated Ste2p was still fuctional and able to form dimers [48]. Single cysteine mutants from L291C to A296C can be constructed in the truncated Ste2p and dimer formation patterns can be compared with those of the full length Ste2p by same methods as performed in this study.

List of References for Part IV

1. Kobilka, B.K., et al., Chimeric alpha 2-,beta 2-adrenergic receptors: delineation of domains involved in effector coupling and ligand binding specificity. Science, 1988. 240(4857): p. 1310-6.
2. Schoneberg, T., J. Liu, and J. Wess, Plasma membrane localization and functional rescue of truncated forms of a G protein-coupled receptor. J Biol Chem, 1995. 270(30): p. 18000-6.
3. Filipek, S., et al., G protein-coupled receptor rhodopsin: a prospectus. Annu Rev Physiol, 2003. 65: p. 851-79.
4. Hargrave, P.A., H.E. Hamm, and K.P. Hofmann, Interaction of rhodopsin with the G-protein, transducin. Bioessays, 1993. 15(1): p. 43-50.
5. Khorana, H.G., Rhodopsin, photoreceptor of the rod cell. An emerging pattern for structure and function. J Biol Chem, 1992. 267(1): p. 1-4.
6. Rao, V.R., G.B. Cohen, and D.D. Oprian, Rhodopsin mutation G90D and a molecular mechanism for congenital night blindness. Nature, 1994. 367(6464): p. 639-42.
7. Hauser, M., et al., The first extracellular loop of the Saccharomyces cerevisiae G protein-coupled receptor Ste2p undergoes a conformational change upon ligand binding. J Biol Chem, 2007. 282(14): p. 10387-97.
8. Jones, K.A., et al., GABA(B) receptors function as a heteromeric assembly of the subunits GABA(B)R1 and GABA(B)R2. Nature, 1998. 396(6712): p. 674-9.

9. Pin, J.P., et al., Allosteric functioning of dimeric class C G-protein-coupled receptors. Febs J, 2005. 272(12): p. 2947-55.

10. Kristiansen, K., Molecular mechanisms of ligand binding, signaling, and regulation within the superfamily of G-protein-coupled receptors: molecular modeling and mutagenesis approaches to receptor structure and function. Pharmacol Ther, 2004. 103(1): p. 21-80.

11. Meyer, B.H., et al., FRET imaging reveals that functional neurokinin-1 receptors are monomeric and reside in membrane microdomains of live cells. Proc Natl Acad Sci U S A, 2006. 103(7): p. 2138-43.

12. Prinster, S.C., T.G. Holmqvist, and R.A. Hall, Alpha2C-adrenergic receptors exhibit enhanced surface expression and signaling upon association with beta2-adrenergic receptors. J Pharmacol Exp Ther, 2006. 318(3): p. 974-81.

13. Uberti, M.A., et al., Heterodimerization with beta2-adrenergic receptors promotes surface expression and functional activity of alpha1D-adrenergic receptors. J Pharmacol Exp Ther, 2005. 313(1): p. 16-23.

14. Lee, Y.H., F. Naider, and J.M. Becker, Interacting residues in an activated state of a G protein-coupled receptor. J Biol Chem, 2006. 281(4): p. 2263-72.

15. Mentesana, P.E. and J.B. Konopka, Mutational analysis of the role of N-glycosylation in alpha-factor receptor function. Biochemistry, 2001. 40(32): p. 9685-94.

16. Li, J.H., et al., Ligand-specific changes in M3 muscarinic acetylcholine receptor structure detected by a disulfide scanning strategy. Biochemistry, 2008. 47(9): p. 2776-88.

17. Li, J.H., et al., Distinct structural changes in a G protein-coupled receptor caused by different classes of agonist ligands. J Biol Chem, 2007. 282(36): p. 26284-93.

18. Ward, S.D., et al., Use of an in situ disulfide cross-linking strategy to study the dynamic properties of the cytoplasmic end of transmembrane domain VI of the M3 muscarinic acetylcholine receptor. Biochemistry, 2006. 45(3): p. 676-85.

19. Yu, H., et al., A general method for mapping tertiary contacts between amino acid residues in membrane-embedded proteins. Biochemistry, 1995. 34(46): p. 14963-9.

20. Yu, H., M. Kono, and D.D. Oprian, State-dependent disulfide cross-linking in rhodopsin. Biochemistry, 1999. 38(37): p. 12028-32.

21. Srinivasan, N., et al., Conformations of disulfide bridges in proteins. Int J Pept Protein Res, 1990. 36(2): p. 147-55.

22. Guo, W., et al., Crosstalk in G protein-coupled receptors: changes at the transmembrane homodimer interface determine activation. Proc Natl Acad Sci U S A, 2005. 102(48): p. 17495-500.

23. Mancia, F., et al., Ligand sensitivity in dimeric associations of the serotonin 5HT2c receptor. EMBO Rep, 2008. 9(4): p. 363-9.

24. Shi, C., et al., N-terminal residues of the yeast pheromone receptor, Ste2p, mediate mating events independently of G1-arrest signaling. J Cell Biochem, 2009. 107(4): p. 630-8.

25. Lee, G.F., et al., Deducing the organization of a transmembrane domain by disulfide cross-linking. The bacterial chemoreceptor Trg. J Biol Chem, 1994. 269(47): p. 29920-7.

26. Struthers, M., et al., Tertiary interactions between the fifth and sixth transmembrane segments of rhodopsin. Biochemistry, 1999. 38(20): p. 6597-603.

27. Wang, H.X. and J.B. Konopka, Identification of Amino Acids at Two Dimer Interface Regions of the alpha-Factor Receptor (Ste2). Biochemistry, 2009.

28. Avery, S.V., N.G. Howlett, and S. Radice, Copper toxicity towards Saccharomyces cerevisiae: dependence on plasma membrane fatty acid composition. Appl Environ Microbiol, 1996. 62(11): p. 3960-6.

29. Shi, C., et al., In vitro characterization of ligand-induced oligomerization of the S. cerevisiae G-protein coupled receptor, Ste2p. Biochim Biophys Acta, 2009. 1790(1): p. 1-7.

30. Alisio, A. and M. Mueckler, Relative proximity and orientation of helices 4 and 8 of the GLUT1 glucose transporter. J Biol Chem, 2004. 279(25): p. 26540-5.

31. Giron-Monzon, L., et al., Mapping protein-protein interactions between MutL and MutH by cross-linking. J Biol Chem, 2004. 279(47): p. 49338-45.

32. Kovalenko, O.V., et al., Evidence for specific tetraspanin homodimers: inhibition of palmitoylation makes cysteine residues available for cross-linking. Biochem J, 2004. 377(Pt 2): p. 407-17.

33. Lee, B.K., et al., Tyr266 in the sixth transmembrane domain of the yeast alpha-factor receptor plays key roles in receptor activation and ligand specificity. Biochemistry, 2002. 41(46): p. 13681-9.

34. He, J., et al., Glycosylation of beta(1)-adrenergic receptors regulates receptor surface expression and dimerization. Biochem Biophys Res Commun, 2002. 297(3): p. 565-72.

35. Michineau, S., F. Alhenc-Gelas, and R.M. Rajerison, Human bradykinin B2 receptor sialylation and N-glycosylation participate with disulfide bonding in surface receptor dimerization. Biochemistry, 2006. 45(8): p. 2699-707.

36. Fernandes, H., S. Cohen, and S. Bishayee, Glycosylation-induced conformational modification positively regulates receptor-receptor association: a study with an aberrant epidermal growth factor receptor (EGFRvIII/DeltaEGFR) expressed in cancer cells. J Biol Chem, 2001. 276(7): p. 5375-83.

37. Wheatley, M. and S.R. Hawtin, Glycosylation of G-protein-coupled receptors for hormones central to normal reproductive functioning: its occurrence and role. Hum Reprod Update, 1999. 5(4): p. 356-64.

38. Milligan, G., G protein-coupled receptor dimerization: function and ligand pharmacology. Mol Pharmacol, 2004. 66(1): p. 1-7.

39. Milligan, G., G-protein-coupled receptor heterodimers: pharmacology, function and relevance to drug discovery. Drug Discov Today, 2006. 11(11-12): p. 541-9.

40. Milligan, G., G protein-coupled receptor dimerisation: molecular basis and relevance to function. Biochim Biophys Acta, 2007. 1768(4): p. 825-35.

41. Milligan, G., G protein-coupled receptor hetero-dimerization: contribution to pharmacology and function. Br J Pharmacol, 2009.

42. Overton, M.C. and K.J. Blumer, The extracellular N-terminal domain and transmembrane domains 1 and 2 mediate oligomerization of a yeast G protein-coupled receptor. J Biol Chem, 2002. 277(44): p. 41463-72.

43. Cleverley, R.M., et al., Selection of membrane protein targets for crystallization using PFO-PAGE electrophoresis. Mol Membr Biol, 2008. 25(8): p. 625-30.

44. Ramjeesingh, M., et al., Novel method for evaluation of the oligomeric structure of membrane proteins. Biochem J, 1999. 342 (Pt 1): p. 119-23.

45. Yang, Z.G., et al., Dimerization of human XPA and formation of XPA2-RPA protein complex. Biochemistry, 2002. 41(43): p. 13012-20.

46. Rath, A., R.A. Melnyk, and C.M. Deber, Evidence for assembly of small multidrug resistance proteins by a "two-faced" transmembrane helix. J Biol Chem, 2006. 281(22): p. 15546-53.

47. Guo, W., et al., Dopamine D2 receptors form higher order oligomers at physiological expression levels. Embo J, 2008. 27(17): p. 2293-304.

48. Overton, M.C. and K.J. Blumer, G-protein-coupled receptors function as oligomers in vivo. Curr Biol, 2000. 10(6): p. 341-4.

VITA

Heejung Kim was born in Seoul, Korea on Febrarury 22, 1979. She entered the Ewha Woman's University, Seoul, Korea, in March, 1997 and graduated with a Bachelor degree in Biology in February, 2000. She started her graduate study at the Seoul National University in 2000 and completed her non-thesis program in Oceanography in 2003. In August of 2003, she entered Graduate School at the University of Tennessee in Microbiology. Throughout the course of her time in this program, she served as a Graduate Teaching Assistant (2003-2007) and as a Graduate Research Assistant (2008-2009). She officially received a Doctor of Philosophy degree in Microbiology in December, 2009.

In February of 2010, she will take a position as a post-doctoral fellow in the laboratory of Dr. Brad Binder at the University of Tennessee.